UNIVERSITY OF CINCINNATI

Date: 10-Nov-2010

I, Karolin Kroening **,**

hereby submit this original work as part of the requirements for the degree of:

Doctor of Philosophy

in Chemistry

It is entitled:

Small to large molecule speciation: Metallomics approaches stretch the horizons.

Student Signature: Karolin Kroening

This work and its defense approved by:

Committee Chair: Joseph Caruso, PhD
Joseph Caruso, PhD

Small to large molecule speciation: Metallomics approaches stretch the horizons

A dissertation submitted to the

Division of research and Advanced Studies
of the University of Cincinnati

In partial fulfillment of the requirements for the degree of

Doctor of Philosophy (Ph.D.)

In the Department of Chemistry of the
McMicken College of Arst and Sciences

2010

By

Karolin Katrin Kroening

B.S. Chemistry, Università degli Studi di Firenze, Italy, 2003

M.S. Analytical Chemistry, Università degli Studi di Bologna, Italy, 2006

Committee Chair: Dr. Joseph A. Caruso

Abstract of Dissertation

Metallomics is the study of the metallome, interactions, and functional connections of metal ions and other metal species with genes, proteins, metabolites, and other biomolecules in biological systems. Its application can handle a variety of sample, from biomedical to environmental. Elemental speciation is a fundamental component of the concept of Metallomics. It permits to investigate the chemical form of metals and metalloids containing species.

Speciation analyses with metallomics approaches can be performed best by high performance liquid chromatography (HPLC) coupled to inductively coupled plasma mass spectrometry (ICP-MS). HPLC represents a suitable separation technique and a variety of different chromatographic techniques, from conventional to capillary, can be applied to obtain good baseline separated peaks corresponding to different species. ICP-MS is the state-of-the-art instrument when elemental mass spectrometry for the detection of ultra trace levels (parts per quadrillion) takes place. ICP-MS is renowned for its phenomenal sensitivity and selectivity as elemental analyzer. Chromatography can be applied to molecular mass spectrometry as well. In the presented works electrospray ionization is the technique of choice. Nano liquid chromatography-Chip-electrospray ionization- ion trap mass spectrometry (NanoLC-Chip-ESI-ITMS) is an excellent tool for the research performed.

The aforementioned instrumentations have been applied to environmental applications in the first part of this dissertation. Chemical warfare agents (CWAs) are present in the environment (sea and soil) because discarded due over production during World War I and II. Those CWAs easily degrade, especially in aquatic surrounding, and give birth to chemical

warfare agent degradation products (CWADPs) whose toxicity is not well know. In the following pages a complete study about some of these CWADPs and their speciation and toxicity is reported.

The second part of the dissertation analysis a more complex matrix with metallomics approaches. The combination of subarachnoid hemorrhage (SAH) with cerebral vasospasm (CV) leads to severe debilitation or death of an estimated one million people worldwide every year. A biomarker that would predict CV after a SAH has yet to be found.

The focus of this study is to explore differences in protein phosphorylation in cerebral spinal fluid (CSF) among healthy patients, SAH patients and SAH-CV patients. A significant difference in the phosphorproteom could be one step towards the discovery of a diagnostic marker that may predict CV after SAH. The significance of phosphorylated proteins as a marker is manifested in the constitutive nature of intracellular signaling involved in the pathological events seen post SAH.

Capillary liquid chromatography (cap-LC) coupled to inductively coupled plasma mass spectrometry (ICPMS) and nanoliquid chromatography-PhosphoCHIP/ion trap mass spectrometry (nanoLC-P-CHIP/ITMS) are used to identify and measure protein phosphorylation changes in the CSF of the aforementioned three groups. ICPMS represents a suitable method for screening phosphorous (^{31}P), while nanoLC-P-CHIP/ITMS can be used to identify phosphoproteins and match these with protein database entries.

Table of contents

Chemical warfare agents degradation products (CWADPs) containing Arsenic, Phosphorus and Sulfur and their simultaneous detection as oxides with HPLC-ICPMS

CHAPTER 6:

Cytotoxicity of Arsenic containing Chemical Warfare Agent Degradation Products with Metallomics Approaches for metabolite analysis

Figures

Figure 3.3. HPLC-ICPMS chromatogram of the diluted standards. Concentration: 20 µL mL^{-1}. Injection volume, 100 µL , 10mM acetate buffer (pH 4.0)-methanol (85:15, v/v). 0%, 0.50%, 1.00%, 1.50%, 2.00% 3-pentanol and 2.00% 2-methyl-3-pentanol in every run. Method 1.

Figure 3.4. HPLC-ICPMS chromatogram of the diluted standard. Concentration: 10µL mL^{-1}. Injection volume, 100 µL, 10mM acetate buffer (pH 4.0)-methanol (98:2, v/v). 2.00% 3-pentanol, 2.00% 2-methyl-3-pentanol and 3.00% 2,2 dimethyl-3-pentanol. Method 2.

Figure 3.5. Reconstructed electrospray ion chromatograms of the five hydrolysis products: TDG m/z 123 (A), BHETM m/z 169 (B), BHETE m/z 183 (C), BHETPr m/z 197 (D), BHETBu m/z 211(E) and total ion chromatogram accomplished with HPLC-ESI-MS separation Method 2 (F).

Figure 3.6. HPLC-ICPMS chromatogram of the five hydrolysis products spiked into Little Miami River (OH) water. Concentration: 10µL mL^{-1}. Injection volume, 100 µL, 10mM acetate buffer (pH 4.0)-methanol (85:5, v/v). 2.00% (v/v) 3-pentanol, 2.00% (v/v) 2-methyl-3-pentanol.

Figure 4.1. Structures and p*K*a values of CWADPs analyzed. $H_2PO_4^-$ is the last breakdown product of many CWAs but is considered an interference in this study because it is prevalent in many common sample matrices

Figure 4.2. Separation of a 100-ng/mL mixture of MPA, EMPA, and IMPA.

Figure 4.3. LC–ICP-MS chromatogram of CWADPs mixture including $H_2PO_4^-$ in distilled deionized water at a concentration of 10 µg/mL for each analyte. Dashed line represents the gradient program. Peaks: 1 = EHDAP (GA acid), 2 = MPA, 3 = EPA, 4 = DMHP, 5 = PPA, 6 = EMPA (VX acid), 7 = IMPA (GB acid), 8 = DEHP, 9 = IPHEP, 10 = IBHMP (RVX acid), 11 = H_3PO_4.

Figure 7.3. CSF Control, CSF C, CSF V (< 5 kDa) LC-ICPMS chromatograms. A peak at 12.1 min in the CSF C is being distinguished from CSF Control and CSF V. Also, a peak at around 38 min in the CSF Control and CSF V samples is not present in the samples from patients that have suffered a SAH without vasospasm.

Figure 7.4. Regulator of G-protein signaling 12 (RGS12) average mass spectrum showing characteristic masses as ATK, m/z 575.3: AQSNR, m/z 728.4: m/z GWLKPK, m/z 1193.6: LAFSAVCPDDR, m/z 1796.9: INLDEAEEFFELISK etc., being indication of peptide fragmentation.

Tables

Chapter 1

Introduction to elemental speciation analysis and Metallomics

1.1. Overview of elemental analysis

Elemental analysis is the quantitative and qualitative study of the amount and type of an element in a compound. Sometimes isotopic information is included in the elemental analysis. The process of elemental analysis is essential in the determination of a variety of matrices. Common samples where elemental analysis is requested can go from liquid to solid compounds, e.g. urine, clay, wine, cells etc. The application of this kind of investigation can also be a multiplicity of fields: environmental, biomedical, clinical, nutritional and "daily life" complex matrices. For instance, the elemental composition of clay is fundamental for the determination of the kind of the type of rock it is. The rock composition refers to the weight percentages (wt %) of elements (more in specific minerals) contained in the rock.

Elemental analysis belongs to the branch of analytical chemistry and a variety of instrumentation can determine the amount and which elements are present in a matrix. Few examples of instruments commonly used include:

- Thermal Ionization Mass Spectrometry (TIMS)
- Inductively Coupled Plasma-Mass Spectrometry (ICP-MS)
- Inductively Coupled Plasma-Atomic Emission Spectrometry (ICP-AES)
- X-Ray Diffraction (XRD) & Micro X-Ray Diffraction (Micro XRD)
- X-Ray Fluorimetry (XRF)

- Carbon Analyzer
- Nitrogen/Oxygen Analyzer

One step in elemental analysis is the determination of elements at trace levels. Those levels are commonly referred to as ranges of parts per million (ppm), parts per billion (ppb), and parts per trillion (ppt), depending on the sample being tested. But in few cases reported in the literature femto levels (10^{-15}) have been reported. Separation of DMBA-oligosaccharides was achieved on a graphitized carbon column and the DMBA-oligosaccharides were detected by positive-ion mode ESI-ITMS allowing sample amounts down to ~30 fmol of single DMBA-oligosaccharides.[1] In cases like these, ultra trace elemental analysis would be the proper descriptors.

Ultra trace level analysis requires more than a simple laboratory structure; possibly experiments will need to be performed in clean rooms, where the level of dust and other common environmental and airborne pollutants is held at the minimum. The level of contamination is controlled depending on number of particles of a specific size per cubic meter.

Sample preparation is a crucial step in the analytical world. Without it being done properly, there would be little point in doing the analysis. Sample preparation has to reduce interferences and allow for minimal contamination plus losses of trace elements during sample preparation have to be reduced at the bare minimum. Depending on the sample type, each sample preparation is different for obvious reasons, but few factors are common in almost all the procedures and that is the use of ultrapure/ high purity solvent or ultrapure filtered deionized water as well as the cleanliness of the sample preparation area. As mentioned

before, the sample preparation step is a very important aspect concerning the quality in trace analysis.

Element speciation determines the different forms that a chemical element can take within a given compound or sample, enabling chemists to predict possible ramifications for the environment and human health.[2] Elemental speciation analysis has become exceptionally important in environmental, food, and biomedical studies. This is because, for many elements, properties such as those listed below depend on the species or chemical form of the element present in the sample.

- Toxicity or nutritional value
- Environmental mobility and persistence
- Bioavailability
- Volatility
- Chemical reactivity

A common example would be the measurement of Cr (VI) – toxic – and Cr (III) – non-toxic – as opposed to total Cr in environmental samples. Similar examples of elemental speciation include As (III)/As (V), Se (IV)/Se (VI) and other elements that can exist at different stable oxidation states. [3]

While the concept of ***"element speciation"*** in the sense of distinguishing fractions of the total element concentration, according to some peculiar properties such as being "bioavailable," grew slowly in the late 1950s, it was only during the late 80's, that instrumental elemental analysis reached the detection power necessary to measure small fractions of trace elements in environmental and biological samples. [4]

It is almost impossible not to associate elemental speciation analysis with Metallomics – the analysis of metals/metalloids and metal/metalloid species and their interactions within biological and ecological systems.

1.2. Metallomics

Metallomics has had a variety of definitions over the past years. The term "metallome" was coined by Williams who referred to it as an element distribution, equilibrium concentrations of free metal ions, or as free element content in a cellular compartment, cell, or organism.[5] The latter would therefore be characterized not only by its genome or proteome but also by the metallome, the inorganic complement. The meaning of the term "metallome" was then proposed to extend to the entirety of metal and metalloid species present in a cell or tissue type.[6, 7] The characterization of the pool of metal-containing species in living organisms and of their inter actions with the genome, transcriptome, proteome, and metabolome requires dedicated analytical approaches to *in vivo* detection, localization, identification, and quantification, *in vitro* functional analysis and "*in silico*" prediction using bioinformatics.[8] The

term “metallomics” was coined by Haraguchi to denote the ensemble of research activities related to metals of biological interest.[9, 10]

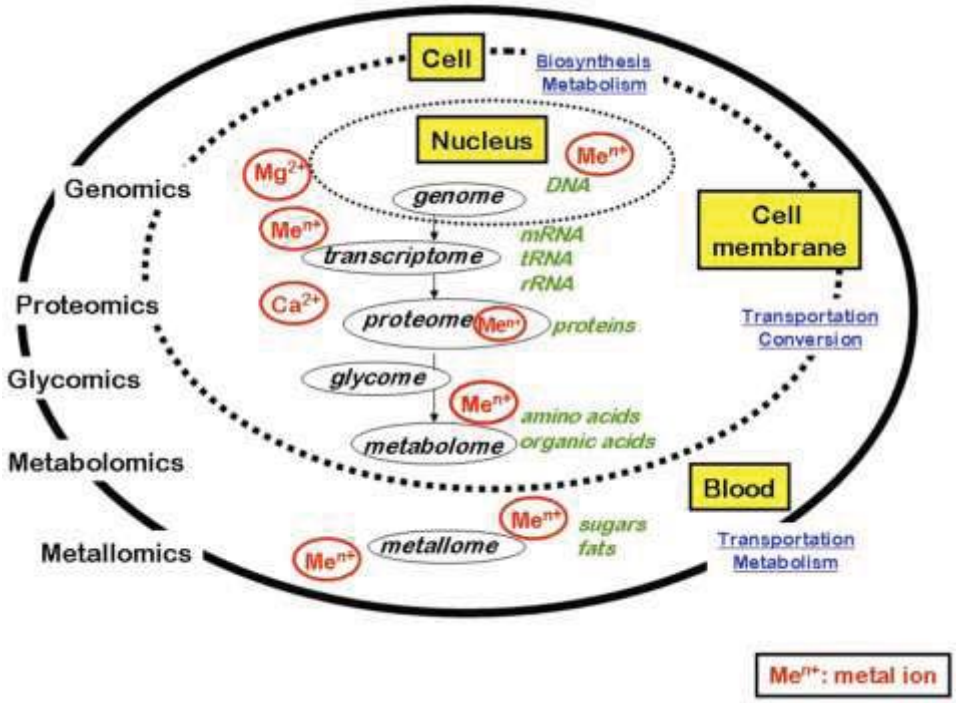

Figure 1.1 Simplified model of biological system and related -omics sciences. The outer area surrounded with the continuous line is showing, e.g., an organ or whole body, and the inner area surrounded with the dotted line is showing a biological cell. Biological fluid, e.g., blood, is circulating in the intermediate area. The Mg2+ and Ca2+ ions are given as examples because of their large affinities with DNA and proteins, respectively, in the biological cell. Reproduced from Metallomics as integrated biometal science.

Hiroki Haraguchi,*J. Anal. At. Spectrom.*, 2004, 19, 5-14,DOI: 10.1039/B308213J .

The definition of metallome and Metallomics has been defined by Lobinski et al. and has found an International Union of Pure and Applied Chemistry (IUPAC) acceptance. [12]

Metallome

Entirety of metal- and metalloid species* present in a biological system, defined as to their identity and/or quantity.

Note 1: The metallome can be determined in a bulk biological sample representative of the system [or its component(s)] or at specific location(s).

Note 2: The metallome can be characterized with different degrees of approximation, such as

- a set of total element concentrations,
- a set of metal complexes with a given class of ligands, e.g., proteins or metabolites or
- a set of all the species of a given element (e.g., copper metallome).

Note 3: In contrast to the genome of which the analysis has a specific endpoint (the determination of a finite number of DNA sequences), the description of a metallome, like that of a proteome or metabolome[11], can never be complete. In particular, the numerous known and possible metal coordination complexes with biological ligands can be described only in terms of kinetic constants with defined thermodynamic equilibria. [12]

Metallomics

Study of the metallome, interactions, and functional connections of metal ions and other metal species with genes, proteins, metabolites, and other biomolecules in biological systems. A metallomics study is expected to imply:

• a focus on metals (e.g., copper, zinc, iron, manganese, molybdenum, nickel, calcium, …., cadmium, lead, mercury, uranium) or metalloids (e.g., arsenic, selenium, antimony) in a biological context;

• a link between the set of element concentrations or element speciation with the genome. This link may be statistical (an enrichment of an element coincides with the presence of a particular gene), structural (sequence of a metalloprotein is traceable to a gene) or functional (the presence of a bio ligand is the result of a gene-encoded mechanism); or

• a systematic or comprehensive approach. The identification of a single metal species, however important, without specifying its significance and contribution to the system should not be referred to as metallomics.[12]

1.3. References

(1) Broberg, A. *Carbohydrate Research* **2007**, *342*, 1462-1469.
(2) Caroli, S. *Element Speciation in Bioinorganic Chemistry*; Wiley, April 1996.
(3) http://www.chem.agilent.com/en-us/products/instruments/icp-ms/pages/gp56894.aspx.
(4) http://www.speciation.net/Public/Document/2003/09/11/500.html.
(5) Williams, R. J. P. *Coord. Chem. Rev.* **2001**, *583*, 216–217.
(6) Szpunar., J. *Anal. Bioanal. Chem.* **2004**, *378*.
(7) D. W. Koppenaal, G. M. H. *J. Anal. At. Spectrom* **2007**, *22*.
(8) S. Mounicou, J. S., R. Lobinski *Chem. Soc. Rev.* **2009**, *28*.
(9) H. Haraguchi, T. M., E. Enomoto (Ed.), RIKEN (Research Institute of Physics and Chemistry), Wako 2002.
(10) Haraguchi, H. *J. Anal. At. Spectrom.* **2004**, *19*.
(11) J. H. Duffus, M. N., D. M. Templeton *Pure. Appl. Chem* **2007**, *79*, 1153.
(12) Lobinski Ryszard, B. J. S., Haraguchi Hiroki, Sarkar Bibundhendra *Pure Appl. Chem* **2010**, *82*, 493–504.

Chapter 2

Instrumentation adept for elemental speciation and Metallomics studies

2.1. Elemental speciation technique

2.1.1 High performance liquid chromatography (HPLC) systems

A vast amount of the work presented in this dissertation is concerning elemental speciation. One of the most common methods to perform speciation is high performance liquid chromatography (HPLC), coupled to mass spectrometry. Several chromatography types allow for a variety of applications, depending on the chemical properties of the matrix to be analyzed. In the following chapters representing several applications, chromatography types as reversed phase chromatography, ion pairing chromatography and displacement chromatography, as well as conventional and capillary chromatography have been used.

HPLC is a universal method for separating polar, non-polar, hydrophobic, hydrophilic and charged species which are not charged in nature.[1] The HPLC instrumentations used in this work were Agilent series 1100 and 1200 high-performance liquid chromatographic systems.

2.2. Overview Chromatographic techniques

2.2.1.Reversed phase chromatography

Reversed phase chromatography is very common as speciation technique. The separation mechanism depends on the hydrophobic binding interaction between the solute molecule in the mobile phase and the immobilized hydrophobic ligand, i.e.

stationary phase. Reversed phase chromatography is an adsorptive process by experimental design, which relies on a partitioning mechanism to effect separation. The solute molecules partition between the mobile phase and the stationary phase and the distribution of the solute between the two phases depends on the binding properties of the medium, the hydrophobicity of the solute and the composition of the mobile phase. [2]

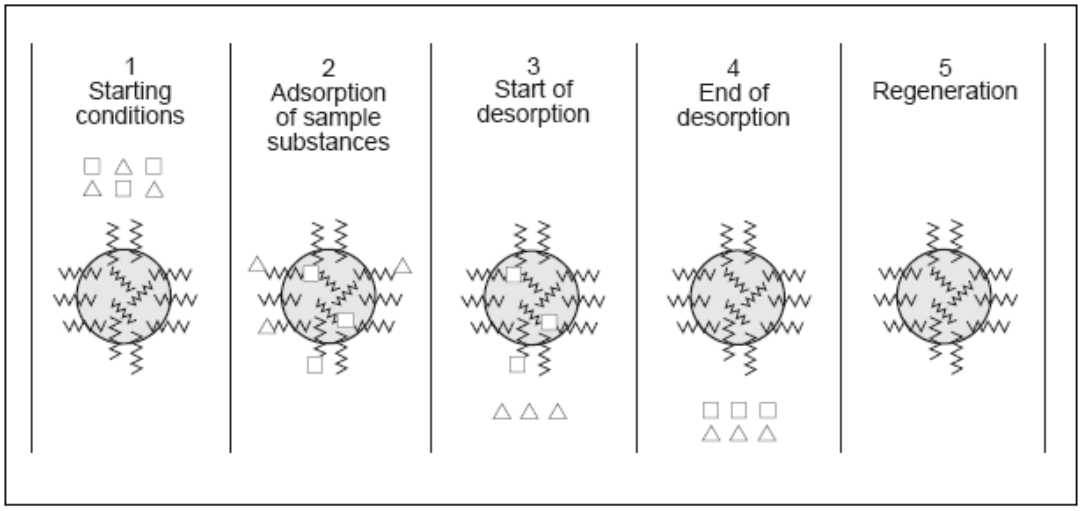

Figure 2.1. Principle of reversed phase chromatography with gradient elution. [2]

In most of the work in this dissertation uses reversed phase chromatography to separate biomolecules. Reversed phase chromatography of biomolecules generally uses gradient elution instead of isocratic elution. While biomolecules strongly adsorb to the surface of a reversed phase matrix under aqueous conditions, they desorb from the matrix within a very narrow window of organic modifier concentration. Along with these high molecular weight biomolecules with their unique adsorption properties, the typical

biological sample usually contains a broad mixture of biomolecules with a correspondingly diverse range of adsorption affinities. The only practical method for reversed phase separation of complex biological samples, therefore, is gradient elution. [3] In summary, separations in reversed phase chromatography depend on the reversible adsorption/desorption of solute molecules with varying degrees of hydrophobicity to a hydrophobic stationary phase. The majority of reversed phase separation experiments are performed in several fundamental steps as illustrated in **Figure 2.1**.[2]

2.2.2.Ion-pairing chromatography

Because of the polar nature of the matrix t be separated, sometimes reversed phase can present not the ideal choice of methodology. Ion pairing chromatography (IPC) is a more general and applicable approach that allows the separation of complex mixtures of polar and ionic molecules. The selectivity is determined by the mobile phase: the organic eluent is supplemented with a specific ion-pairing reagent. The IPC reagents are large ionic molecules having a charge opposite to the analyte of interest, as well as a hydrophobic region to interact with the stationary phase. The counter-ion combines with the ions of the eluent, becoming ion pairs in the stationary phase. This results in different retention, thus facilitating separation of analytes.

Important parameters for IPC are:

- Type of analyte matrix (e.g. charged, hydrophobicity).

- Type of IP-agent.
- Concentration of IP agent.
- Type of organic modifier in the mobile phase.
- Concentration of organic modifier in the mobile phase.
- Ionic strength and type of ions in the mobile phase.

Figure 2.2 illustrates the multistep ion pairing formation equilibrium. What sets ion pairing apart from forming a complex is the absence of directional covalent coordinative bonds resulting from a Lewis acid-base interaction and a special geometrical arrangement. [4]

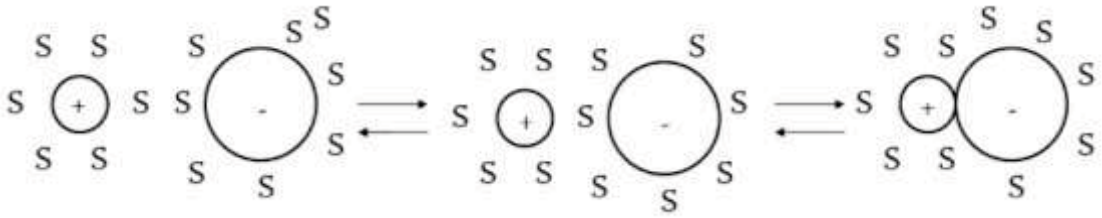

Figure 2.2. Multistep ion pairing formation equilibrium.[4]

2.2.3.Displacement chromatography

Displacement is a universal concept to indicate that one competitor is strong enough to replace the other competitor from its recent position or situation. The displacement mode of chromatography is a normal method of development in separation techniques.

Displacement chromatography works with the same instrumentation (hardware) generally used for analytical separation (the only usual exception is a large-volume sample loop)[3] . The key difference is in the quality and order of mobile phases. Elution-type HPLC employs one (isocratic elution) or several similar eluents (stepwise gradient), or mixtures of two eluents with changing concentration (gradient elution) as the mobile phase. On the other hand, displacement chromatography employs three basically different mobile phases, such as the carrier, displacer, and regenerant(s). The carrier serves to facilitate the load; the carrier has to be able to dissolve the sample, and the sample components have to be definitely retarded on the stationary phase. The function of the displacer is to displace the sample components from the stationary phase; during this step the individual components also displace each other. By the end of the displacement step, the displacer occupies all binding sites of the stationary phase. Finally, the regenerant removes the displacer from the stationary phase and it prepares the column for the separation of the next sample.[3] The consecutive steps of displacement chromatography are shown in **Figure 2.3**.

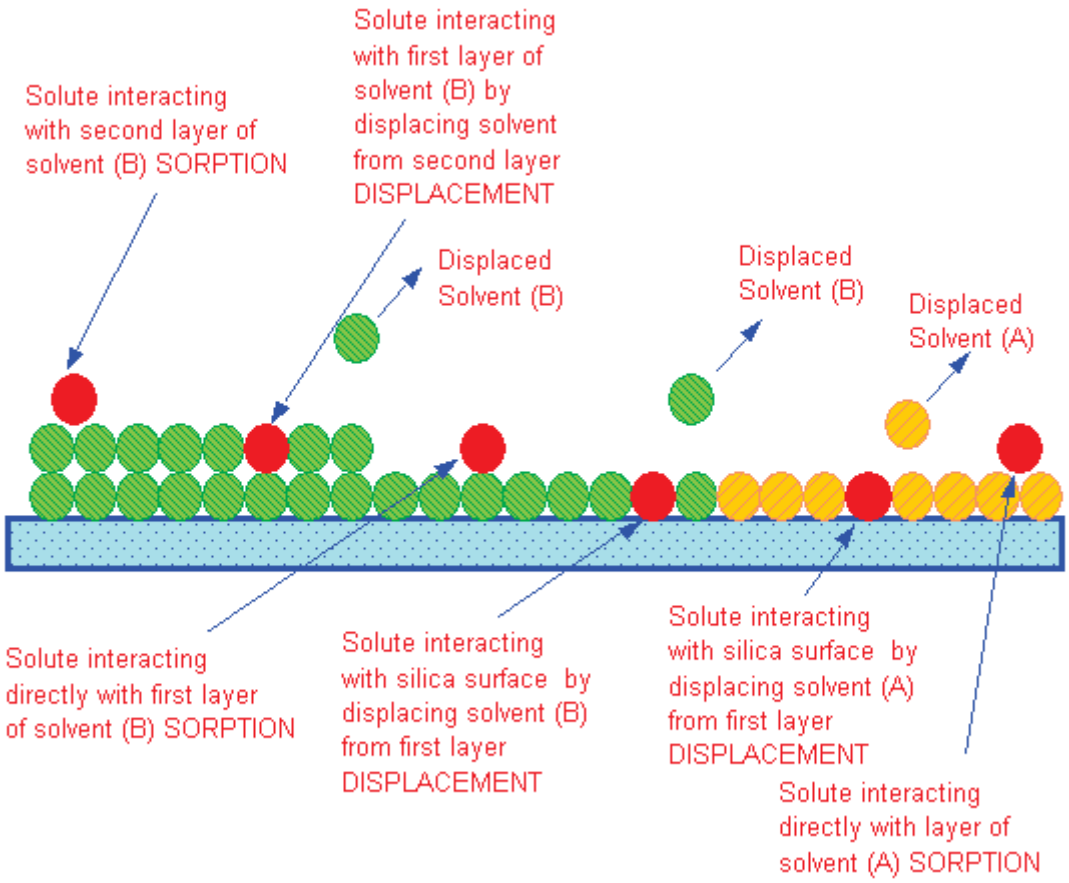

Figure 2.3. Scheme of the displacement chromatographic technique.[4]

2.3. Inductively coupled plasma mass spectrometry (ICP-MS)

Inductively coupled plasma mass spectrometry (ICP-MS) has several advantages compared to other atomic spectrometry techniques: it is rapid, sensitive, multi-elemental, it has a wide dynamic range and with the introduction of the latest instrumentations on the markets, very good control of interferences. Furthermore, ICP-MS can give isotopic information and is an excellent chromatographic detector. **Figure**

2.4 represents the sample introduction process, from liquid matrix (solid, in case of laser ablation ICP-MS) to ion.

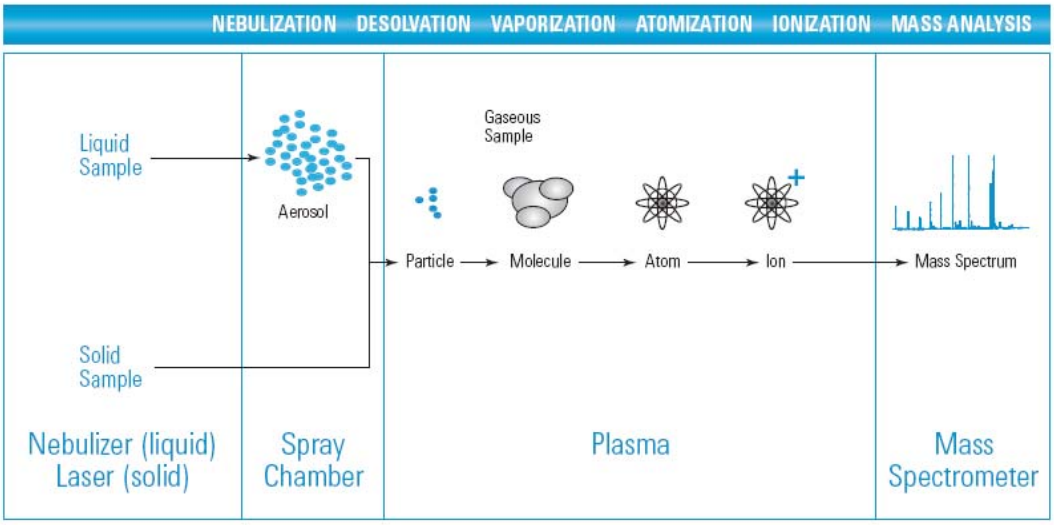

Figure 2.4. Schematic representation of processes in ICP-MS from sample introduction to mass analysis. [5]

One of the most important steps in ICP-MS analyses is the sample introduction and ion generation in the ICP. Spray chamber and torch need specific designs and requirements in order to optimize those processes. The interface and ion focusing extract the positively charged ions in the high vacuum area. These processes are taking over by a pair of cones (sampling cone and skimmer cone) and by a set of electrostatic lenses that keep the ions in a compact ion beam.

At this stage the collision reaction cell (CRC) becomes important in order to minimize polyatomic interferences. The CRC is basically an ion guide, which is enclosed in a cell that can be pressurized with a gas and is located after the main ion lenses.

At the end ions pass from the CRC to the analyzer vacuum stage, where they are separated by a quadruple, according to their mass to charge ratio. Because of the complexity of the instrument it is useful to refer to the Agilent Primer Guide, that represent an optimum tool to better understand the functionality of the ICP-MS used in these studies. **Figure 2.5** shows a schematic representation of an Agilent 7500 Series ICP-MS.

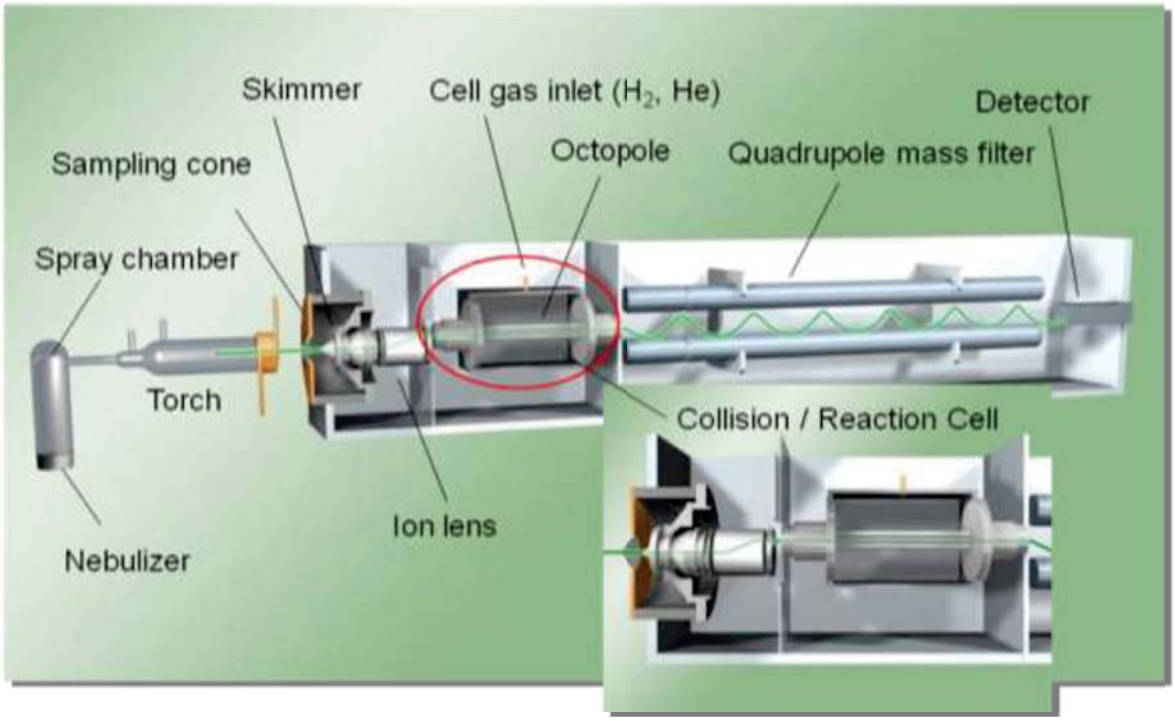

Figure 2.5. Agilent 7500 Series ICP-MS [5]

2.4. Ion Trap LC/MS

The Agilent 6300 Series Ion Trap LC/MS used in this dissertation work consists of the following components (**Figure 2.6**):

- interface to generate ions
- ion optical elements to guide the ions from the interface to the mass analyzer (ion trap)
- ion trap to collect the ions and then release them according to mass-to-charge ratio
- ion detector (and its electronics, firmware and software) to convert the ions to a mass spectrum
- vacuum pumps to keep the system at low

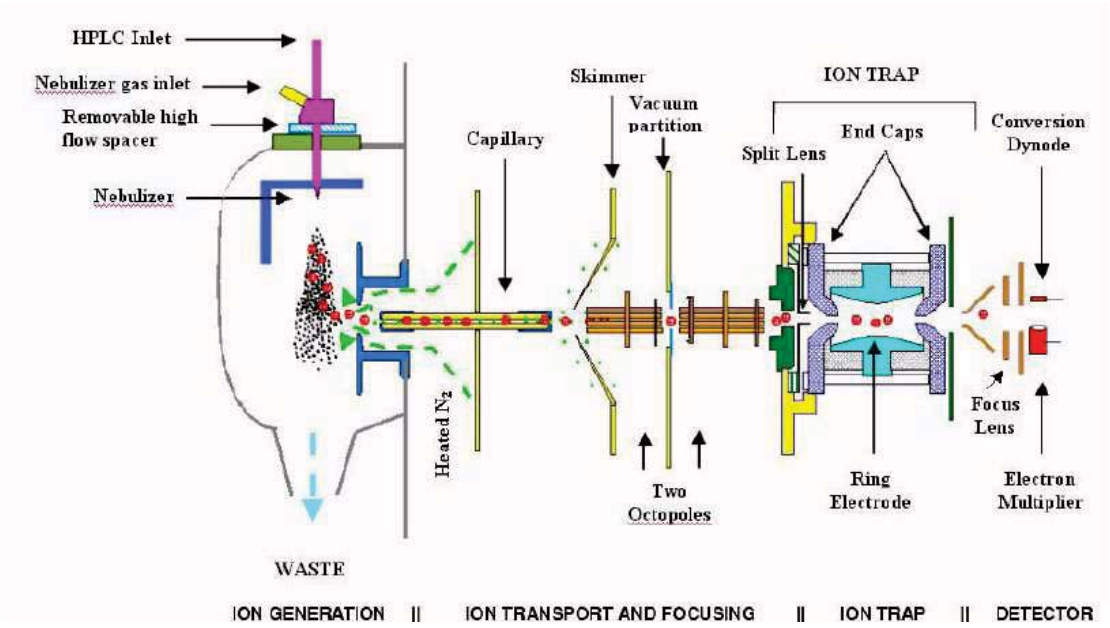

Figure 2.6. Trap mass spectrometer for ion transmission and detection. [6]

An ion trap performs several important steps to produce mass spectra:

- mass accumulation,
- selective mass isolation and excitation for collision-induced dissociation (MS/MS), and
- sequential mass ejection to produce a mass spectrum.

With such flexibility, the ion trap has some advantages over linear quadrupole systems for use in highly sensitive and selective mass measurements. Ions are generated outside the trap by one of several possible API (Atmospheric Pressure Ionization) sources, which produces a continuous source of ions. These naturally divergent ions have to be focused from the source into the trap by a combination of electrostatic lenses and a split RF octopole ion guide.

During the first part of the mass analysis cycle, ions are accumulated in the trap. During later parts of the mass analysis the continuous ion beam from the source must be prevented from passing through the trap, which would result in detector noise. Appropriate voltages ("block voltages") are applied to the elements in the ion transport and focusing region to deflect the ion beam during these later stages of mass analysis.

During the "scanning" step, ions of a particular mass are ejected in increasing order of mass from the trap. The trap can also isolate a precursor ion, which is then fragmented into product ions to produce MS/MS spectra. You can also tell the trap to fragment the product ions as well, to give the trap MS(n) capability.[6]

2.5. References

1. Bélanger J.M.R. et al., Techniques and Instrumentation in Analytical ChemistryVolume 18, 1997,1-35.
2. http://teachline.ls.huji.ac.il/72682/Booklets/AmershamRPCManual.pdf
3. Kalász et al., Journal of Chromatographic Science, ISSN 0021-9665 Volume 41, Number 6, July 2003, pp. 281-283.
4. http://www.chromatography-online.org/HPLC/HPLC-Mobile-Phases/Stationary-Phase-Interactions/rs72.html
5. http://www.agilenticpms.com/primer/ICP-MS%20Primer.pdf
6. http://www.chem.agilent.com/Library/usermanuals/Public/G2440-90096_Concepts_6.1.pdf

Chapter 3

Screening hydrolysis products of sulfur mustard agents by high-performance liquid chromatography with inductively coupled plasma mass spectrometry detection

Reproduced from Karolin K. Kroening, Douglas D. Richardson, Scott Afton, Joseph A. Caruso. Screening hydrolysis products of sulfur mustard agents by HPLC with ICPMS detection. *Analytical and Bioanalytical Chemistry*, **2009**; 393(8): 1949-56.

3.1 Introduction

The need to find effective methods for the detection and measurement of chemical warfare agents (CWAs) has increased in recent years. Current stockpiles need to be monitored to ensure their safe storage and ultimate disposal. The remediation of sites containing CWAs requires analysis in support of safe removal and destruction of agents. More recently, counterterrorism efforts have underscored the need for methods to accurately detect and measure CWAs at low levels.[1] Therefore, detection at lowest levels possible of these agents and their degradation products is necessary.

Mustard agents, including sulfur mustard, are schedule 1 CWA regulated under the 1993 Chemical Weapons Convention (CWC), which banned the production, acquisition, retention and direct or indirect transfer of all chemical weapons.[2] Mustard gas has been used during World War I and II and during the Iran-Iraq war in the 1980s. In addition, American soldiers were exposed to Iraqi chemical agents when arms dumps were destroyed during and after the 1991 Gulf War.[3]

Mustard gas is a strong vesicant, resulting in severe skin blistering as well as eye and lung lesions upon exposure. Blister agent exposure over more than 50% body surface area is usually fatal.[4] Mustard gas is also carcinogenic and mutagenic.[5]

Chemically, sulfur mustard is a thioether, 2,2-dichlorodiethyl sulfide, $(ClCH_2CH_2)_2S$. The point of departure for this study is to improve previous studies concerning the detection of hydrolysis degradation products of sulfur mustards. These hydrolysis products

include: thiodiglycol (TDG), bis(2-hydroxyethyl thio)methane (BHETM), 1,2-bis(2-hydroxyethyl thio)ethane (BHETE), 1,3-bis(2-hydroxyethylthio)propane (BHETPr), 1,4-bis(2-hydroxyethylthio)butane (BHETBu). Their molecular weights and pKa values are listed in **Table 3.1**.[6]

Compound name	Structure	MW (g mol^{-1})	pKa
Thiodiglycol (**TDG**)	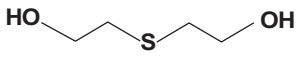	122.19	14.19 ± 0.10
Bis(2-hydroxyethylthio)methane (**BHETM**)	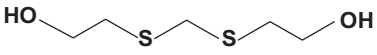	168.28	14.10 ± 0.10
1,2-bis(2-hydroxyethylthio)ethane (**BHETE**)	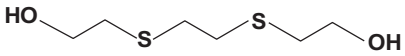	182.31	14.16 ± 0.10
1,3-bis(2-hydroxyethylthio)propane (**BHETPr**)	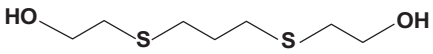	196.33	14.19 ± 0.10
1,4-bis(2-hydroxyethylthio)butane (**BHETBu**)	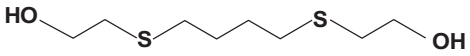	210.36	14.20 ± 0.10

Table 3.1. Structure of the studied compounds

Due to high sensitivity and specific element detection of ICP-MS these hydrolysis degradation products have been identified with HPLC coupled to ICP-MS detection, resulting in the first study utilizing ICP-MS with ^{32}S element-specific detection for the

analysis of vesicant chemical warfare agent degradation products. Sulfur detection with ICP-MS has presented difficulties in the past due to several polyatomic interferences on ^{32}S. But the use of a collision/reaction cell with xenon as optional gas represents a step forward for sulfur detection. Also, reversed-phase high-performance liquid chromatography (RP-HPLC) coupled with electrospray mass spectrometry (ESI-MS) data were collected to confirm to and compare with ICP-MS detection.

This study also employs peak compression chromatography (increase of peak concentration and reduction of peak tailing). The general term peak compression is used to describe the concentration of analyte bands during the chromatographic run and not before it. One of these techniques is displacement chromatography.[7] In displacement chromatography the substances are resolved into consecutive zones (displacement train) by displacers, usually alcohols, of the respective pure substance, which leave the column in the order of their affinity for the stationary phase. A big advantage of the displacement mode is that the separated products are obtained in higher concentration than in the normal elution mode, also solvent consumption is less and peak tailing is reduced.[8] Displacement chromatography is not often used due to difficulty in finding specific displacers.

Two different methods were tested in this study. The difference in these methods consists of the use of different columns and displacers for the chromatographic separations.

Previous studies have successfully utilized methods such as reversed-phase microcolumn liquid chromatography (micro-RPLC) coupled on-line with sulfur flame photometric detection (FPD) and electrospray ionization mass spectrometry (ESI-MS) for the analysis of the hydrolysis degradation products of sulfur mustards.[7-9]

3.2. Experimental

3.2.1 Reagents

Ammonium sulfate 1 μg mL^{-1} (Fisher Scientific, Fairlawn, NJ, USA) was used to tune the ICP-MS parameters, diluted in 2% HNO_3 (Pharmco, Brookfield, CT, USA). A 10 mM ammonium acetate (Fisher Scientific), pH 4.0, was used as the chromatographic buffer. Acetic acid (Fisher Scientific) was used to adjust the pH of the buffer. Methanol (Tedia Company, Fairfield, OH, USA) was added to the buffer solution in different percentages to create a more polar stationary phase.

Certified reference standards (1000 μg mL^{-1}) of sulfur mustards hydrolysis products TDG, BHETM, BHETE, BHETPr and BHETBu were purchased from Cerilliant Corp., Round Rock, TX, USA. Displacer compounds used in this work were 2-methyl-3-pentanol 99+% (Aldrich Chemical Company Inc., Milwaukee, WI, USA), 3-pentanol ≥ 99.5% GC (Fluka, Buchs, Switzerland), 2,2-dimethyl-3-pentanol and 2,4-dimethyl-3-pentanol (Aldrich Chemical Company Inc.).

The reagents utilized throughout this experiment were of analytical grade and prepared fresh daily through dilution of stock standards with DDI water. All water was prepared by passing through a NanoPure (18 MΩ) treatment system (Barnstead, Boston, MA, USA).

3.3 Instrumentation

3.3.1 High-Performance Liquid Chromatography (HPLC)

An Agilent 1100 (Agilent Technologies, Santa Clara, CA, USA) HPLC system equipped with a binary pump, autosampler, vacuum degasser, thermostated column compartment, and UV detector was used for the separation of the hydrolysis products of sulfur mustards. A C18 column (Agilent Technologies), Zorbax Eclipse XDB, 150 x 4.6 mm, 5 µm and a C8 column (Alltech Associates, Deerfield, IL, USA), Alltima, 150 x 3.2 mm, 5 µm were used for all separation experiments for Method 1 and Method 2, respectively.

A 100 µL aliquot of the standard mixtures (20 µg mL^{-1} for Method 1 and 10 µg mL^{-1} for Method 2 of each compound) containing sulfur hydrolysis products was injected into the HPLC coupled with ICP-MS with a flow rate of 1.0 mL min^{-1}.

3.3.2 Inductively coupled plasma mass spectrometer (ICP-MS)

An Agilent 7500ce (Agilent Technologies) ICP-MS equipped with shield torch and collision/reaction cell technology was used for element-specific detection of sulfur at

m/z 32. The collision/reaction cell consisted of an octopole ion guide operated in RF only mode which also served for the removal of polyatomic interferences. Xenon was used as the collision gas throughout all experiments. Electronic coupling of the ICP-MS with the HPLC was accomplished through the use of a remote cable which allowed for simultaneous starting prior to each chromatographic run.[10] A detailed description of the operating parameters for HPLC and ICP-MS is provided in **Table 3.2.1 and Table 3.2.2.**

ICP-MS parameters

Forward power	1500 W (with shielded torch)
Plasma gas flow rate	15.6 L min^{-1}
Auxiliary gas flow rate	1.2 L min^{-1}
Carrier gas flow rate	0.95 L min^{-1}
Nebulizer	Glass expansion micro-concentric
Spray chamber	≈ 2 °C (Scott double channel)
Sampling depth	7.5 mm
Sampling and skimmer cones	Nickel
Dwell time	0.1 s
Isotope monitored (*m/z*)	^{32}S
Octopole reaction system	Xe (Flow optimized prior to experiment)
QP bias	-1 V
Octopole	-46 V

Table 3.2.1 ICP-MS Instrumental Parameter

HPLC parameters	
Instrument	Agilent 1100 HPLC
Flow rate	1.0 mL min^{-1}
Injection volume	100 µL
Buffer	10mM NH_4COOH
	Method 1: 10mM NH_4COOH:MeOH (85:15,v/v)
	Method 2: 10mM NH_4COOH:MeOH (98:2,v/v)
pH	4.00
Column	Method 1: Zorbax Eclipse XDB (C18) 150 x 4.6 mm, 5 µm
	Method 2: Alltima (C8) 150 x 3.2 mm, 5µm
ESI-MS parameters	
Instrument	Agilent 1000 LC/MSD Trap XCT Ultra System
Drying gas: nitrogen	12 L min^{-1}
Temperature	350 ^{o}C
MS capillary voltage:	3000 V
Skimmer	40.0 V
Capillary exit	97.7 V
Trap drive	20.9 V

Table 3.2.2. HPLC and ESI-MS Instrumental Parameters

3.3.3 Electrospray mass spectrometry (ESI-MS)

All electrospray experiments were accomplished on an Agilent 1000 LC/MSD Trap XCT Ultra system (Agilent Technologies). Standard solutions (10 µg ml^{-1}) of each hydrolysis product were injected using a syringe pump first to detect their characteristic masses in positive ion mode. The 1100 LC was then connected to the instrument and the separation as performed in Method 1 was accomplished with a flow rate of 1.0 ml min^{-1}. Although the electrospray source can accommodate flow rates up to 1.0 mL min^{-1}, the flow was split post column to 200 µL min^{-1}. The following MS conditions were used: 12 L min^{-1} nitrogen drying gas at a temperature of 350 ^{o}C; MS capillary voltage: 3000 V; skimmer: 40.0 V; capillary exit: 97.7 V; trap drive: 20.9 V. The MS scan range was 50-400 m/z in standard-enhanced scan mode. ESI-MS, ESI-MS/MS experiments were run.

3.4 Results and Discussion

3.4.1 Optimization ICP-MS parameters

Even if HPLC coupled to ICP-MS is an effective speciation technique using sulfur specific detection, its determination suffers from high background problems. Specifically, $^{32}S^{+}$ (95.02 % abundant isotope) is interfered by $^{16}O^{16}O^{+}$ and $^{14}N^{18}O^{+}$.[11]

Collision/reaction cell technology has proven to be an effective method for alleviating the above mentioned interferences in the ICP-MS analysis through a collision/energy discrimination process for the most part, although other mechanisms may play a role.

For the analysis of sulfur containing compounds, xenon was used as the collision gas. Optimization of the xenon gas flow rate was found to be 0.25 mL min^{-1}. After overcoming the polyatomic interferences, selective ion transmission through adjustment of the pole bias plays a vital role in analyte response. The octopole bias was adjusted to -46 V and the quadrupole bias was adjusted to -1 V, (a positive upstream quadrupole voltage of +45 V) resulting in selective transmission of $^{32}S^{+}$ while minimizing the larger positive ion polyatomic interferences. Other operating conditions were close to the normal tuning parameters without any collision gas.

3.4.2 HPLC-ICP-MS separation

Owing to the hydrophobic and neutral nature of the compounds of interest, reversed-phase chromatography with isocratic conditions was investigated for the separation of sulfur mustard hydrolysis products. The acid dissociation constants for the hydrolysis degradation products of sulfur mustards are: thiodiglycol, pKa: 14.19 ± 0.10, bis(2-hydroxyethyl thio)methane, pKa: 14.10 ± 0.10, 1,2-bis(2-hydroxyethyl thio)ethane, pKa: 14.16 ± 0.10, 1,3-bis(2-hydroxyethyl thio)propane, pKa: 14.19 ± 0.10, 1,4-bis(2-hydroxyethyl thio)butane, pKa:14.20 ± 0.10 (**Table 1**), which indicates that the protonated form is predominant throughout a very wide pH range, limiting any charge interactions with mobile and stationary phases. An organic modifier was employed to separate the hydrolyzed warfare agents on a Zorbax Eclipse XDB C18 column (Method 1) and on an Alltima C8 column (Method 2) with acceptable retention times. Methanol was

selected as modifier and its concentration in the eluent was varied from 0.0 to 15.0 %. 10 mM ammonium acetate/acetic acid buffer at pH 4.0 was the chosen mobile phase. When reversed-phase HPLC is performed under neutral conditions, ammonium acetate is the additive of choice because of its volatility, resulting in efficient aerosol generation for sample introduction. Non-volatile buffer systems may cause clogging of both the torch outlet orifice and the MS sample inlet cone orifice.

A mobile phase with 15.0 % methanol was required to obtain good elution strength for Method 1 and 2.0 % methanol provided good separation for Method 2. Smaller analyte partitioning in the stationary phase is observed with the C8 column vs the C18 allowing a lower concentration of methanol to be used.

Optimum displacer concentration in the analyte solution was determined to be 2.0 % (v/v) 2-methyl-3-pentanol and 2.0 % (v/v) 3-pentanol for Method 1 and in addition to these previous displacers, 3.0 % (v/v) of 2,2-dimethyl-3-pentanol for Method 2 was added. 2,4-dimethyl-3-pentanol was used in comparison to 2,2-dimethyl-3-pentanol, however 2,2-dimethyl-3-pentanol showed better displacer characteristics.

3.4.3 Method 1

This method used a Zorbax Eclipse XDB C18 column and 15.0 % methanol as modifier to obtain an acceptable retention time. Moreover only two displacers 2,2 dimethyl-3-pentanol and 3-pentanol were used to improve the separation.

The loss of sensitivity is small (~ 8%) going from 0.0 to 15.0 % methanol. **Figure 3.1** shows the chromatogram for the separation with 10 mM acetate buffer (pH 4.0) – methanol (85:15, v/v) as mobile phase. The TDG peak slides slightly into the void volume, since the methanol creates a more polar condition, which slightly decreases the degree of hydrophobic interactions, resulting in poor separation for this compound.

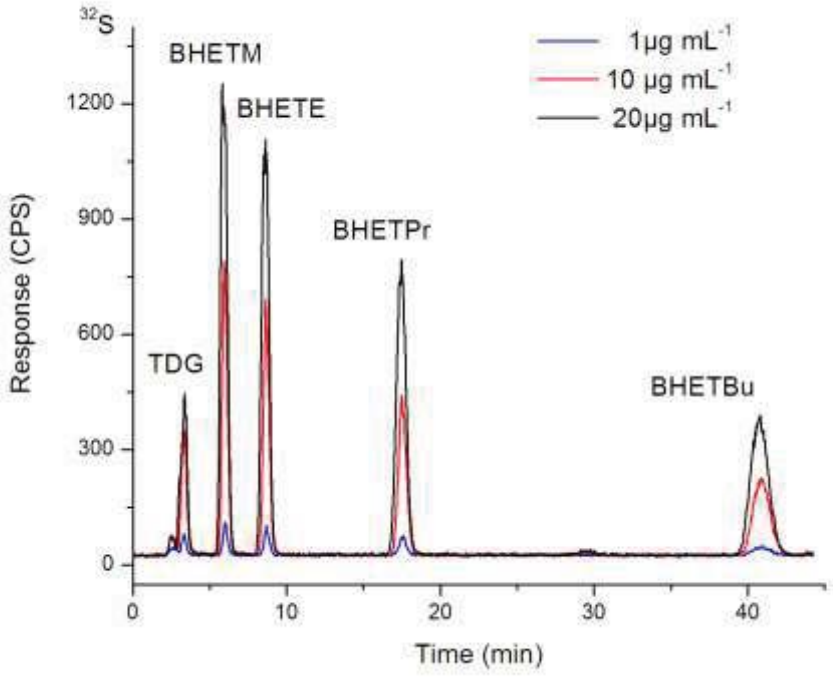

Figure 3.1. HPLC-ICPMS chromatogram of the diluted standards. Concentrations: 1µg mL^{-1}, 10 µg ml^{-1} and 20 µg mL^{-1}. Injection volume, 100 µL, 10mM acetate buffer (pH 4.0)-methanol (85:15, v/v).

Calibration curves showed good reproducibility, except for TDG because of its early elution which comes in the void volume. However, the BHET-alkenes are well separated within about 41.0 min and with good linearity over the concentration range of 1, 10 and 20 µg mL^{-1}.

3.4.4 Peak compression

The displacers used in Method 1 for peak compression were 2-methyl-3-pentanol and 3-pentanol. The choice of these two displacers was based on a previous study [7]. These alcohols are polar and the capacity factors are close to those of the analytes of interest. The displacer 2-methyl-3-pentanol acts as a specific displacer for BHETBu and the displacer 3-pentanol is specific for BHETPr. BHETBu and BHETPr bands elute more quickly, while at the same time, the specific displacers serve to increase the hydrolyzate concentrations observed and reduce their width by competing for the stationary phase with the analyte. These displacers have no significant effect on the other BHET-alkenes or TDG.

The best percentage of displacer added for BHETBu was found to be 2.0 % (v/v) 2-methyl-3-pentanol and 2.0 % (v/v) of 3-pentanol for BHETPr. It can be seen from **Figure 3.2** and **Figure 3.3** that 2-methyl-3-pentanol, which seems to have high affinity for BHETBu, has a slight effect also on BHETPr. On the other hand, the displacer 3-pentanol, which competes for stationary phase interaction with BHETPr has a slight effect on BHETBu. This suggests that the displacers are not entirely specific to the displaced

hydrolysis products, but the specificity also results from the retention time of the displacers, which are close to the retention time of the analytes.

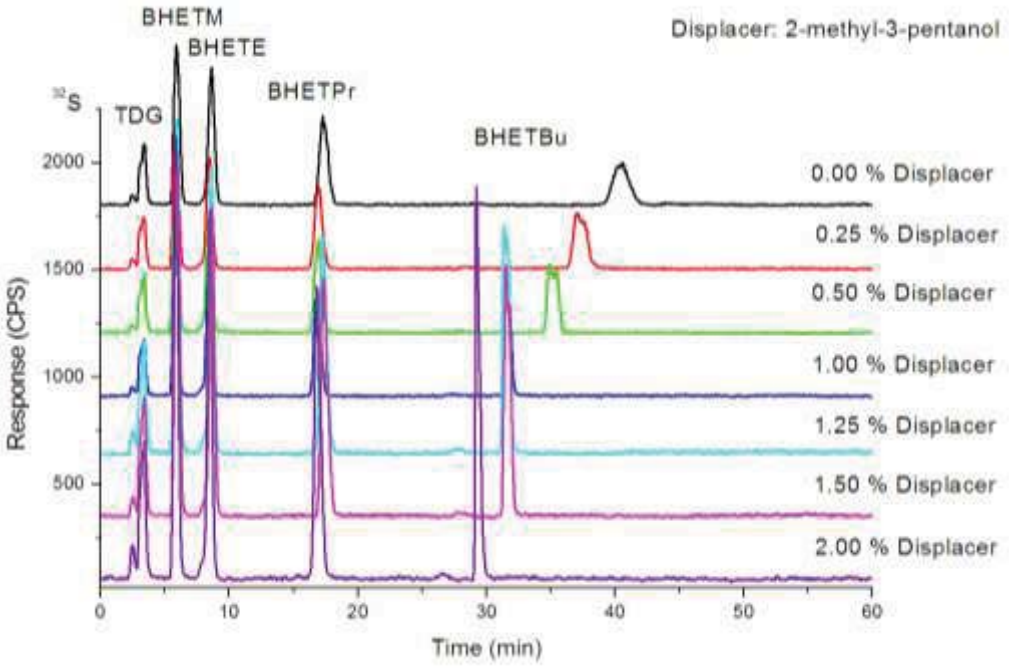

Figure 3.2. HPLC-ICPMS chromatogram. Concentration: 20µL mL^{-1}. Injection volume, 100 µL, 10mM acetate buffer (pH 4.0)-methanol (85:15, v/v). 0%, 0.25%, 0.50%, 1.00%, 1.25%, 1.50%, 2.00% of 2-methyl-3-pentanol. Method 1.

Figure 3.2 shows the addition of only 2-methyl-3-pentanol as a displacer. The retention time decreased from 40.5 min to 29.2 min. The number of plates rose from 5.2 x 10^3 m^{-1} to 43.4 x 10^3 m^{-1} for the BHETBu peak with the peak compression technique, demonstrating a good enhancement in the chromatographic efficiency. It can be seen

that there is almost no effect on TDG and the other BHET-alkenes, except for BHETPr. The effect on BHETPr is about 4 % in retention time decrease with respect to BHETBu.

Addition of both displacers (2.0 % (v/v) 2-methyl-3-pentanol and 0 %, 0.25 %, 0.50 %, 1.00 %, 1.25 %, 1.50 %, 2.00 % (v/v) 3-pentanol) was made to the solution containing a mixture of the hydrolysis products (20 µg mL^{-1} of each standard) as shown in **Figure 3.3.**

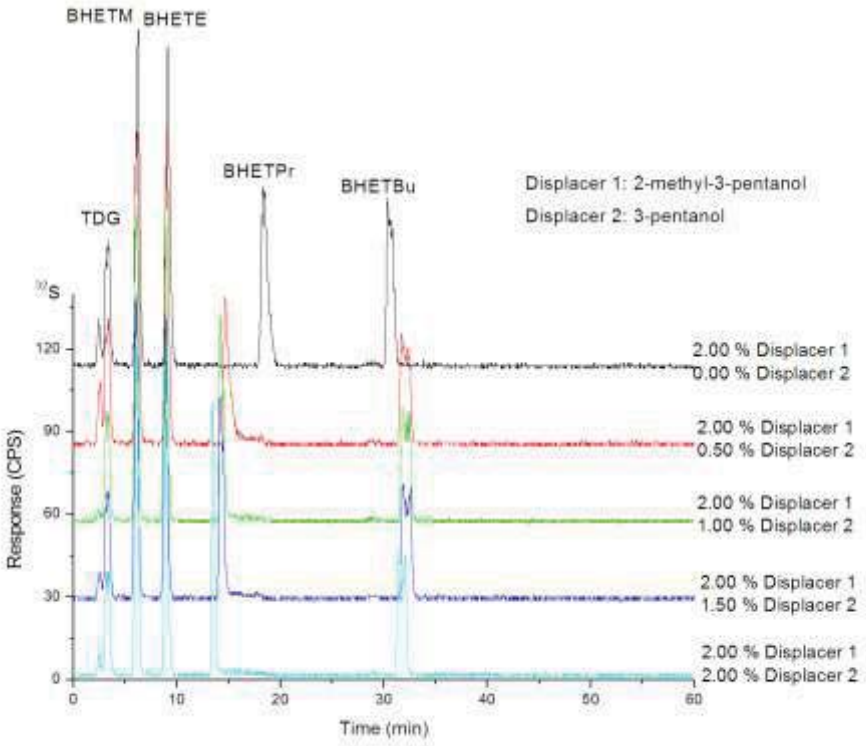

Figure 3.3. HPLC-ICPMS chromatogram of the diluted standards. Concentration: 20 µL mL^{-1}. Injection volume, 100 µL , 10mM acetate buffer (pH 4.0)-methanol (85:15, v/v). 0%, 0.50%, 1.00%, 1.50%, 2.00% 3-pentanol and 2.00% 2-methyl-3-pentanol in every run. Method 1.

The combined effect of these displacers affected the TDG peak and the void volume and a better separation is shown. Since the void volume is likely to relate to free sulfate, it might be due to trace sulfate in the organic displacers, which would be detected by the ICP-MS.

Retention time increases from 29.2 min to 33.3 min as well as decreasing the number of theoretical plates from 9.5 x 10^3 m^{-1} to 7.5 x 10^3 m^{-1} by adding 2.0 % of the specific displacer for BHETPr. The effect of both displacers in the solution had a slightly negative effect on BHETBu, that is its retention time increases of about 2.0 min. The BHETBu peak is more strongly retained. The BHET-alkenes and TDG can now be separated within 34.0 min.

3.5 Method 2

This method uses an Alltima C8 column to produce a better separation between the TDG peak and the void volume peak obtained with the C18 column. Optimization for the best separation was found to be the addition of 2.0 % of the methanol modifier with the same mobile phase used in Method 1, 10 mM acetate buffer, pH 4.0.

The BHET-alkenes are well separated within 52.5 minutes, which results in a longer retention time than Method 1, but the separation between the void volume and the TDG peak is better. This can be explained by the more hydrophobic interaction between the hydrolysis products and the stationary phase using the C8 column.

Two additional displacers over those of Method 1 were tried to improve the separation efficiency: 2,2 dimethyl-3-pentanol and 2,4-dimethyl-3-pentanol. By using 2,2 dimtheyl-3-pentanol the resolution was slightly better, but not significant. However 2,2 dimethyl-3-pentanol was chosen to be the third displacer in the analyte mixture.

By adding the displacers 2-methyl-3-pentanol and 3-pentanol (**Figure 3.4**), it was possible to see how the displacers' effect shifted in comparison to Method 1. 2-methyl-3-pentanol did not affect BHETBu anymore, but BHETPr and 3-pentanol did not affect BHETPr anymore, but BHETE was affected. 2,2 dimethyl-3-pentanol is now the displacer specific for BHETBu. These shifts are due the different stationary phase that mainly differentiates the two methods.

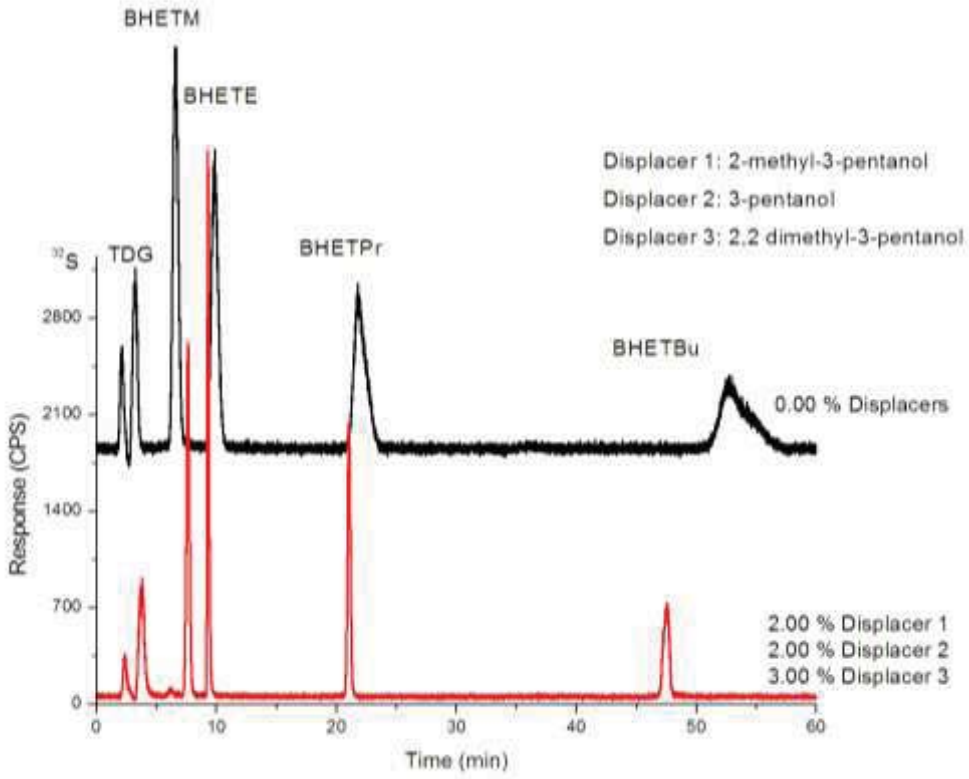

Figure 3.4. HPLC-ICPMS chromatogram of the diluted standard. Concentration: 10µL mL^{-1}. Injection volume, 100 µL, 10mM acetate buffer (pH 4.0)-methanol (98:2, v/v). 2.00% 3-pentanol, 2.00% 2-methyl-3-pentanol and 3.00% 2,2 dimethyl-3-pentanol. Method 2.

Retention time decreased from 52.5 min to 47.0 min. The number of plates increased from 2.6 x 10^3 m^{-1} to 38.9 x 10^3 m^{-1} for BHETBu, from 2.2 x10^3 m^{-1} to 46.3 x 10^3 m^{-1} for BHETPr and from 1.4 x10^3 m^{-1} to 18.9 x 10^3 m^{-1} for BHETE by adding 2.0 % (v/v) of 2-methyl-3-pentanol, 2.0 % (v/v) of 3-pentanol and 3.0 % (v/v) of 2,2 dimethyl-3-pentanol to the warfare agent degradation product mixture.

Retention time decreased 5.7 min for BHETBu, 0.7 min for BHETPr and 0.6 min for BHETE. The addition of the displacers is not a usual way to obtain shorter retention time and a cleaner separation, as can be seen from the increase of number of plates.

3.6 HPLC-ESI-MS separation and detection

To confirm the separation and identity of TDG and the BHET- alkenes, molecular MS detection was performed (**Figure 3.5a-3.5e**) as well as the total ion chromatogram is shown (**Figure 3.5f**). The following compounds in methanol solution were acquired in the positive ion mode by injection using a syringe pump: TDG m/z = 123, BHETM m/z = 169, BHETE m/z = 183, BHETPr m/z = 197 and BHETBu m/z = 211.

As expected, the five hydrolysis degradation products show $[M+H]^+$ ions in their positive ESI mass spectra. BHETE, BHETPr and BHETBu spectra are dominated by the protonated molecular ions and the loss of water $[M+H–H_2O]^+$ and ethanol $[M+H–C_2H_5OH]^+$.

The 1100 HPLC system was then coupled with ESI-MS and the Method 2 separation was performed. The ion chromatogram reconstructed from the mass spectrum confirms retention times and compound identity.

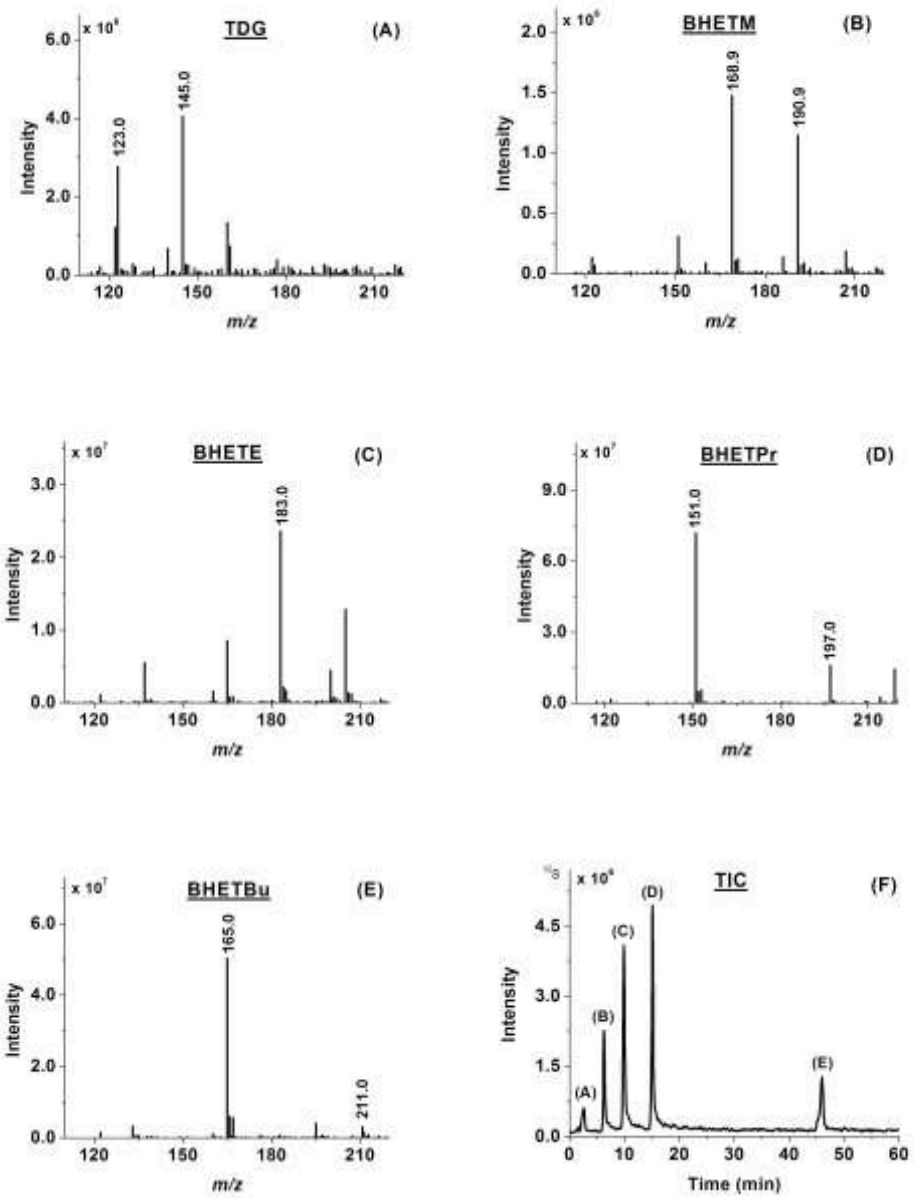

Figure 3.5. Reconstructed electrospray ion chromatograms of the five hydrolysis products: TDG m/z 123 (A), BHETM m/z 169 (B), BHETE m/z 183 (C), BHETPr m/z 197 (D), BHETBu m/z 211(E) and total ion chromatogram accomplished with HPLC-ESI-MS separation Method 2 (F).

3.7 Analytical figures of merit

Calibration curves were prepared from HPLC-ICP-MS experiments through the use of standard mixtures. The concentrations were 1, 5, 10 and 20 μg mL^{-1}. All regression coefficients values, r^2, based on n = 3 (n represents the number of independent analytical replicates) are acceptable with the lowest value being 0.998, except for the TDG peak in Method 1, where r^2 = 0.945. Linearity of the calibration curve has been verified with Mandel's fitting test. Detection limits (3σ) based on three times the standard deviation of seven replicates of the blank areas (IUPAC) for the analysis of the percentage of sulfur present in the compounds TDG, BHETM, BHETE, BHETPr and BHETBu were 4.6, 35.3, 79.3, 98.5 and 73.2 ng mL^{-1}, respectively, for Method 1 and 679.0, 349.9, 261.7, 541.9 and 1255.7 ng $mL,^{-1}$ respectively, for Method 2. The blank was the same matrix in all experimental runs. The large differences in detection limits between the two methods may be associated with S/B for these. These detection limits appear to be lower than the 1 ppm reported from a previous study using displacement chromatography Hooijschuur et al. [7] as summarized in **Table 3.3**. The precision for repeated injections of 10 and 20 μg mL^{-1} standard mixtures were less than 2.0 % for retention times and less than 8.0 % for peak areas. Column recovery was calculated and showed the efficiency to be from 61-85 %. Analytical figures obtained in the ESI-MS analysis are different than those from the ICP-MS due to fragmentation that takes place in the electrospray. Sulfur is more spread out leading to superior detection limits.

Compound / Detection technique	TDG	BHETM	BHETE	BHETPr	BHETBu
LODs previous paper compression technique (ng mL^{-1})	1000	1000	1000	1000	1000
LODs Present work compression technique Method 1 (ng mL^{-1})	4.6	35.5	79.3	98.5	73.2
LODs Present work compression technique Method 2 (ng mL^{-1})	679	350	262	542	1260
QLs Present work complex matrix (river water) (ng mL^{-1})	750	690	1000	1160	3300

Table 3.3. Detection limits and quantifiable limits of previous paper[7] and present work.

3.8 Complex samples

Both methods were applied to real world samples. Investigation was made on samples collected from the Little Miami (Ohio) River water. Samples were spiked with the five sulfur mustard hydrolysis degradation products and treated with the same procedure described in Experimental section. **Figure 3.6** shows the separation of the mustard gas hydrolysis degradation products by applying Method 1. The actual quantifiable limits calculated were: TDG 750 ng mL^{-1}, BHETM 690 ng mL^{-1}, BHETE 1000 ng mL^{-1}, BHETPr 1160 ng mL^{-1} and BHETBu 3300 ng mL^{-1}.

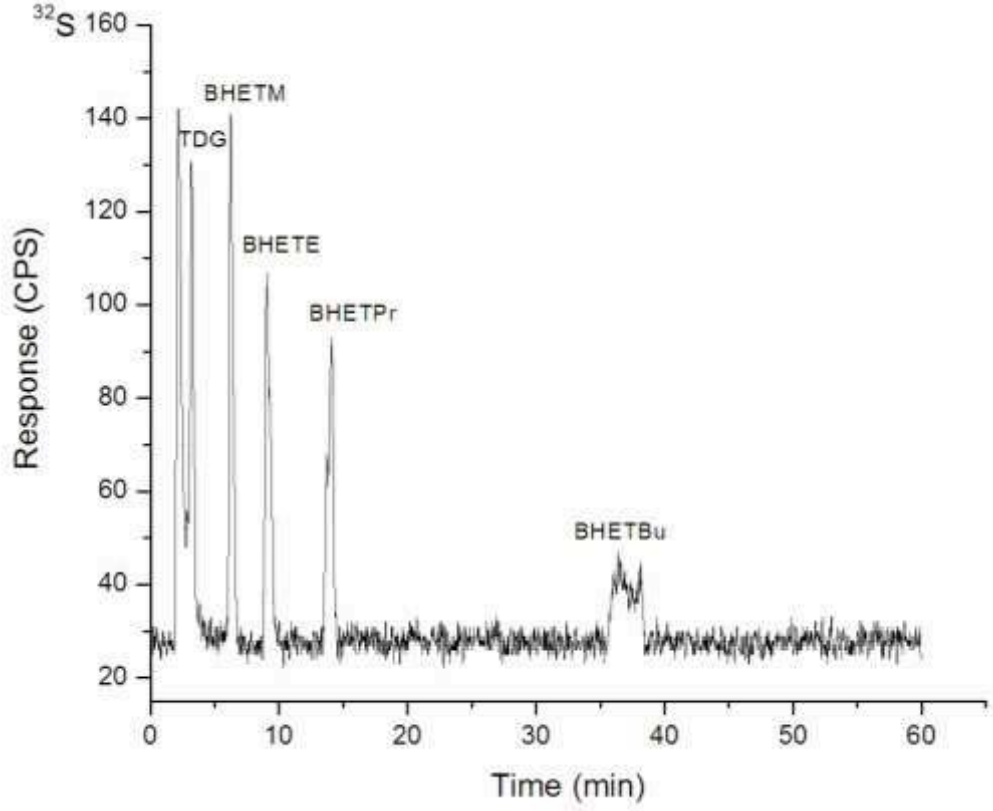

Figure 3.6. HPLC-ICPMS chromatogram of the five hydrolysis products spiked into Little Miami River (OH) water. Concentration: 10µL mL^{-1}. Injection volume, 100 µL, 10mM acetate buffer (pH 4.0)-methanol (85:5, v/v). 2.00% (v/v) 3-pentanol, 2.00% (v/v) 2-methyl-3-pentanol.

Column recovery was 75% by applying Method 1 and 81% with Method 2. It is interesting to see how the separation of the degradation products is still possible even by applying the method with the lowest signal response. All methods were applied to

the real world sample showing successful separation, even if the noise level is relatively high in complex samples as shown in **Figure 3.6**.

3.9. Conclusions

RP-HPLC coupled with ICP-MS, presents a selective and rapid procedure for the separation of sulfur mustard hydrolysis products TDG, BHETM, BHETE, BHETPr and BHETBu. The effect of peak compression by displacement chromatography can lower the retention time and at the same time can lead to high sensitivity and low detection limits. The decrease of retention time was 11.3 min with Method 1 and 5.5 min for Method 2, relative to the experiments without any use of displacers as shown in Figure 2 and 4. Detection limits were in the ng mL^{-1} range for all five hydrolysis degradation products. The use of displacers showed an increase of number of plates for each separation. Separation confirmation was successfully provided by HPLC-ESI-MS. To date this is the first study utilizing HPLC-ICP-MS for the analysis of sulfur mustard hydrolysis products. All compounds were identified by their protonated molecular ions and separation was similar to those for RP-HPLC-ICP-MS.

3.10 References

(1) Bruce D. Quimby, M. S. *Agilent Technologies* **2003**.
(2) Agency, U. S. B. o. A. C. a. D., Washington DC **1997**.
(3) L. Perharic Walton, R. L. M., V.S.G. Murray, IPCS Inchem, **1996**.
(4) (ATSDR), A. f. T. S. a. D. R.: Atlanta, GA, **2001**; Vol. Volumes 1, 2, 3.
(5) Takeshima, Y., et al. *Carcinogenesis* **1994**, *15*, 2075-2079.
(6) Advanced Chemistry Development; Solaris, S. V. f., Ed.; ACD/Labs, **1994-2008**.
(7) Hooijschuur, E. W. J. K., Charles E.; Hulst, Albert G.; Brinkman, Udo A. Th., *Analytical Chemistry* **2000**, *72*, 1199-1206.
(8) Colin F. Poole *The Essence of Chromatography*, **2002**.
(9) V. V. S. Lakshmi, M. R. V. S. M., T. Jagadeshwar Reddy, M. Ravikumar, S. Prabhakarand M. Vairamani, *Rapid Commun. Mass Spectrom* **2006**, *20*, 981–986.
(10) Douglas D. Richardson, B. B. S., Joseph Caruso, *J. Anal. At. Spectrom.* **2006**, *21*, 396-403.
(11) Douglas D. Richardson, S. S. K., Rodolfo G. Wuilloud, Joseph A. Caruso, *Analytical Chemistry* **2004**, 76, 7137-7142.

Chapter 4

Review of analytical techniques to detect CWADPs (nerve agents, mustard agents, sternutator agents)

Reproduced from Karolin K. Kroening, Douglas D. Richardson, Kevin M. Kubachka, Joseph A. Caruso. Chemical Warfare Nerve Agents - Analyzing Their Degradation Products. *Spectroscopy,* **2008**; 23(9): 68-73**.**

4.1 Abstract

America's security has become the top priority of the government at every level, especially in view of worldwide terrorist activity and the continuing threat of chemical warfare agents. Research regarding detection of these agents has become vital for finding solutions that will help make government action timely and effective. A class of nerve agents, organophosphorus agents, typically hydrolyze readily to presumably less toxic degradation products and can be analyzed by collision cell inductively coupled plasma-mass spectrometry (ICP-MS) for phosphorus at its only natural isotope of *m/z* 31.

4.2 Introduction

In a 1995 incident, members of Aum Shinrikyo released sarin (GB) at a Tokyo subway, killing 12 people and injuring many more.[1] Due to this and other more recent activities, the threat of terrorists acquiring and using chemical warfare agents (CWAs) is of extreme importance. Also, current stockpiles of CWAs must be monitored to ensure their safe storage and disposal. The remediation of sites containing abandoned CWAs in the world requires analysis in support of safe removal and destruction of agents. So the need for methods able to accurately analyze those agents with lowest levels of detection possible is desirable; therefore, ^{31}P detection with ICP-MS is highlighted here.

The Chemical Weapons Convention (CWC), which came into effect on April 29, 1997, bans the production, acquisition, and direct or indirect transfer of chemical weapons, and also mandates the destruction of all chemical weapons held in reserve by member states.[2] A United Nations

report from 1969 defines chemical warfare agents as "chemical substances, whether gaseous, liquid or solid, which might be employed because of their direct toxic effects on man, animals and plants".[3] Chemical warfare agents can be classified as lethal agents; blood agents (cyanogens chloride), blister agents (sulfur mustard gas), nerve agents (tabun, sarin), pulmonary agents (chlorine), and nonlethal agents: incapacitating agents (Agent 15) and riot-control agents (pepper spray). Of these, nerve agents are the most notorious. These agents are a class of phosphorus-containing organic chemicals (organophosphates) that bind in blood primarily and extremely rapidly to the enzymes acetyl- and butyrylcholinesterase.[4] There are two main classes of nerve agents based upon alkylphosphonic acid esters. The members of the two classes share similar properties and both are given a common name (such as sarin), and a two-character NATO identifier (such as GB for sarin).

G-Series. The G-series is thus named because German scientists first synthesized them. All of the compounds in this class were discovered and synthesized during or soon after World War II.

V-Series. The V-series is the second family of nerve agents (the *V* apparently standing for "venomous")> and contains four members: VE, VG, VM, and VX. The most studied agent in this family is the VX.[4] As G-type and V-type agents enter the environment, they hydrolyze rapidly into their degradation products (CWADPs), specifically into organophosphorus acid degradation products, which generally are thought to be less toxic (**Figure 4.1**).[5]

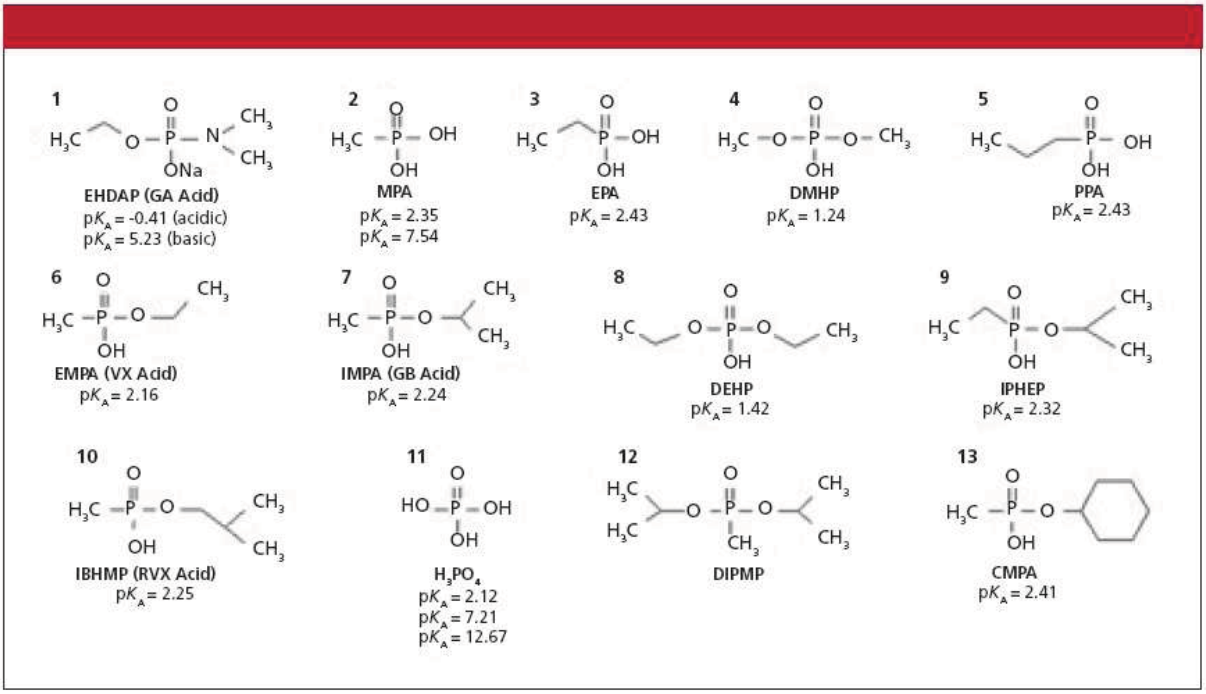

Figure 4.1. Structures and p*K*a values of CWADPs analyzed. $H_2PO_4^-$ is the last breakdown product of many CWAs but is considered an interference in this study because it is prevalent in many common sample matrices.[5]

Although the toxicities of CWADPs are thought to be significantly lower than their parent agents, the exact health risk is relatively unknown.[6] The large number of possible CWADPs leads to the incomplete knowledge regarding toxicity. Phosphorus-containing nerve agents along with their degradation products present difficulties for ultratrace analysis due to their high polarity, extremely low (or lack) of volatility for the degradation products, and lack of a good chromophore. Previous studies have successfully utilized methods such as gas chromatography-mass spectrometry (GC-MS), ion mobility-mass spectrometry (IM-MS), and liquid

chromatography- mass spectrometry (LC-MS) for the analysis of organophosphoms-containing degradation products with detection limits in the nanograms-per-milliliter range.[7-10]

GC with various detection methods such as atomic emission detection[11,12], flame photometric detection[13], inductively coupled plasma-mass spectrometry (ICP-MS)[14], MS [15-18],and tandem MS [19,20] has been employed for analysis of CWADPs. The low volatility of CWADPs requires them to be derivatized for GC separation analysis, and divalent metals can cause interferences with derivatization steps. [16] LC-MS and LC-MS-MS are commonly used techniques for the detection of CWADPs because of their selectivity, sensitivity, and structural identification capabilities. However, ionization involving conventional MS sources such as atmospheric pressure chemical ionization (APCI) or electrospray ionization (ESI) can pose difficulties from the constituents of various mobile phases and extraneous sample matrix components. [21]

Considering the lethal doses of the degradation products, lower detection limits require a more selective analytical detection technique such as ICP-MS. Also, for the most part, ICP-MS is more tolerant of difficult matrices, and can be used with mobile phases not suitable for APCI or ESI-MS.[22]

ICP-MS is an element-specific detection technique capable of qualitative and quantitative determination. It has a large dynamic range, high sensitivity, low detection levels (often at low to sub part per- trillion levels for some analytes), and it is interfaced easily with LC. Elemental speciation analysis by ICP-MS allows for high sensitivity, low level detection, and elemental selectivity, making it an excellent choice for ultratrace elemental speciation studies. [23-25]

Phosphorus (m/z = 31) analysis by ICP-MS was limited for many years due to its high first ionization potential (10.5 eV) and due to the polyatomic interferences such as $^{14}N^{16}O^{1}H^{+}$ and $^{15}N\ ^{16}O^{+}$ (m/z - 31). Since about the turn of the century, there have been major technological advancements with the application of collision-reaction cells to ICPMS with various gases for collision, reaction, or energy discrimination. This enhancement allows for the analysis of elements prone to isobaric and polyatomic interferences. Though ICP-MS can detect ^{31}P specifically in complicated matrices, its inability to differentiate various compounds containing naturally occurring ^{31}P requires Chromatographic separation before detection. Reversed phase ion-pairing chromatography, coupled to ICP MS, represents a detection method for the analysis of organophosphorus degradation products of nerve agents. Both GC and LC separation methods are highlighted.

4.3 LC with ICP-MS Detection

4.3.1 Project 1

This study [23] has provided details of the detection of organophosphorus degradation products of sarin (GB) and VX. In this work, the coupling of ion-pairing reversed-phase high performance liquid chromatography (HPLC) with ICP-MS, equipped with a collision- reaction cell allowed for trace analysis of three organophosphorus chemical warfare degradation products: methylphosphonic acid (MPA, degradation product of VX and sarin), ethyl methylphosphonic acid (EMPA, degradation product of VX), and isopropyl methylphosphonic acid (IMPA, degradation product of sarin). Due to the charged nature of the compounds of interest, ion-

pairing chromatography was investigated as the chromatographic separation technique. The acid dissociation constants for the chemical warfare degradation products are as follows: MPA pKa_1 2.41, pKa_2 7.54; EMPA, pKa 2.16; IMPA pKa 2.24. This information was used to select the buffer system. Myristyl trimethylammonium bromide (TTAB), consisting of an intermediate length alkyl chain, along with an ammonium acetate-acetic acid buffer (pH 4.85) and 2% (v/v) methanol for the mobile phase, allowed separation of methylphosphonic acid, ethyl methylphosphonic acid, and isopropyl methyl phosphonic acid with the selected column (150 mm x 3.2 mm, 5-μm Alltima C8, Grace Davison Discovery Sciences, Deerfield, Illinois) in less than 15 min (**Figure 4.2**). Some comparative data, available at the time of this study, are summarized in **Table 4.1** and illustrate the excellent compound detection limits with ^{31}P selective detection.

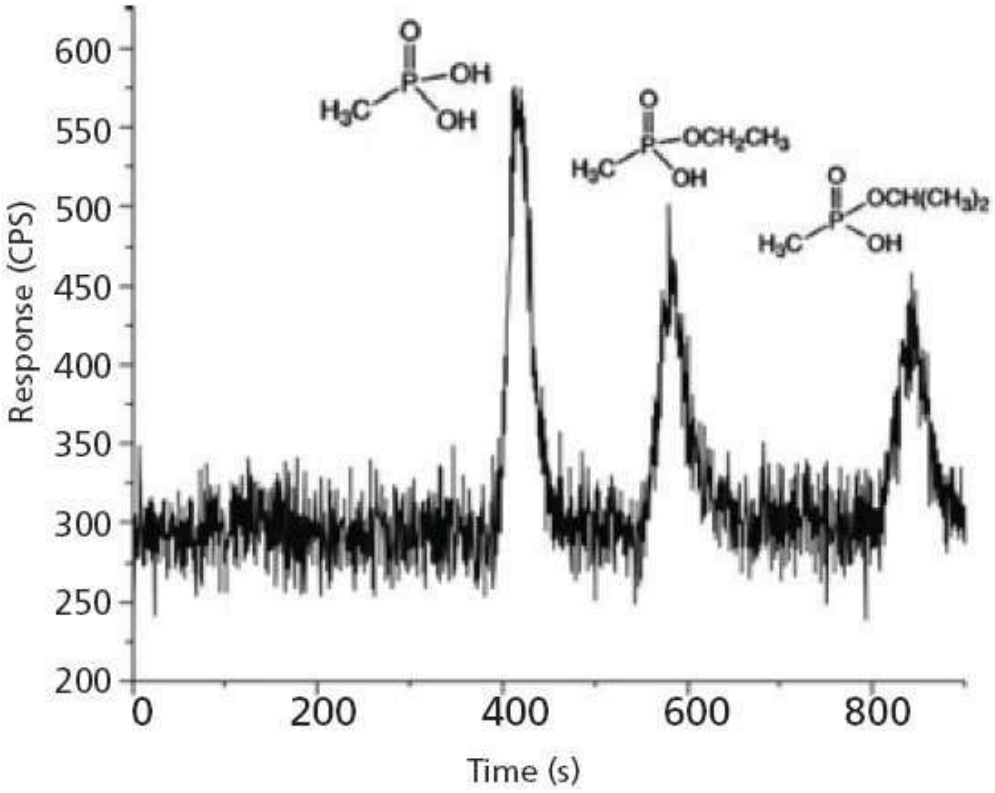

Figure 4.2. Separation of a 100-ng/mL mixture of MPA, EMPA, and IMPA.

Table I: Figures of merit comparison table for three degradation products

Chemical warfare degradation product	Detection limit/pg mL	Column recovery	RDS (%) peak area	RSD (%) retention time
MPA	140	86.2	2.75	0.38
EMPA	260	69.2	5.39	0.55
IMPA	180	73.0	5.96	0.65

J. Anal. At. Spectrom. **21**, 396–403 (2006). Reproduced by permission of The Royal Society of Chemistry.

Table 4.1. Figures of merit comparison table for three degradation products.

Complex samples of the Little Miami River (Ohio) water, tap water, topsoil, and potting soil samples were analyzed. Although good results were obtained, phosphate interference was associated with the EMPA retention time. This resulted in continuing the study, investigating four methods with ion exchange chromatography coupled to ICP-MS.[5]

4.3.2 Project 2

Four separation methods for the determination of CWADPs using LC-ICPMS were developed. The best separation was able to separate 10 CWADPs (MPA, EMPA, dimethyl hydrogen phosphate [DMHP], diethyl hydrogen phosphate (DEHP), ethyl hydrogen dimethylamidophosphate sodium salt [EHDAP], isopropyl methylphosphonic acid [IMPA], isopropyl hydrogen ethylphosphonate [IPHEP], isobutyl hydrogen methylphosphonate (IBHMPj, ethylphosphonic acid [EPA], and propylphosphonic acid [PPA]) in the presence of $H_2PO_4^-$. It had the best tolerance for $H_2PO_4^-$ and is applicable to several matrices. In previous studies [26,27] authors discussed conditions under which MPA could be separated from $H_2PO_4^-$ using flame photometric detection (FPD) for detection and concluded that a gradient separation was needed in which 70% methanol must be used. Unfortunately, this compromises or extinguishes the plasma using standard-bore columns and standard nebulizers. By adjusting the mobile phases and PRP X-100 ion-exchange column (Hamilton Company, Reno, Nevada) dimensions, a gradient utilizing various levels of formic acid, methanol, and ammonium format was developed, resulting in the separation shown in **Figure 4.3** with figures of merit that address reproducibility and detection limits (calculated as recommended by IUPAC, 3σ of integrated

peak area of seven blanks divided by the slope of the calibration curve) displayed in **Table 4.2**.[5] The chromatogram in Figure 3 illustrates the separation possibilities for nine degradation products.

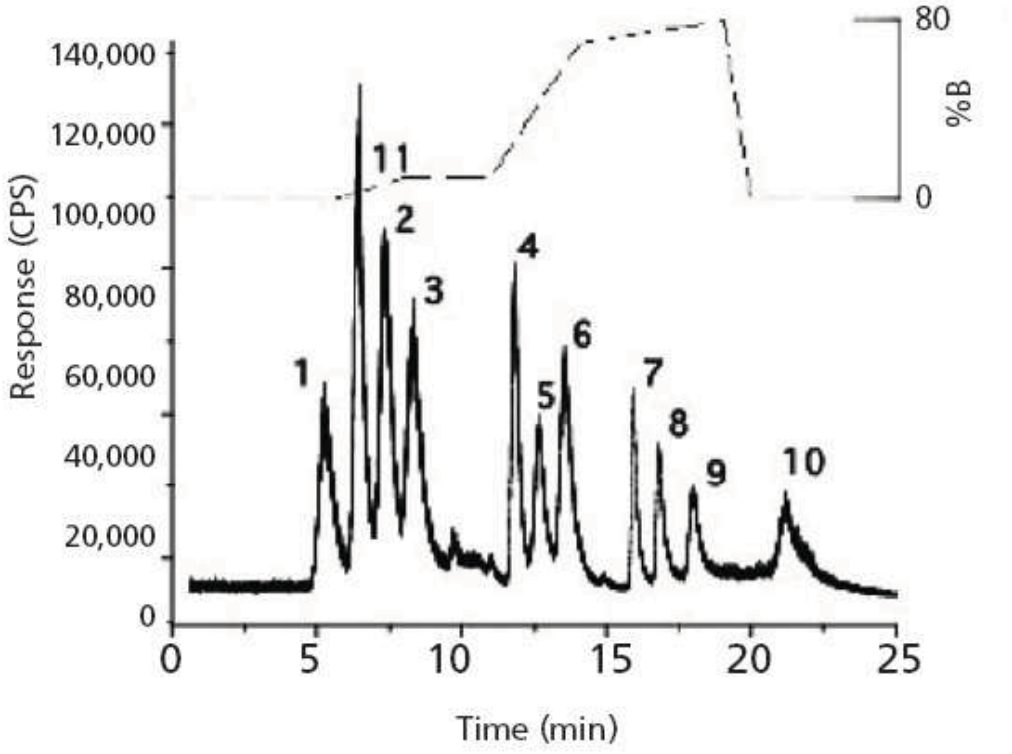

Figure 4.3. LC–ICP-MS chromatogram of CWADPs mixture including $H_2PO_4^-$ in distilled deionized water at a concentration of 10 μg/mL for each analyte. Dashed line represents the gradient program. Peaks: 1 = EHDAP (GA acid), 2 = MPA, 3 = EPA, 4 = DMHP, 5 = PPA, 6 = EMPA (VX acid), 7 = IMPA (GB acid), 8 = DEHP, 9 = IPHEP, 10 = IBHMP (RVX acid), 11 = H_3PO_4.

Table II: Figures of merit for the separation method of 10 CWADPs using ICP-MS for detection, based on 250 ng/mL CWADPs mixture			
CWADPS	RSD (%) retention time	RSD (%) peak area	Detection limit ng of standard mL
EHDAP	0.6	2.5	21.7
MPA	0.3	4.1	18.3
EPA	0.4	8.1	19.9
DMHP	0.3	2.5	10.0
PPA	0.4	7.1	22.9
EMPA	0.6	3.3	20.4
IMPA	0.1	6.6	19.5
DEHP	0.1	11.5	26.6
IPHEP	0.1	3.4	61.5
IBHMP	0.3	16.1	81.1

Table 4.2. Figures of merit for the separation method of 10 CWADPs using ICP-MS for detection, based on 250 ng/mL CWADPs mixture.

Applications were made by analyzing tap water, bottled water, grape juice, apple juice, soda, and sport drinks. Beverages that had a high level of $H_2PO_4^-$ showed overlap with the EPA peak. But highly positive results show the separation of EMPA, IMPA, and MPA from sarin and VX, the most widely discussed CWAs, to be separated completely from the phosphate interference, as shown in **Figure 4.4**.

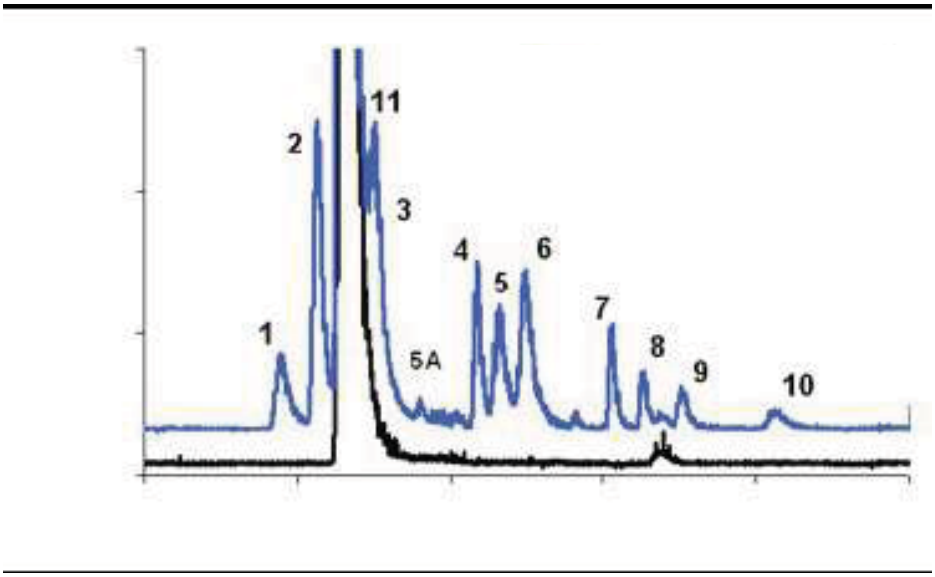

Figure 4.4. LC–ICP-MS chromatogram of diluted lettuce extract unspiked (blue trace) and spiked with 1 µg/mL of CWADPs 2–10 (black trace). Peaks: 1 = EHDAP (GA acid), 2 = MPA, 3 = EPA, 4 = DMHP, 5 = PPA, 6 = EMPA (VX acid), 7 = IMPA (GB acid), 8 = DEHP, 9 = IPHEP, 10 = IBHMP (RVX acid), 11 = H_3PO_4.

Analysis was attempted for a sample of infant formula, which has a high number of interferences (in addition to $H_2PO_4^-$), but only six (MPA, DMHP, EMPA, DEHP, IPHEP, and IBHMP) of the spiked standards could be identified due to the high background of the blank infant formula. Detection limits were lower than or comparable to the majority of currently published LC methods and easily meet the required limits of detection of 1 mg/mL for the OPCW tests.[5]

4.4 GC with ICP-MS Detection

GC-ICP-MS is an excellent method to detect organophosphorus nerve agent degradation products, providing that volatile derivatives are attainable.[14] This work analyzed several organophosphorus nerve agent degradation products, alone or in the presence of mixtures of common organophosphorus pesticides (OPPs). OPPs are the most widely used type of chemical for insecticides, herbicides, and fungicide applications. [28-32] Due to the extensive use of these OPPs as agricultural products, their presence has been detected in ground waters, drinking waters, fruits, and vegetables.[28,30,33] Because of this high environmental presence, OPPs must be considered as possible interfering species for the analysis of organophosphorus nerve agent degradation products. The first degradation products of sarin (isopropyl methylphosphonic acid, GB acid), cyclo-sarin (cyclohexyl methylphosphonic acid, GF acid), and soman (pinacolyl methylphosphonic acid), as well as their common final hydrolysis product, MPA, were utilized throughout these experiments. Due to the nonvolatile nature of these alkyl phosphonic acid degradation products, derivatization was performed to generate the volatile *tert*-butyl dimethylsilyl (TBDMS) species.[22]

Degraded organophosphorus pesticide standards were obtained for acephate, chlorpyrifos, dichlorvos, ethion, and parathion ethyl. Mixtures consisting of three pesticides in the presence of a single nerve agent degradation product were prepared. GC-ICP-MS allowed for the separation and detection of all four degradation products in the presence of pesticide mixtures in just over 12 min. Elemental speciation with GC-ICPMS requires high chromatographic

resolution to ensure that no interfering species overlap the degradation product standards, leading to false positives. **Figure 4.5** shows the analysis of the final hydrolysis product.

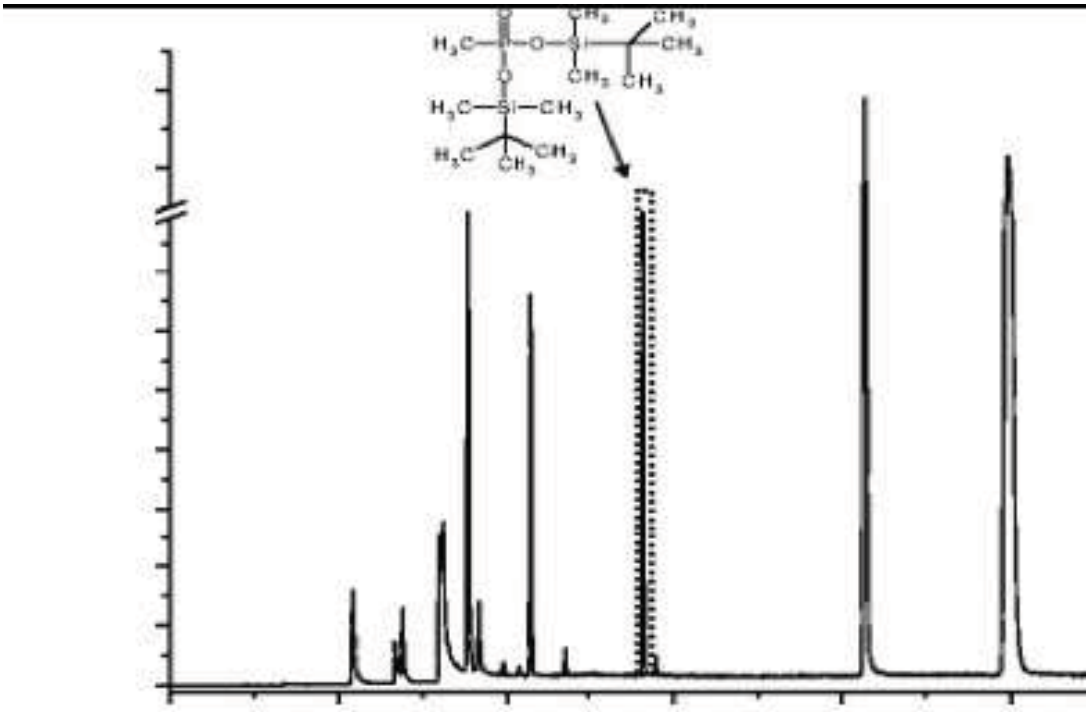

Figure 4.5. GC-ICP-MS analysis of 5 ng of methylphosphonic acid-TBDMS in a mixture with 25 ng of acephate, ethion and chlorpyrifos.

MPA TBDMS, in the presence of a concentration of acephate, ethion, and chlorpyrifos that was five times higher. MPA typically is used to verify release of all organophosphorus nerve agents. As a result of the highly specific hydrolysis pathway, it also is predicted that MPA will be present at higher concentrations relative to the other alkyl phosphonic acid degradation products following release into the environment. Other separations were obtained by successfully separating IMPA-TBDMS (sarin, GB acid) in the presence of a concentration of dichlorvos,

ethion, and parathion ethyl pesticides that was 10 times higher. It was possible to outline specific peak to IMPA-TBDMS among multiple phosphorus-containing peaks corresponding to various hydrolysis products of the three pesticides. Similar results were obtained for CMPA and PMPA-TBDMS (cyclosarin-GF acid and soman) derivatives in the presence of pesticide mixtures. Parent pesticide peaks are still observed at the longer retention times; however, due to the age and storage of the standards, degradation would be expected. This is the first study analyzing pesticides as interfering species for analysis of nerve agent degradation products by GC-ICP-MS.

4.5. References

(1) K. Miyaki, Y. Nishiwaki, K. Maekawa, Y. Ogawa, N. Asukai, K. Yoshimura, N. Etoh, Y. Matsumoto, Y. Kikuchi, N. Kumagai, and K. Omae, *J. Occup. Health* 47, 299–304 (**2005**).
(2) OPCW, Washington D.C., April 29, 1997; United States Bureau of Arms Control and Disarmament Agency.
(3) Foreign Relations, 1969-1976-, Volume E-2, Documents on Arm Control. **1969-1972**.
(4) Markku Mesilaakso, Chemical Weapons Convention Chemicals Analysis, Editor Wiley. 11, 250, 275 (**2005**).
(5) Kevin M. Kubachka, Ph.D. dissertation, Elemental speciation analysis of arsenic, selenium and phosphorus: exploring foods and plants, Chapter 5, University of Cincinnati, **2007**.
(6) "Review of the U.S. Army Proposal for the Off-Site Treatment and disposal of Caustic VX Hydolysate from Newport
(7) Chemical Agent Disposal Facility," Department of Health and Human Services: Centers for Disease Control and Prevention, **2005**.
(8) W.E. Steiner, B.H. Clowers, L.M. Matz, W.F. Siems, and H.H. Hill, Jr., *Anal. Chem*. 74, 4343–4352 (**2002**).
(9) J.R. Smith and M.L. Shih, *J. Appl. Toxicol*. 21, S27–S34 (**2001**).
(10) R.M. Black and R.W. Read, *J. Chromatogr., A* 794, 233–244 (**1998**).
(11) A.B. Kanu, P.E. Haigh, and H.H. Hill, *Anal. Chim. Acta* 553(1–2), 148–159 (**2005**).
(12) P.A. D'Agostino, J.R. Hancock, C.L. Chenier, and C.R.J. Lepage, *J. Chromatogr., A* 1110, 86–94 (**2006**).
(13) W.R. Creasy, A.A. Rodriguez, J.R. Stuff, and R.W. Warren, *J. Chromatogr., A* 709, 333–344 (**1995**).
(14) D.D. Richardson and J.A. Caruso, *Anal. Bioanal. Chem*. 388, 809–823 (**2007**).
(15) S.V. Vasilevskii, A.F. Kireev, I.V. Rybal'chenko, and V.N. Suvorkin, *J. Anal. Chem*. 57, 491–497 (**2002**).
(16) M. Kataoka, N. Tsunoda, H. Ohta, K. Tsuge, H. Takesako, and Y. Seto, *J. Chromatogr., A* 824, 211–221 (**1998**).
(17) H. Gu, L. Zhou, G. Cai, and Y. Zhong, *Sepu* 14, 41–44 (**1996**).
(18) Cai, G.; Gu, H.; Zhou, L.; Qu, G.; Zhong, Y. Fenxi Huaxue, 24, 886-889 (**1996**).
(19) M.-I. Lei, H.-I. Xi, D.-N. Xu, and Z.-S. Chen, *J. Mass Spectrom.* 41, 1453–1458 (**2006**).
(20) J. Riches, I. Morton, R.W. Read, and R.M. Black, *J. Chromatogr., B: Anal. Technol. Biomed. Life Sci*. 816, 251–258 (**2005**).
(21) M.Kataoka, N. Tsunoda, H. Ohta, K. Tsuge, H. Takesako, and Y. Seto, *J. Chromatogr., A* 824, 211–221 (**1998**).
(22) P.A. D'Agostinoand C.L. Chenier, "Analysis of Chemical Warfare Agents: General Overview, LC-MS Review, In- House LC-ESI-MS Methods and Open Literature Biography," Defence Research and Development Canada, **2006**.
(23) D.D. Richarson and J.A. Caruso, *Anal. Bioanal. Chem*. 389, 679–682 (**2007**).
(24) D.D. Richardson, B.B.M. Sadi, and J.A. Caruso, *J. Anal. At. Spectrom*. 21, 396–403 (**2006**).

(25) P. Leonhard, R. Pepelnik, A. Prange, N. Yamada, and T. Yamada, *J. Anal. At. Spectrom*. 17, 189–196 (**2002**).
(26) E.W.J. Hooijschuur, C.E. Kientz, and U.A.T. Brinkman, *J. Chromatogr., A* 928, 187–199 (**2001**).
(27) C.E. Kientz, A. Verweij, G.J. de Jong, and U.A. Brinkman, *J. Microcolumn Sep*. 4, 477–483 (**1993**).
(28) A.P. Vonderheide, J. Meija, M. Montes-Bayon, J.A. Caruso, J. Anal. At. Spectrom., 18, 1097-1102 (**2003**).
(29) R.G. Wuillod, M. Shah, S.S. Kannamkumarath, J.C. Altamirano, Electrophoresis, 26, 1598-1605 (**2005**).
(30) N. Fidalgo-Used, M. Montes-Bavon, E. Blanco-Gonzales, A. Sanz-Mendel, J. Anal. At. Spectrom., 20, 876-882 (**2005**).
(31) S.O. Pehkonen, Q. Zhang, Crit. Rev. Environ. Sci. Technol., 32, 17-72 (**2002**).
(32) S.A. Lacorte, S.B. Lartiges, P. Garrigues, D. Barcelo, Environ. Sci. Technol. 29, 431-438 (**1995**).
(33) D. Proefrock, P. Leonhard, S. Wilbur, A. Prange, J. Anal. At. Spectrom., 19, 623-631 (**2004**).

Chapter 5

CWADPs containing As, P and S simultaneous detection as oxides HPLC-ICPMS

5.1 Introduction

Chemical warfare agents (CWAs) belong not only to the past, but they still represent a problem from a terrorist threat point of view as well as environmental concerns.

Chemical warfare agents can be divided in several classes, but three types of chemical warfare agents represent the majority of environmental related problems. They can be divided as:[1]

- **Nerve agents**: class of organophosphates that disrupt the mechanism by which nerves transfer messages to organs. (GX, Sarin)
- **Blister agents**: strong vesicants, resulting in severe skin blistering as well as eye and lung lesions upon exposure. (Mustard gas)
- **Sternutator agents:** mixture of gases used as "mask breakers" in WW I and II, causing prolonged systematic effects, such as headache, vomiting and abdominal cramps. (Clark I, Clark II, known as "Blue Cross")

5.2 Environmental concerns

Chemical warfare agents were produced in enormous amounts in the past 100 years and their disposal is very expensive. A safe disposal procedure requires secure "packaging", appropriate handling with safety precautions and from experts, careful transportation of hazardous material with many document requests etc[2]. As it can be seen, the cost of their disposal is sky-high.

Unfortunately some governments have found as means of disposal, discarding CWAs into the environment, and more often it can be found in the sea instead of in the soil. **Figure 5.1** represents a map of known dumpsites, it is a US Army report reporting sites containing CWAs in the sea water in the Atlantic Ocean. [3]

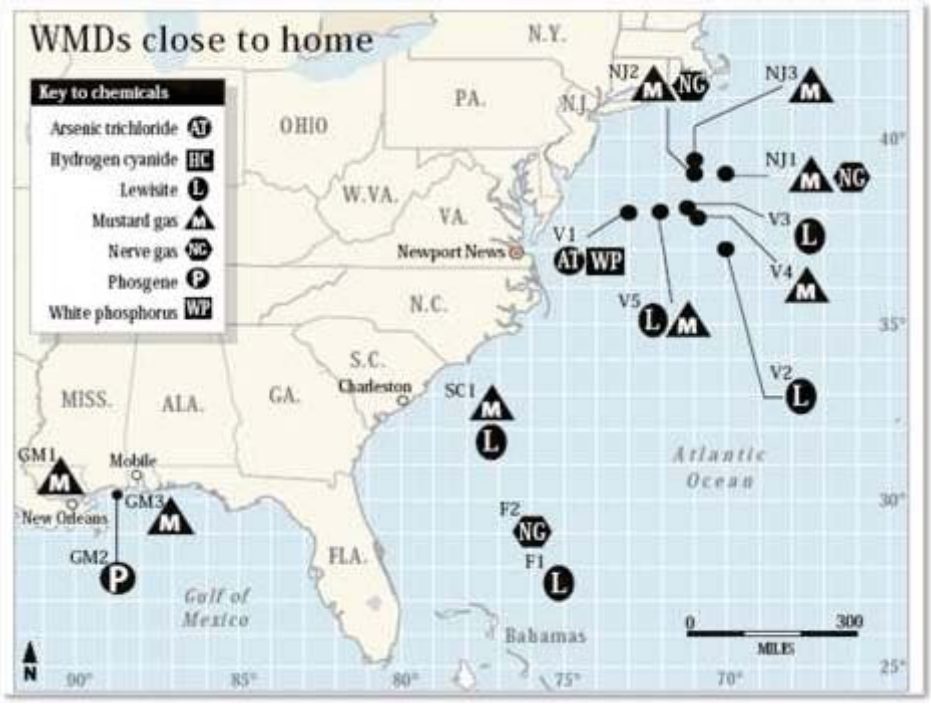

Figure 5.1. Known dumpsites in the Atlantic Ocean, U.S. Army reports (2005)[3]

These dumpsites are close to the United States, however worldwide episodes of contamination from CWA pollution is known. One example is in Bari, Italy, where fishermen have been exposed to shells containing mustard gas from a bombardment on Bari's harbor during World War II. Those shells have been lying in the sea for over 40 years and still were able to produce burns and almost fatal consequences.[4]

A further example can be reported in Kamisu City, Japan, where a drinking water contamination damaged the health of more than 200 people. The speculation is that arsenic containing CWAs were buried underneath the soil close to Kamisu City [5]and once they started degrading due to certain environmental conditions, they contaminated the drinking water that was for the citizens common use. These and many more health concerns related to CWAs in the environment are a good *raison d'être* to develop methods that allow detection of CWAs at the lowest levels possible.

5.3 Chemical warfare agent degradation products

Not only are the above mentioned parent agents important to be identified, but their degradation products as well, because they also have toxicity concerns. [6] Many of the nerve agents, mustard gas agents and sternutator agents produce chemical warfare agent degradation products (CWADPs), especially after their disposal in an aquatic environment. Most of these parent agents undergo hydrolysis, giving birth to CWADPs whose toxicity can be alarming [7] as shown in **Table 5.1**, even if their toxicity is lower than the original CWA, However, this may not always be the case and concentrations, exposure times, cell uptake effectiveness, etc. will have a major influence, mandating their detection as well.

Type	CWA	Active component	CWADPs
Nerve Agent	GX, GB (Sarin), VE, VG, VM, VX	Alkylphosphonic acid esters	• MPA - $CH_3P(O)(OH)_2$ • IMPA (GB acid) - $CH_3P(O)(OH)(C_3H_7O)$ • EMPA (VX acid) - $CH_3P(O)(OH)(C_2H_5O)$
Blister Agent	Mustard gas	2,2-dichlorodiethyl sulfide $(CLCH_2CH_2)_2S$	• TDG - $(HOCH_2CH_2)_2S$ • BHET-alkenes - $(CH_2)n$ $(S\text{-}CH_2\text{-}CH_2\text{-}OH)_2$
Sternutator Agent	Blue Cross	DA, diphenylchloroarsine $(Ph)_2AsCl$, DC diphenylcyanoarsine $(Ph)_2AsCN$	• PAO - PhAsO • PAA - $PhAs(O)(OH)_2$ • DPAA - $(Ph)_2As(O)(OH)$ Byproducts • TPA - $(Ph_3)As$ • TPAO - $(Ph_3)AsO$

Table 5.1. Common to these CWAs is their rapid breakdown to much longer lived degradation products listed in the table.

When a small sample of soil or water is given for analysis, it is important to identify low levels (down to parts per trillion range) of these compounds and a fast detection technique is needed. Low levels can be identified by hyphenated techniques as chromatography coupled to inductively coupled plasma mass spectrometry (ICP-MS).

5.4 Instrumental conditions

The aforementioned chemical warfare agents contain a heteroatom identifiable with the ICP-MS instrumentation. Nerve agents contain phosphorus, that can be detected by the ICP-MS using helium as collision reaction gas for minimizing interferences on ^{31}P. Mustard agents

contain sulfur, ^{32}S. Xenon can be used in the octopole reaction cell in order to reduce polyatomic interferences that might take place to detect low levels of sulfur. ^{75}As is the heteroatom of the sternutator agents Clark I and Clark II, and the use of helium or hydrogen can lower the interferences and thereby optimized the arsenic signal. In **Table 5.2**, some common polyatomic interferences of P, S and As are listed.

Polyatomic Interference	Element
$^{14}N^{16}O^{1}H^{+}$, $^{15}N^{16}O^{+}$	^{31}P
^{32}O	^{32}S
$^{40}Ar^{35}Cl$	^{75}As

Table 5.2. Common polyatomic interferences of P, S and As.

Table 5.3 represents the optimized conditions to detect P, S and As and the type of chromatography that allows for speciation studies to detect the specific degradation product

Heteroatom	ICP-MS conditions	Reaction gas	Chromatography
^{31}P	Oct RF: - 16 V Quad: RF: -18 V	Hydrogen/Helium	Ion pairing
^{32}S	Oct RF: -1 V Quad: RF: -46 V	Xenon	Displacement
^{75}As	Oct RF: -16 V Quad: RF: -18 V	Helium	Ion pairing

Table 5.3. Optimized parameters of the LC-ICP-MS conditions for the elimination of polyatomic interferences for the detection of P, S and As.

5.5 Previous studies

A HPLC-ICP-MS separation and identification has been reported by Richardson et al. [8] The method uses to separate by HPLC-ICPMS analysis a 50 µg mL^{-1} mixture of MPA, EMPA and IMPA in river water. The reversed phase-ion pairing chromatographic conditions were as follows: C 8 column, Alltima, 3.2 x 150 mm, 5µm, Flow Rate 0.5 mL min^{-1}, Inj. Volume 100 µL. Mobile phase: 50mM NH_4Ac + 2% MeOH, pH 4.85. IP agent: 5 mM Myristyltrimethylammonium Bromide and the ICP-MS Parameters: Oct Bias: - 18 V, QP Bias: -16 V, Reaction gas : He 3.0 mL min^{-1}. Detection limits were 0.139 ng mL^{-1} for MPA, 0.263 ng mL^{-1} for EMPA and 0.183 ng mL^{-1} for IMPA.

The separation and detection of mustard gas degradation products, as TDG and the BHET-alkenes, have been reported in Chapter 3, the separation is shown in Figure 3.2. The detection limits were in the parts per billion range and are reported in **Table 5.4**.

	TDG	**BHETM**	**BHETE**	**BHETPr**	**BHETBu**
Retention time (min)	3.3	7.4	10.2	18.8	29.2
LOD, 3σ (ng ml^{-1})	5.01	35.2	79.8	99.1	73.6

Table 5.4. Detection limits and retention times for the main degradation products of mustard gas.

One of the separations that can detect the sternutator agents main degradation products as PAO, PAA, DPAA and distinguish them from other common As species, as inorganic species As (III) and As (V) that can be found in our daily diet in small quantities, can be accomplished by the following HPLC-ICP-MS conditions for an analysis of a 10 µg mL^{-1} mixture: Ion pairing chromatography, 10mM NH_4Ac + 2% MeOH, pH 8.7, IP agent: 400µM SDS, C3 column. ICP-MS parameters: Oct Bias: - 18 V,QP Bias: -16 V Reaction gas : He 3.5 mL min^{-1}. **Figure 5.2** shows the separation and emphasizes the distinction between common As species.

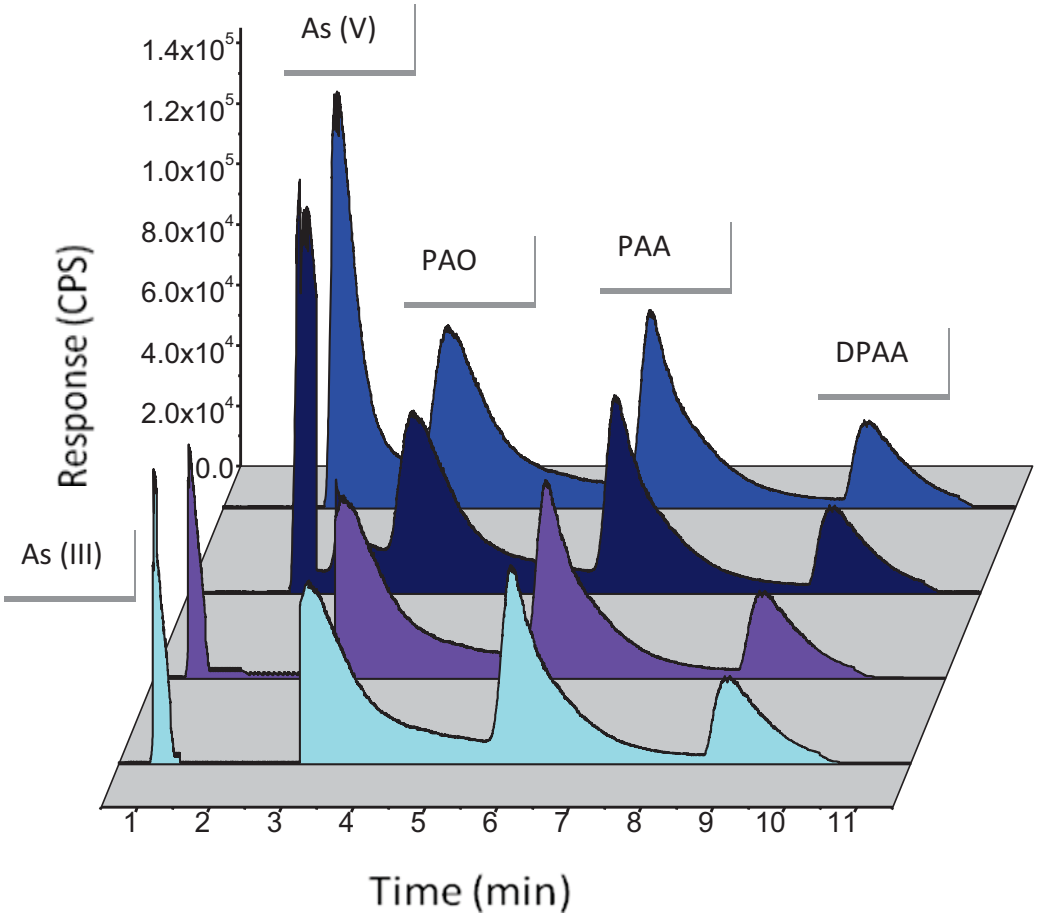

Figure 5.2 HPLC-ICP-MS separation between inorganic As species and CWADPs.

5.6 Results and discussion

As mentioned earlier the main goal of this study is to produce a fast and low level method of detection for the three main classes of CWADPs. The methods shown and mentioned above are very productive in case a the detection of a single heteroatom, but in case of a simultaneous detection of all three heteroatoms, the conditions and reaction gases from Table 5.3 cannot be used. The reaction gas that is necessary for a clean detection for one heteroatom, would suppress the signal for the other heteroatom. For instance, helium would work best for the detection at low levels of phosphorus and arsenic (therefore for the main degradation products of nerve agents and sternutator agents, but helium would as well and almost completely suppress the signal of sulfur, the main heteroatom of the mustard gas agent degradation products). One possible solution is the use of oxygen in the collision reaction gas. In this way detection of oxides PO+ (m/z=47), SO+ (m/z=48) and AsO+ (m/z=91) can be performed.

Figure 5.3 represents the separation with HPLC-ICP-MS applied for some of the main degradation products of nerve agents, mustard gas agents and sternutator agents. Conditions were as follows: HPLC-ICPMS analysis (50 μg mL^{-1} mixture), Ion pairing chromatography, 10mM NH_4Ac,pH 8.0,IP agent: 800μM SDS, Zorbax SB-Phe,1.5x3.4mm, 5μm, Displacer:2-methyl-3-pentanol, ICPMS parameters: Oct Bias: - 3.8 V,QP Bias: -3.1 V, Reaction gas : O_2 3.5 mL min^{-1} (Masses monitored: m/z = 47, 48, 91).

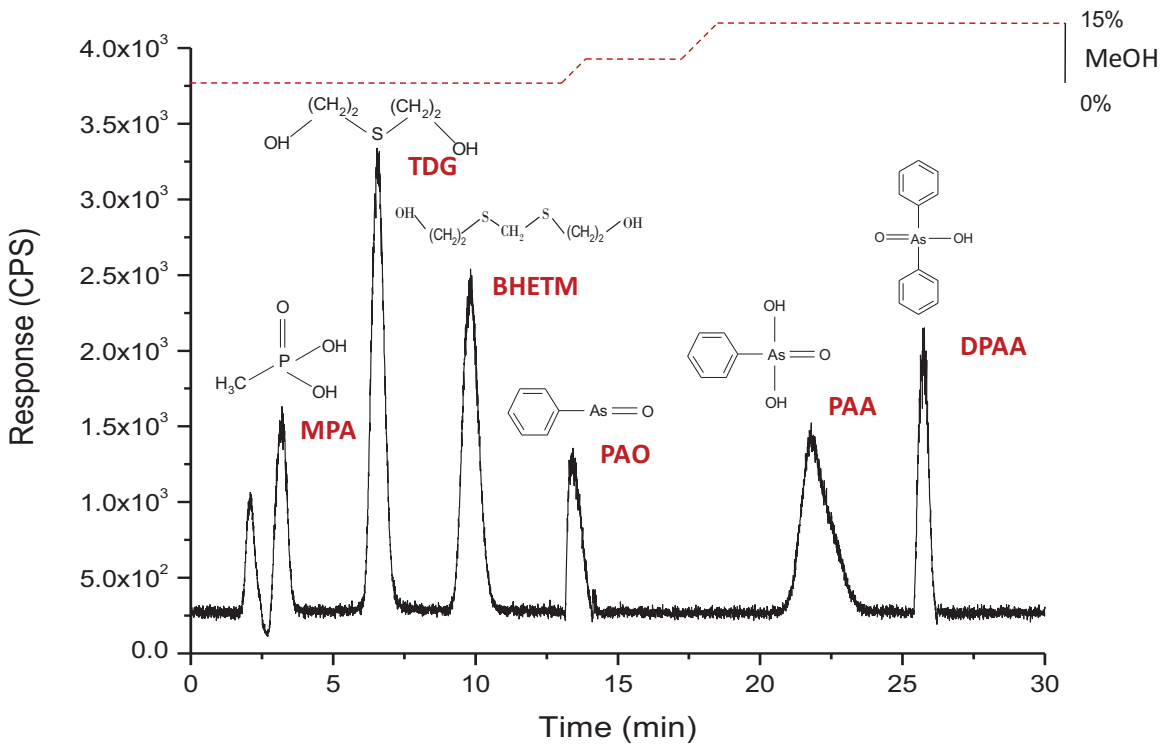

Figure 5.3 HPLC-ICP-MS analysis applied for some of the main degradation products of nerve agents, mustard gas agents and sternutator agents.

Table 5.5 shows the detection limits, which are still in the ng mL^{-1}, but some are improved from the previously shown separations for the single heteroatom and some are worse. In the case of phosphorus the detection with oxygen as reaction gas is worse for and for As remains the same. In the case of sulfur, the combination of oxygen improves the ultra trace detection availability.

The application has been shown in a real world sample (Ohio River water, Cincinnati, OH) as shown in **Figure 5.4**

Chemical Warfare Degradation Product	Detection Limit* ng mL^{-1}	Column Recovery (%)	RSD (%) Peak Area	r^2 Calibration Curve
MPA	46.1	83.2	4.13	0.997
TDG	3.20	67.5	5.64	0.999
BHETM	11.5	73.0	5.02	0.998
PAO	2.46	81.1	3.89	0.995
PAA	2.78	75.9	4.87	0.999
DPAA	23.5	83.2	6.01	0.998

Table 5.5. Detection limits and retention times for the degradation products of mustard gas.

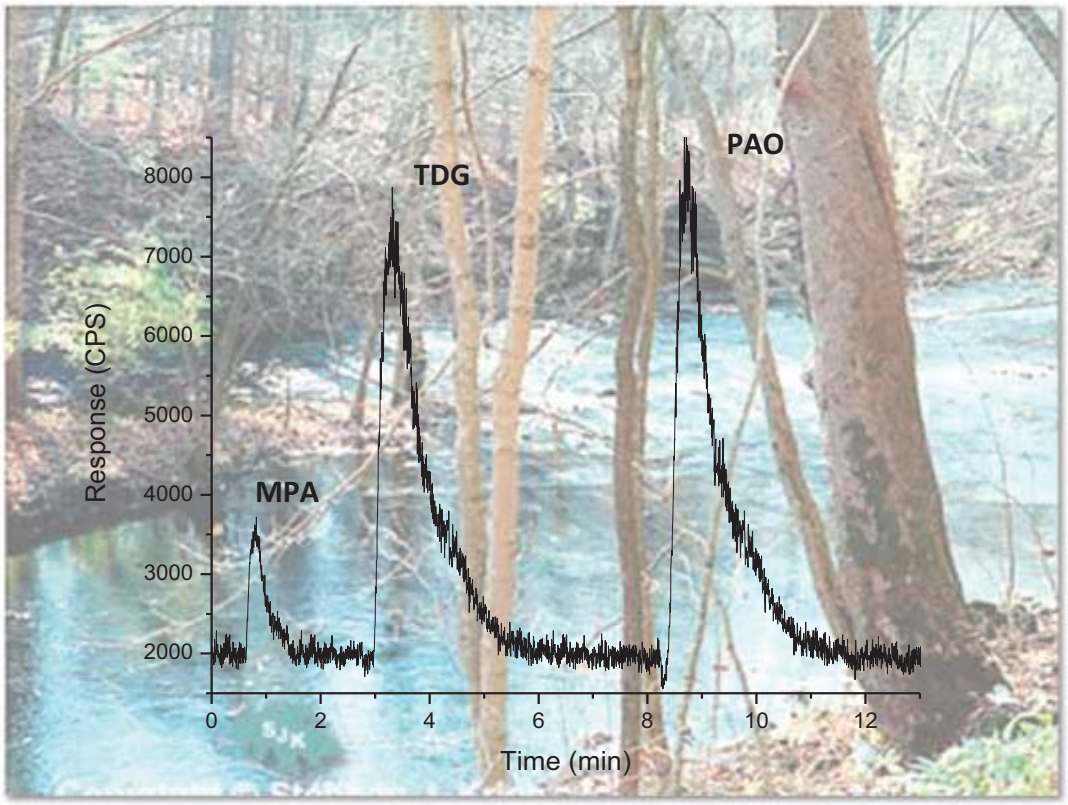

Table 5.4. Ability to identify CWDPs of nerve agents, mustard gas and sternutator agents from common river water (Ohio River, Cincinnati, OH).

Chapter 6

Cytotoxicity of Arsenic containing Chemical Warfare Agent Degradation Products with Metallomics Approaches for metabolite analysis

Reproduced from Karolin K. Kroening, Morwena J. V. Solivio, Monica Garcia-Lopez, Alvaro Puga, Joseph A. Caruso. Cytotoxicity of arsenic-containing chemical warfare agent degradation products with metallomic approaches for metabolite analysis. *Metallomics*, **2009**; 1:59-66.

6.1 Abstract

In this study the arsenic metallome in African Green Monkey kidney (**Figure 6.1**) cells is probed by measuring cytotoxicity, cellular arsenic uptake and speciation studies on arsenic containing chemical warfare agent degradation products (CWDPs) during cell uptake. Inorganic arsenic compounds and methylated species also were studied during cell uptake as a means of providing cytotoxicity information relative to the CWDPs. The degradation products used were phenylarsine oxide (PAO), phenylarsonic acid (PAA), diphenylarsinic acid (DPAA), triphenylarsine (TPA) and triphenylarsine oxide (TPAO). These are the warfare agent's degradation products. The parent warfare agents (red agents) are diphenylarsine chloride (DA or referred to as Clark I) and diphenylarsine cyanide (DC or Clark II), sternutator agents, sneezing gases able to cause bronchial irritation. Cytotoxicity levels and cellular uptake were compared to those of inorganic species: sodium arsenite, $NaAsO_2$ (As III), sodium arsenate Na_2HAsO_4 (As V) and methylated arsenicals such as dimethylarsinic acid (DMA) and methylarsonic acid (MMA).

The arsenic uptake was demonstrated in an African Green monkey kidney cell line, CV-1. Quantification of lactate dehydrogenase activity released from damaged/dying cells was then measured *via* an LDH assay. The purpose of this study is to initially investigate toxicity toward cells when exposed to different arsenic containing compounds over different concentrations and time ranges up to 24 hours. Furthermore, exposed cells were then analyzed for different arsenic species by high performance liquid chromatography (LC) with inductively coupled

plasma mass spectrometry to isolate and speciate arsenic fractions followed by nanoLC electrospray ionization mass spectrometry to analyze the molecular level changes of the arsenic based degradation products in the kidney cells. Metabolic changes to the arsenic species were found and interestingly, at the lowest uptake levels, cytotoxicities were generally higher for the chemical warfare agent degradation products than the inorganic arsenic species.

Figure 6.1 Green African Monkey (*Cercopithecus aethiops)*

6.2 Introduction

Arsenic, a hazardous metalloid, is the inorganic component of a chemical warfare agent named Blue Cross, which consists of diphenylchloroarsine (DA, Clark I) and diphenylcyanoarsine (CDA, Clark II). These agents were mainly used during World War I as vomiting agents; the main purpose was to be “mask breakers” by penetrating the canister, thereby forcing the opposing troops to remove their masks and be further exposed to toxic agents. A concern with these compounds is the possibility of prolonged systemic effects, such as headache, mental depression, chills, nausea, abdominal cramps, vomiting, and diarrhea, all lasting for several hours after exposure. The agents are dispersed as aerosols, and they produce their effects by inhalation or by direct action on the eyes. When released indoors, they can cause serious illness or death.[1,2]

Chemical warfare agent degradation products (CWDPs) include diphenylarsinic acid (DPAA), phenylarsonic acid (PAA) and phenylarsineoxide (PAO). In the degradation pathway, byproducts such as triphenylarsine (TPA) and triphenylarsine oxide (TPAO) are found and their structures are shown in **Figure 6.2**.

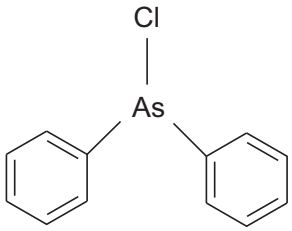

diphenylarsine chloride (CLARK I or DA)

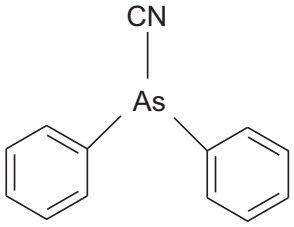

diphenylarsine cyanide (CLARK II or DC)

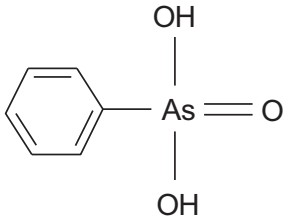

phenylarsonic acid (PAA)

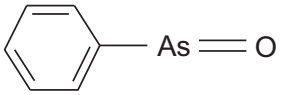

phenylarsine oxide (PAO)

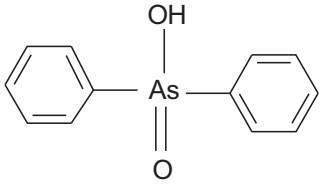

diphenylarsinic acid (DPAA)

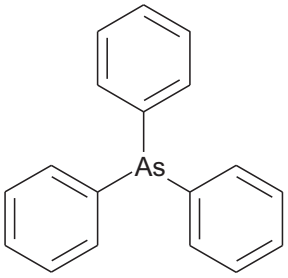

triphenylarsine (TPA)

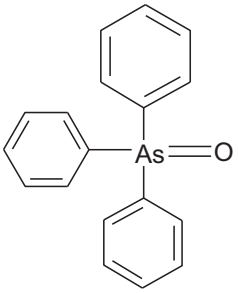

triphenylarsine oxide (TPAO)

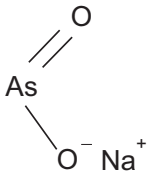

sodium arsenite (As III)

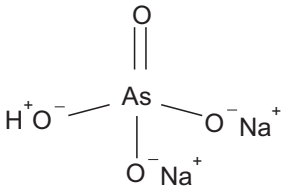

sodium arsenate (As V)

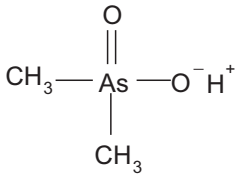

dimethylarsinic acid (DMA)

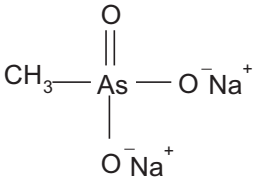

methylarsonic acid (MMA)

Figure 6.2. Structures of primary warfare agents, their degradation products and other arsenic species used in the cytotoxicity study.

Previous papers have mentioned that groundwater and soil has been contaminated from some of these organoarsenical compounds, leading to environmental problems[3,4]. Oyama et al. reported as recently as 2007 the presence of degradation products DPAA, PAA and PAO in groundwater and soil in Kamisu City, Japan.[5] With known population exposure, it is important to understand the biological uptake mechanism for these degradation products in mammalian organisms. Examples of other arsenic species include sodium arsenate, Na_2HAsO_4 (As V), sodium arsenite, $NaAsO_2$ (As III), dimethylarsinic acid (DMA) and methylarsonic acid (MMA) as shown in **Figure 6.2** as well as Clark I and Clark II.

The aim of this work was to initially study the CWDPs cytotoxicity by comparing the effects of different concentrations over different time periods on mammalian cells. To generate metallomics information an As speciation study was performed utilizing liquid chromatography (LC) coupled to both inductively coupled plasma mass spectrometry (ICP-MS) and electrospray mass spectrometry (ESI-MS) to identify the molecular level changes the CWDPs might undergo.

The cytotoxicity evaluation was conducted on an African Green Monkey CV-1 cell line based on quantification of lactate dehydrogenase activity (**Figure 6.3**) as released from damaged/dying cells. Kidney cells were chosen as target cells because kidneys take up and excrete a variety of substances produced by the metabolism. A comparison of different concentration levels over different time ranges was complete, following the toxic compounds addition to the cells. The cells treated with the various arsenic species were then tested for cellular arsenic uptake by ICPMS detection of the monoisotopic ^{75}As.

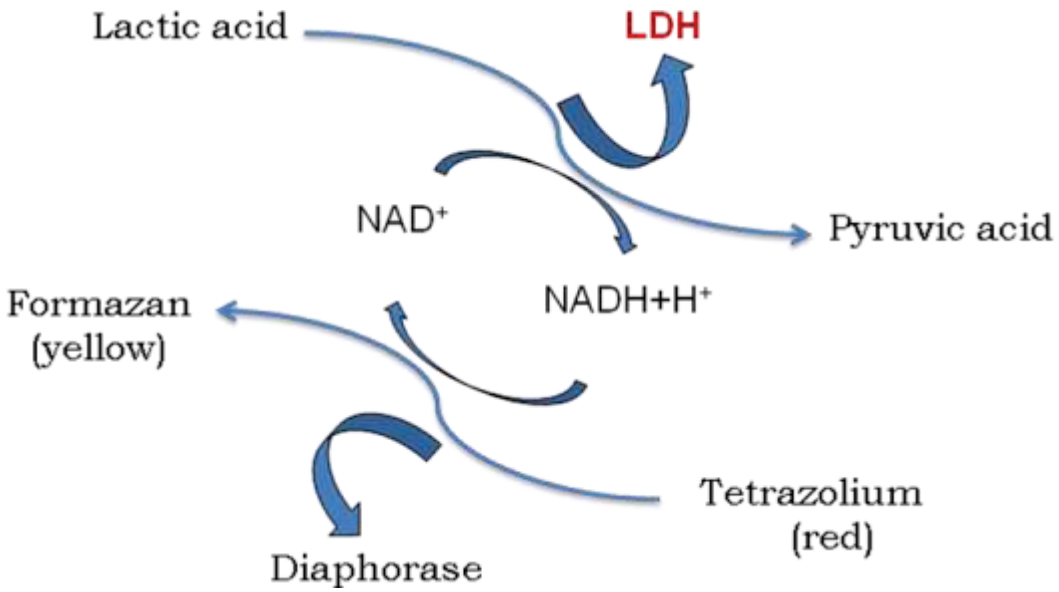

Figure 6.3. LDH (Lactate Dehydrogenase) assay theory

The interest in arsenic speciation analyses continues to grow with the increasing need to assess its biological effects. Total arsenic analyses, though necessary, are insufficient to address the complexities and questions posed by biological systems. While As total concentrations are useful, they provide no information on the various arsenic forms, which have widely varying toxicities. The inorganic species, which are commonly found in the environment, are known to be the most toxic species, but some of the organic arsenic forms are less toxic and even innocuous.[6] Hence, speciation analysis is required and further identification and verification by molecular mass spectrometry is necessary.

6.3 Materials and Methods

6.3.1 Chemicals

Ammonium acetate (Fisher Scientific, Fairlawn, NJ, USA) was the buffer used for liquid chromatography (LC) separation. The buffer pH was adjusted to 8.3 using ammonium hydroxide, also from Fisher Scientific. Methanol (Tedia Company, Fairfield, OH, USA), was the organic modifier used to create a more polar stationary phase. The As (V) standard, sodium arsenate monobasic was acquired from Sigma Aldrich, St. Louis, MO, USA, while the As (III) standard, sodium (meta) arsenite was procured from Sigma Aldrich, Madrid, Spain. The methylated arsenic species standard, methylarsonic acid (MMA) was from Chem. Service, Westchester, PA, USA, while dimethylarsinic acid (DMA) was obtained from Fluka Chemie, Melville, NY, USA. The degradation products, phenylarsine oxide (PAO) and phenylarsonic acid (PAA) were purchased from Alfa Aesar, Lancaster, UK, while diphenylarsinic acid (DPAA) was purchased from Wako Pure Chemical Industries Ltd., Osaka, Japan. CWDPs' byproducts, triphenylarsine (TPA) and triphenylarsine oxide (TPAO) were acquired from Sigma-Aldrich Inc., Steinheim, Germany.

6.3.2 Cells, media and culture conditions

The cell line used for the experiments was ***Cercopithecus aethiops*** (African Green Monkey) kidney cells, CV-1. The CV-1 lines, disease normal, morphology fibroblast, were available from the Puga labs at the University of Cincinnati. The cells were grown in Dulbecco's Modified Eagle's Medium (DMEM; ATCC, Manassas, VA, USA) supplemented with 10% Fetal Bovine

Serum (FBS; Gibco Invitrogen Corporation, Carlsbad, CA, USA) in a humidified incubator under 95% air and 5% CO_2 and at a temperature of 37ºC. Subculture passages were performed twice a week using trypsin-EDTA: 0.05% Trypsin 0.53 mM EDTA x 4Na (Gibco Invitrogen Corporation, Carlsbad, CA, USA). Dimethyl sulfoxide (DMSO; Fisher Scientific, Fairlawn, NJ, USA) was used for frozen stock ampoules at passage 5. Cells used for the experiments were from passages 5 to 12 at a stage of about 80% confluency as estimated by referring to microscopic images.

6.3.3 Cytotoxicity assay

The LDH cytotoxicity detection kit was obtained from Fisher Scientific, Pittsburgh, PA, USA. Triton X-100 (Sigma-Aldrich Chemie, Steinheim, Germany) was used for high controls. This LDH assay was specifically chosen because of its good sensitivity. More specifically it allows for detection based on the lowest number of cells that can be quantified and is compatible with a variety of culture media and liquid handling systems for various detection target applications: cell proliferation, viability (number of live cells), cytotoxicity (number of dead cells). This assay provides a fast and simple method for quantifying cytotoxicity based on lactate dehydrogenase activity released from damaged/dead cells by absorbance measurements at 492 nm.

Unlike many other cytoplasmic enzymes, which exist in many cells either in low or unstable amounts (e.g., alkaline and acid phosphatase), LDH is a stable cytoplasmic enzyme present in all cells and rapidly released into the cell culture supernatant upon plasma membrane damage. LDH activity can be determined by a coupled enzymatic reaction: LDH oxidizes lactate to pyruvate, which then reacts with tetrazolium salt INT to form formazan. The increase in the

amount of formazan produced in culture supernatant directly correlates to the increase in the number of lysed cells. The formazan dye is water-soluble and can be detected spectrophotometrically at 492 nm.[7]

During these experiments the amount of FBS had to be lowered to 1% instead of 10% as recommended because of possible interference during the absorbance measurement. Target cells were seeded in a 96 well microtiter plate (5 x 10^3 cells/well) with different concentrations of the above mentioned As compounds and tested on different incubation time frames.

Triton X-100, known to be highly toxic to the cells was added for a high control to measure the correct cell death. The cell medium was used as low control to indicate the favorable environment for cell growth. These two controls were used for the calculation of cytotoxicity by subtracting the low control from the high control as background correction. A microtiter with blank control has been plated also and has been subtracted from the final values. The LDH assay required the following steps: addition of a mixture of lyophilized catalyst and thawed dye solution and no exposure to light for 30 minutes, centrifugation at 250 x g for 10 minutes, 2 times dilution with DDI water, and the LDH activity measured at 492 nm.

6.4 Instrumentation

6.4.1 Imaging

A Nikon Eclipse TE300 inverted epi-fluorescence microscope (**Figure 6.4**) with a MagnaFire Digital CCD Camera System (BioRad MRC1024. Birad, MO, USA) was used to photograph the cells in various stages of confluency.

Figure 6.4. Nikon Eclipse TE300 inverted epi-fluorescence microscope to identify confluency stage

6.4.2 Microwave Digestion

An Intellivent Explorer microwave digestion/extraction system (CEM Corporation, Matthews, NC, USA) equipped with magnetic stirrer and accelerated cooling profile utilizing compressed gas, was used to digest the arsenic treated cells in preparation for As total analysis in 10 mL

glass tubes sealed with polytetrafluoroethylene faced septa caps. The cells were washed five times to eliminate any residue from the cell culture medium and then digested in the microwave system for 3 minutes with 50:50 v/v nitric acid in DI water at a temperature of 350ºC and a maximum pressure of 1.38MPa.

6.4.3 Sonicator

A Fisher Scientific (Fisher Scientific, Pittsburgh, PA, USA) Ultrasonic Cleaner featuring a 40 kHz industrial transducer with sweep frequency to ensure uniform ultrasonic activity within the tank, was used to disrupt the cellular membrane prior to speciation analyses. One mg (1 mg) cells was washed five times with DDI water, then sonicated for 20 min to accomplish physical cell disruption. Sonication is a good method for samples on the order of 1 mg. To avoid excessive heating the sample was immersed in an ice bath.

6.4.4 Centrifuge

A Sorvall RC-5B Refrigerated Superspeed Centrifuge (Dupont Instruments, ON, Canada), was used to separate the arsenic species from the other cellular contents in preparation for the speciation assay. Lysed cells were centrifuged for 30 minutes at 2500 rpm and 1mL of the supernatant was analyzed under chromatographic separation.

6.4.5 High Performance Liquid Chromatography (LC)

An Agilent (Agilent Technologies, Santa Clara, CA, USA) 1100 high performance liquid chromatography system equipped with a high pressure binary gradient pump, autosampler,

vacuum degasser, column compartment with Peltier heating/cooling, and UV detector was used to separate the arsenic species being investigated in this study. The UV detector was used in line with the ICP-MS. A C3 column (Agilent Technologies), Zorbax 300S-C3, (4.6 x 150 mm, 3.5 µm) was used for the separation and speciation experiments, which were accomplished under isocratic conditions with 10mM ammonium acetate as mobile phase (pH 8.2) and 15% (v/v) methanol as organic modifier using the C3 column. A 100 µL portion of the digested cell sample treated with the arsenic species being investigated was injected into the LC-ICP-MS at a flow rate of 1.0 mL min^{-1}.

6.4.6 Inductively Coupled Plasma Mass Spectrometer (ICP-MS)

An Agilent 7500x ICP-MS (Agilent Technologies, Santa Clara, CA) equipped with a shield torch system and a collision/reaction cell was used for element specific detection of arsenic at m/z 75. Electronic coupling of the ICP-MS with the LC was accomplished through the use of a remote cable, which allowed for synchronized starting prior to each chromatographic run. The experiments have been performed by detecting at m/z of 75 with the ICP-MS by using a flow rate of 3.5 mL min^{-1} of H_2 as cell reaction gas and quadrupole and octopole bias at -16 V and -18 V, respectively, for a net +2V energy discrimination barrier. ICP-MS parameters and LC settings are given in **Table 6.1**.

ICPMS parameters

Instrument	Agilent 7500x ICPMS
Forward power	1500 W (with shielded torch)
Plasma gas flow rate	14.6 L min^{-1}
Auxiliary gas flow rate	1.1 L min^{-1}
Carrier gas flow rate	0.93 L min^{-1}
Nebulizer	Glass expansion micro-concentric
Spray chamber	≈ 2 °C (Scott double channel)
Sampling depth	7.5 mm
Sampling and skimmer cones	Nickel
Dwell time	0.1 s
Isotope monitored (*m/z*)	^{75}As
Octopole reaction system	H_2 (Flow rate: 3.5 mL min^{-1})
QP bias	-16 V
Octopole	-18 V

HPLC parameters

Instrument	Agilent 1100 HPLC
Flow rate	1.0 mL min^{-1}
Injection volume	100 µL
Buffer	10mM NH_4COOH + 15% MeOH
pH	8.2
Column	Zorbax 300S-C3, (4.6 x 150 mm, 3.5 µm)

ESI-MS parameters

Instrument	MSD Ion Trap XCT Ultra system
Flow rate	18 µL/hour
Drying gas	N_2, 4 L min^{-1}
Temperature	300^{o}C
MS capillary voltage	1800 V
Skimmer	25.0 V
Capillary exit	110.7 V
Trap drive	32.3 V

Table 6.1. HPLC, ICPMS and ESI-MS instrumental parameters

6.4.7 Electrospray Ionization Mass Spectrometry (ESI-MS)

All electrospray experiments were accomplished by taking As specific fractions pre-determined by ICPMS and directly infusing them to the ion trap mass spectrometer using a syringe pump on an MSD Ion Trap XCT Ultra system (Agilent Technologies, Santa Clara, CA) equipped with an on-chip nano column of Zorbax 300SB C18 for enrichment (4 mm x 75 µm, 5 µm) and an analytical column Zorbax C18 (45 mm x 75 µm, 5 µm). Sample loading onto the enrichment column was set at a flow rate of 18 µL/hour with the mobile phase used for chromatographic separation. The following MS conditions were used: 4 L min^{-1} nitrogen drying gas at a temperature of 300^{o}C; MS capillary voltage, 1800 V; skimmer, 25.0 V; capillary exit, 110.7 V; trap drive, 32.3 V. The MS scan range was 50-400 m/z in standard-enhanced scan mode. ESI-MS, ESI-MS^2 spectra were taken.

6.5 Results and Discussion

6.5.1 Cytotoxicity of different arsenic species in African Green monkey CV-1 cells

The study of cell viability requires the quantification of the number of viable cells in a cell culture. The LDH assay utilized the detection kit for the above mentioned reasons. Cells were tested with exposure to four different concentrations: 0.5, 5, 50 and 500 µM of the five CWDPs, two inorganic arsenic species (As III and As V) and the methyl organoarsenicals DMA and MMA, in addition to cell medium, low and high controls. Additionally a zero control has been plated for all the above mentioned products. Further, three different time frames (3, 12 and 24 hours) for cell exposure were utilized to assess the prolonged effect on target cells. Cells for the

experiments were chosen when their confluency level reached about 80%. Confluency is an indication of the cell growth phase, referred to proliferation throughout the culture medium (**Figure 6.5**).

Figure 6.5. Confluency: coverage or proliferation that the cells are allowed over or throughout the culture medium

The confluency level was based on microscopic images, for example, those shown in **Figure 6.6.a** and **6.6.b**, showing a distinction in cell density between confluent and non-confluent cells. Figure 6.6.a also demonstrates the difference in appearance between live and dead cells. Live CV-1 cells adhere to the substratum and have fibroblast-like morphology, while dead CV-1 cells are round and are detached. The black dots in the image below are probably organelles or proteins present in the cell.

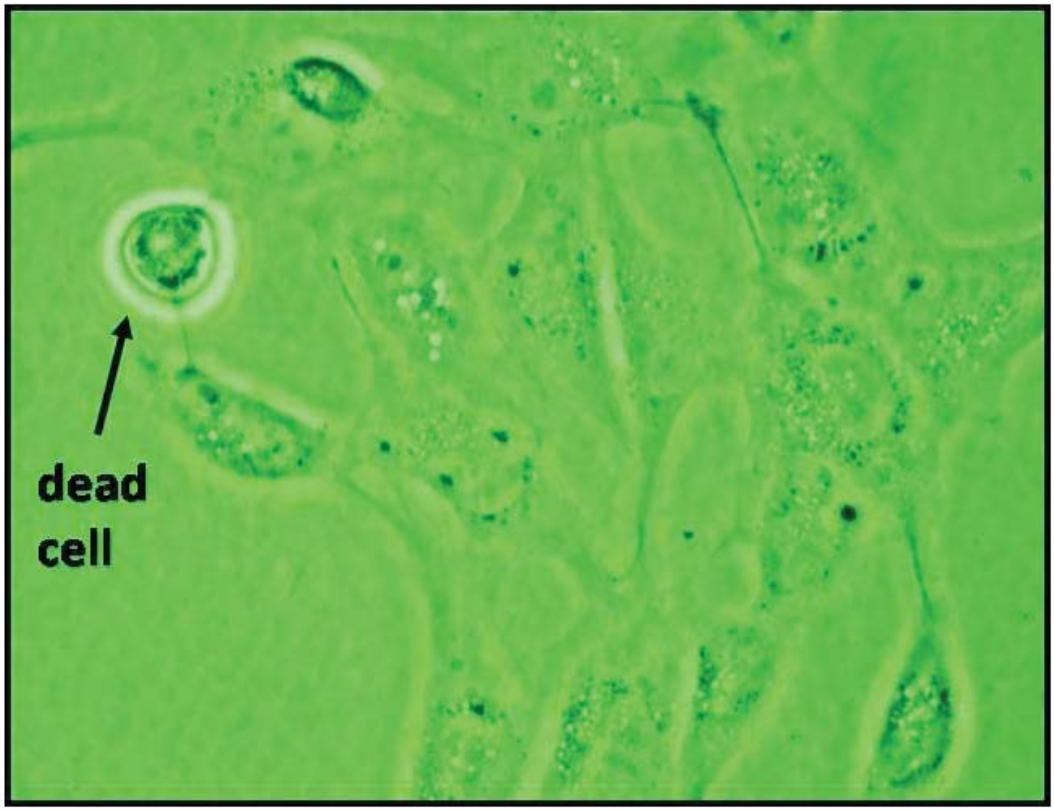

Figure 6.6.a. Image of CV-1 cells after 4 days of cultivation, showing evidence of about 80% confluency and the ability to detect for dead cells

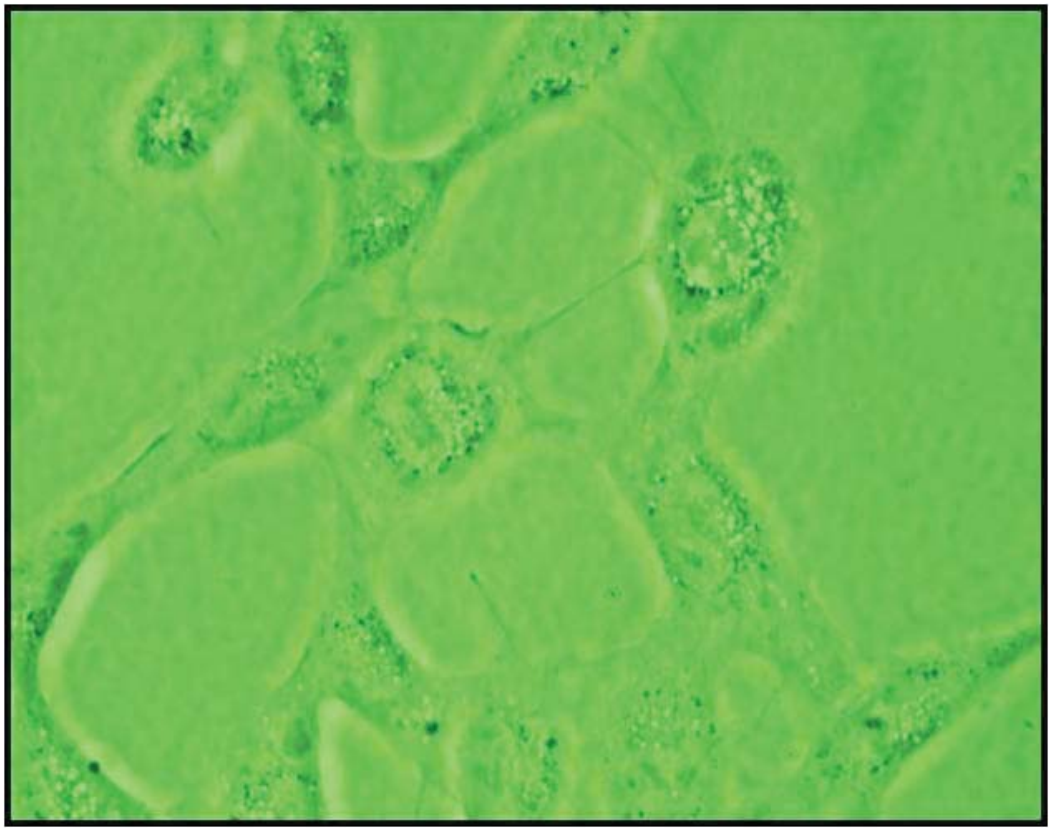

Figure 6.6.b. Cell confluency after 1 day of cultivation, indicating low proliferation, therefore very low confluency.

The results indicate that treatment with CWDPs after 24 hours of incubation resulted in higher cytotoxicity compared to the other arsenic species (**Figures 6.7.a-i)**.

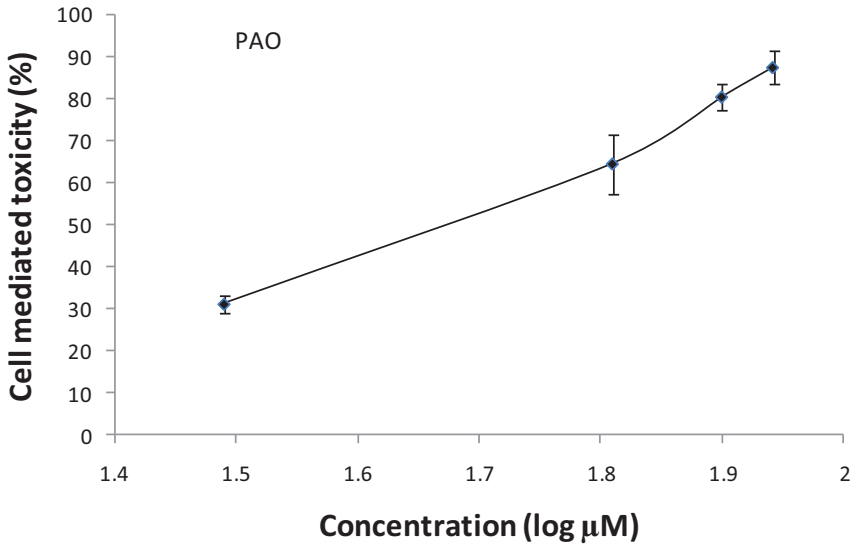

Figure 6.7.a Toxic effect of As containing compound PAO after 24 hours exposure time at different concentration ranges : 0.5,5,50,500 µM.

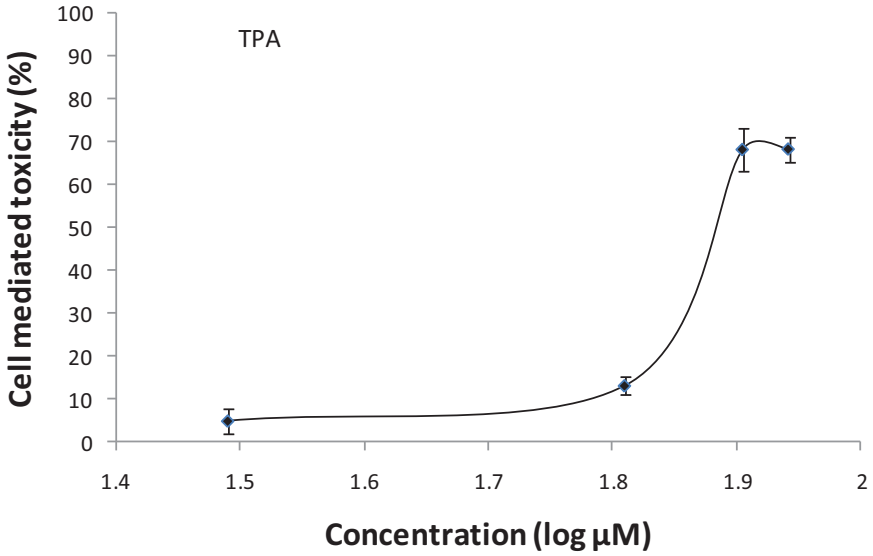

Figure 6.7.b Toxic effect of As containing compound TPA after 24 hours exposure time at different concentration ranges : 0.5,5,50,500 µM.

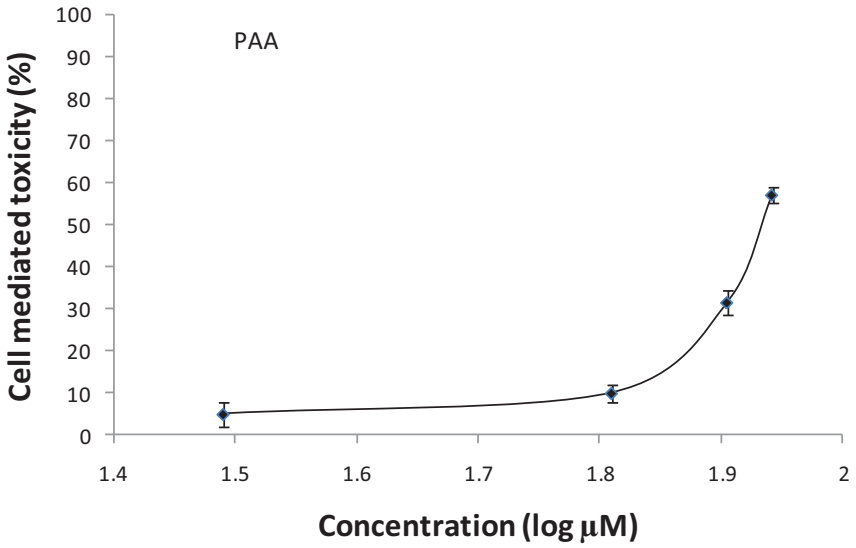

Figure 6.7.c Toxic effect of As containing compound PAA after 24 hours exposure time at different concentration ranges : 0.5,5,50,500 μM.

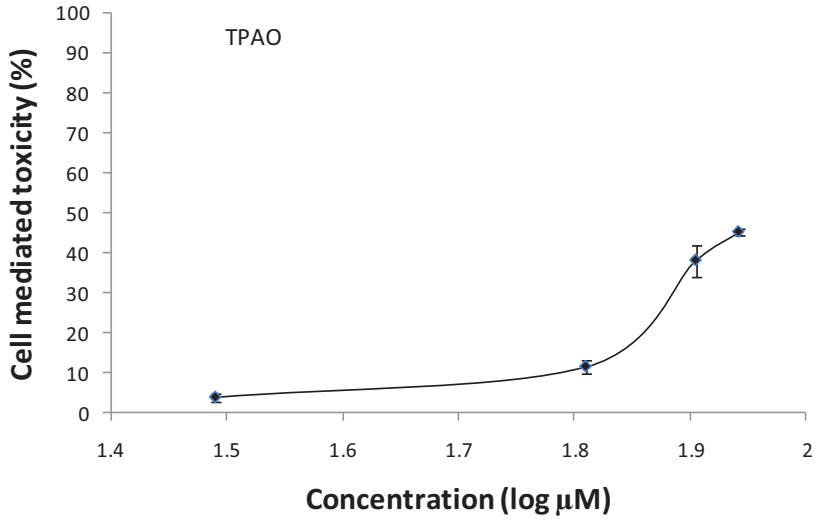

Figure 6.7.d Toxic effect of As containing compound TPAO after 24 hours exposure time at different concentration ranges : 0.5,5,50,500 μM.

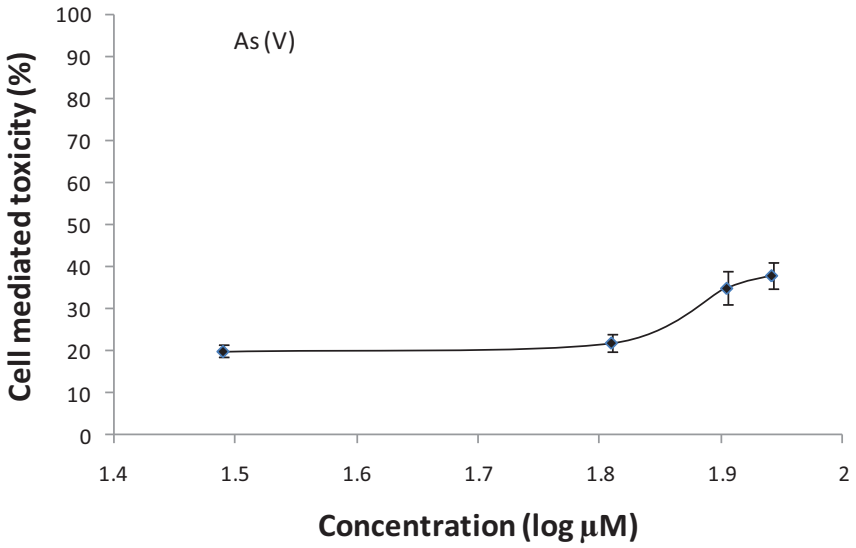

Figure 6.7.e Toxic effect of As containing compound As(V) after 24 hours exposure time at different concentration ranges : 0.5,5,50,500 µM.

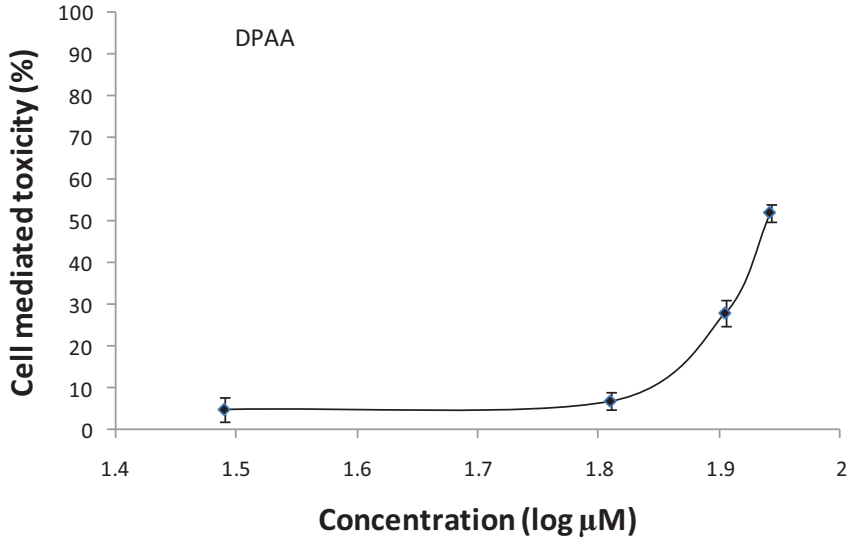

Figure 6.7.f Toxic effect of As containing compound DPAA after 24 hours exposure time at different concentration ranges : 0.5,5,50,500 µM.

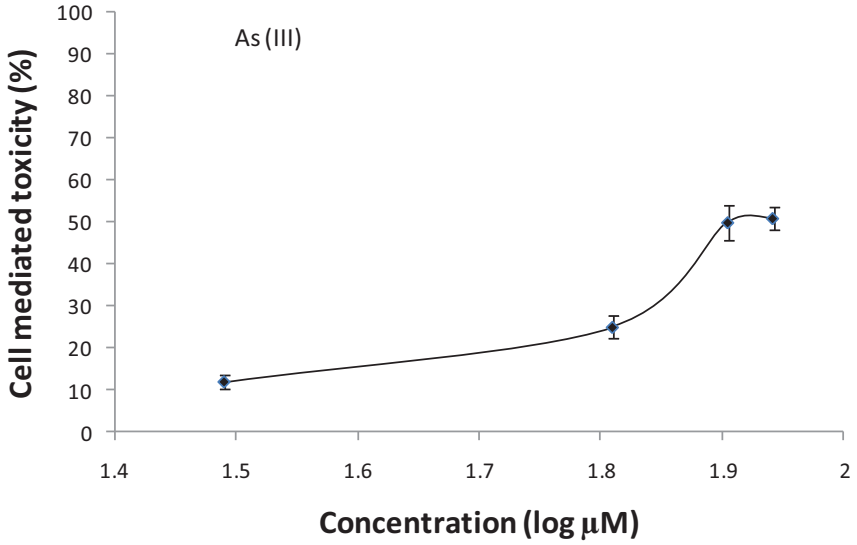

Figure 6.7.g Toxic effect of As containing compound As(III) after 24 hours exposure time at different concentration ranges : 0.5,5,50,500 µM.

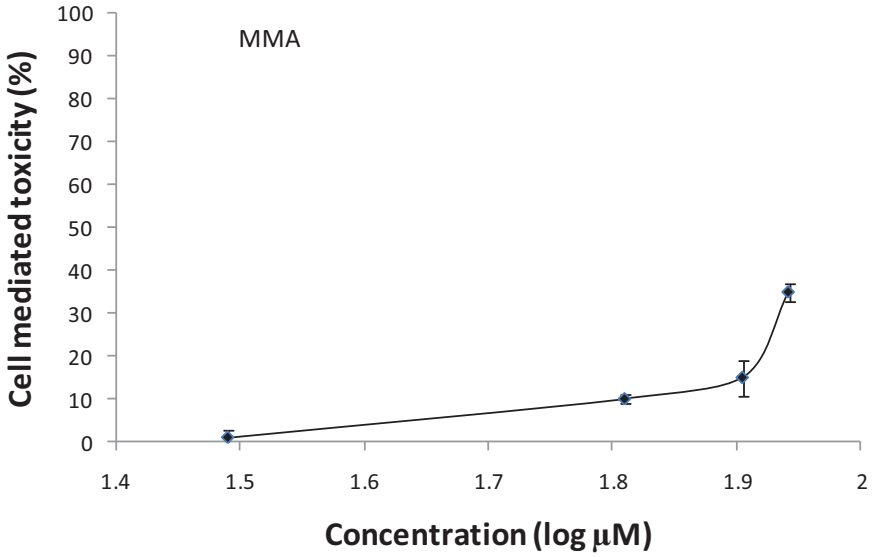

Figure 6.7.h Toxic effect of As containing compound MMA after 24 hours exposure time at different concentration ranges : 0.5,5,50,500 µM.

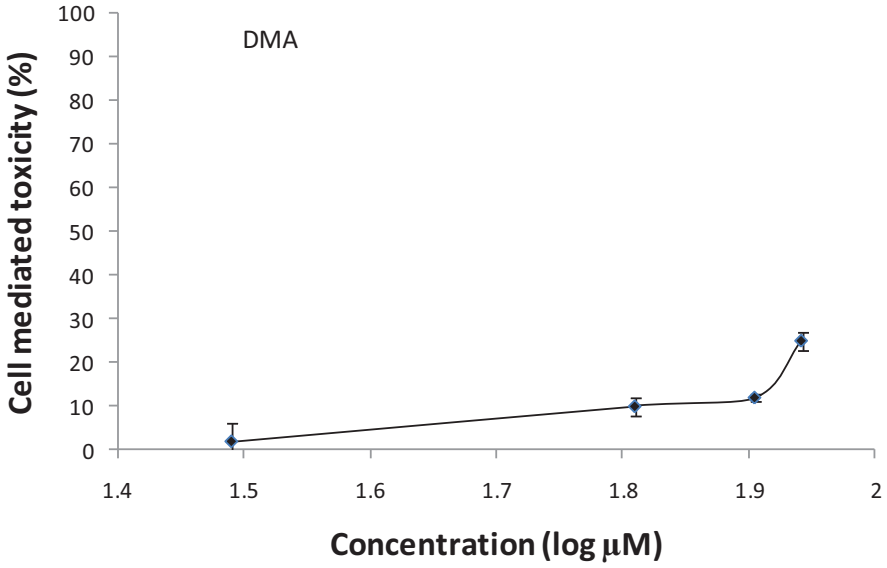

Figure 6.7.i Toxic effect of As containing compound DMA after 24 hours exposure time at different concentration ranges : 0.5,5,50,500 μM.

Overall, PAO caused cell death the most. The cytotoxicity level of PAO at the highest concentration (500 μM) is 3.5 ± 0.3 times higher than DMA, 2.3 ± 0.1 times higher than the As (V) species and 1.7 ± 0.1 higher than As (III). Also TPA and TPAO, other products in the degradation pathway, show still higher toxicity levels compared to species of non CWDPs. It may be possible that species with phenyl groups more easily enter the cell membrane, but the relationship between chemical structure and passage through the mitochondrial membrane is not yet clear [8]. As (III) shows higher toxicity when compared with As (V), but surprisingly lower toxicity relative to several CWDPs. Also it is generally known that As (III) forms of methylated species have genotoxicities similar to inorganic As (III), which may extend to

additional organoarsenicals. It has been suggested that the difference between As (III) and As (V) is due to the faster uptake of As (III) by endothelial cells with inorganic arsenic exerting its toxicity, at least in part, *via* intracellular oxidative stress [9]. The experiment also showed that the higher the concentration of arsenic species added, the stronger the cell damage. Calculations for cytotoxicity were performed based on triplicate experiments and error bars at $\pm$ 1 std. dev. obtained for each experiment (as is generally accepted for these types of experiments).

Figure 6.8 demonstrates cell damage/death after incubated exposure for 3, 12 and 24 hours, respectively, to the arsenic compounds (concentration at 500 μM). Significant differences between different exposure times are noted. The trivalent arsenic species PAO, TPA and sodium arsenite have strong cytotoxicity after 3 hours and the prolonged exposure to arsenic does not significantly increase cell death when compared to the pentavalent species. The relative PAO toxicity on target cells grows only 8.5% from 3 to 24 hours of exposure, while toxicity increases 24% for DMA and 32% for MMA.

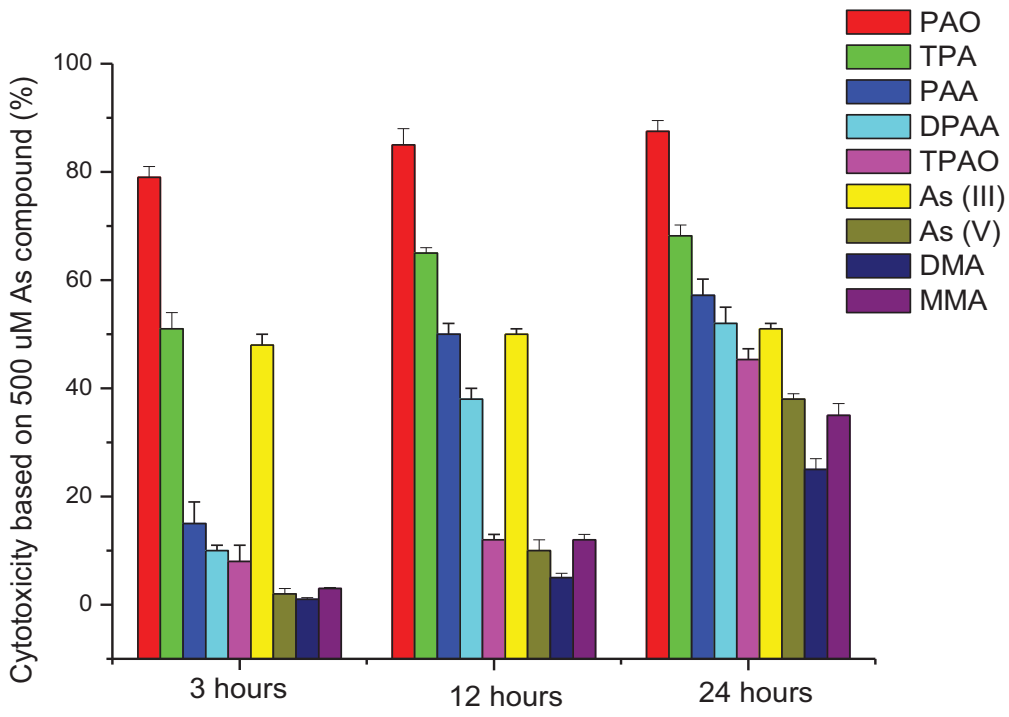

Figure 6.8. Toxicity effects on target cells after 3, 12 and 24 hours based on different As species with 500 μM added in each experiment performed in triplicate with ± 1 std dev shown as the error.

Tsuchiya et al. conducted experiments on the metabolism of arsenic species, providing evidence that pentavalent inorganic arsenic is metabolized to the trivalent form, which is then methylated. Therefore, the most active arsenic compound is trivalent inorganic arsenite, followed by the pentavalent inorganic arsenate.[10] This explanation might be applied to the CWDPs' trivalent arsenic compounds also, but further investigation is required, since very little information about metabolic interactions and toxicity is known about chemical warfare degradation compounds.

6.6 Metallomics approach

6.6.1 Cellular arsenic uptake

Comparison of total arsenic uptake has been studied in the cell culture medium and on the cells. **Figure 6.9** shows evidence of a higher cellular uptake from the CWDPs. PAO arsenic concentration was 4.8 ± 0.7 times higher than MMA. This suggests that the toxicity is associated with the cellular uptake of the arsenicals.

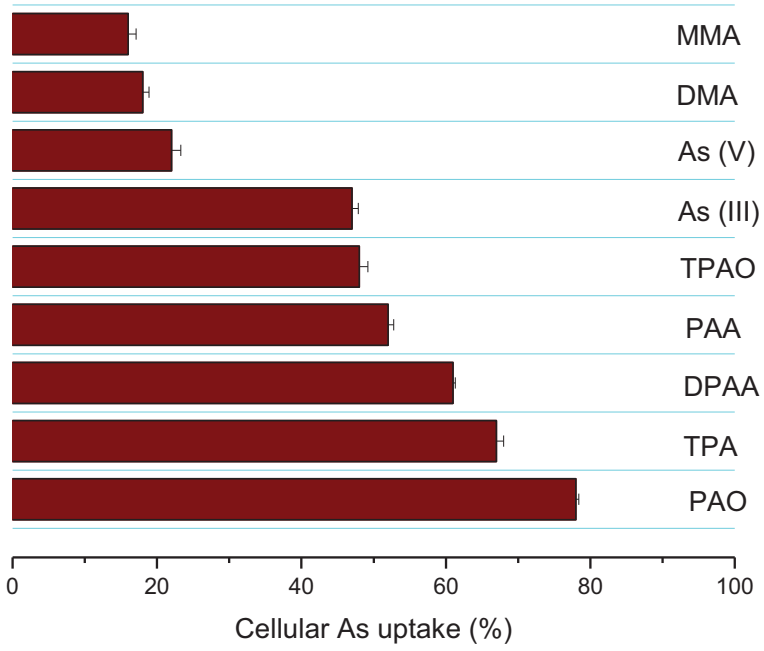

Figure 6.9. Cellular arsenic uptake results based on a 500 µM addition, after 24 hours exposure to varying As species. Cellular As uptake percentage refers to the amount of As present in 1mg of cell pellet. Error bars indicate ± 1 std. deviation.

PAA and DPAA are inverted in **Figure 6.9** (with respect to their III or V arsenic forms), compared to the cytotoxicity results in **Figure 6.7** where PAA is appears to be 1.1 ± 0.2 times more toxic than DPAA, although the error analysis indicates no difference. Considering the As concentration present in the cells, DPAA has a higher uptake of As. As earlier suggested, this may be due to the two phenyl groups on DPAA that permit more interaction with the cell membrane, showing that cytotoxicity and As uptake are not complementary for these two compounds. Relative concentrations with relative standard deviation based on calculations for experiments repeated in triplicate are: MMA 16% ± 1.1, DMA 18% ± 0.8, As (V) 22% ± 1.3, As (III) 47% ± 0.8, TPAO 48% ± 1.2, PAA 52% ± 0.4, DPAA 61% ± 0.3, TPA 67% ± 1, PAO 78% ± 0.4 based on 1 mg of cell pellet after addition of 500 µM of arsenic species and an incubated exposure time of 24 hours.

- As conclusion PAO, TPA and As (III) have high toxicity after already 3 hours and doesn't significantly increase after 24 hours.
- PAA and DPAA show higher toxicity, but increase their toxicity going from 3 up to 24 hours

Figure 6.10 shows the cytotoxicity compared to the As uptake of the As studied species at 24 hours time exposure in the cells.

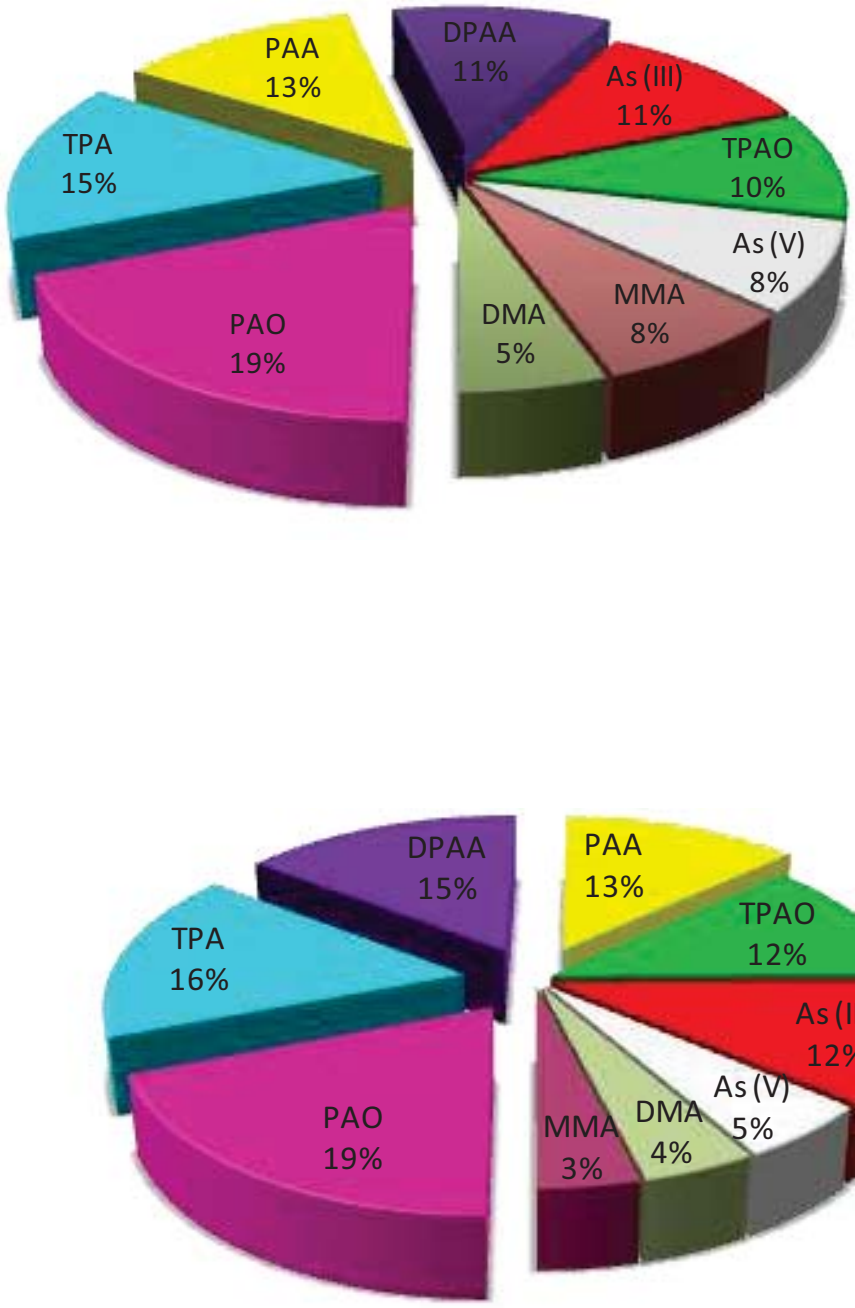

Figure 6.10. Cytotoxicity vs. arsenic uptake

6.6.2 Speciation of arsenic compounds after cell exposure

The aim of this work was not only to measure cytotoxicity levels of cells exposed to different arsenic species, but also to understand what changes these toxicant species might undergo after cell metabolism has taken place. Each cell inoculant was analyzed for total arsenic uptake with ICPMS. Additionally, several compounds have been speciated by using LC coupled to ICPMS and subsequently by ESI-MS for mass identification. Because of low uptake for most of the species, speciation was not possible for all.

For each compound a standard LC separation was run with As species standards, media and cells. The culture medium was treated with the same amount of As species at the same conditions as for the target cells, i.e. after 24 hour As species exposure to 500 µM solution in an incubator.

Figure 6.11.a shows that DPAA was not present in its original form after metabolism, but it is still present in the medium, indicating the species changes occur during cell metabolism. An unknown low intensity peak at 160 sec, when compared to the peak from DPAA in the medium, is due to the lower arsenic uptake and possible sample loss during cell lysis.

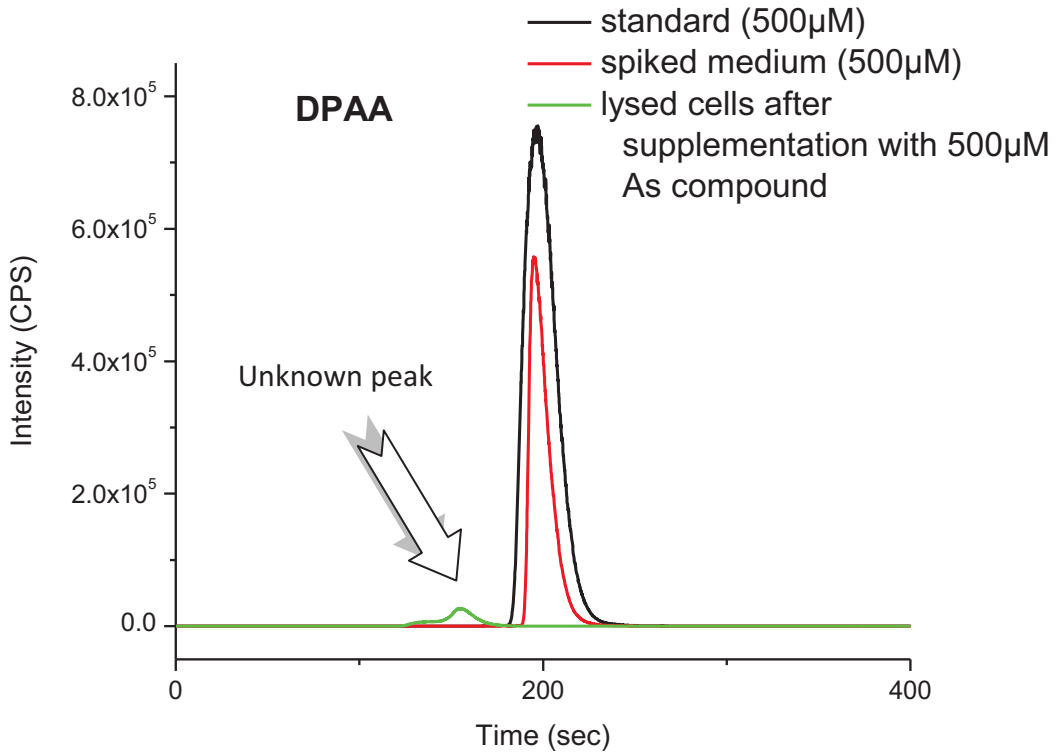

Figure 6.11.a. LC-ICPMS for speciation analysis with DPAA standard, spiked medium, and target cells showing complete loss of DPAA to PAA as determined by spike addition.

Identification of the unknown LC-ICPMS peak with nanoLC-CHIP-ITMS (+ ion mode) and spiked LC-ICPMS analysis demonstrates the complete chemical transformation of DPAA to PAA after cell interaction (**Figure 6.11.b).**

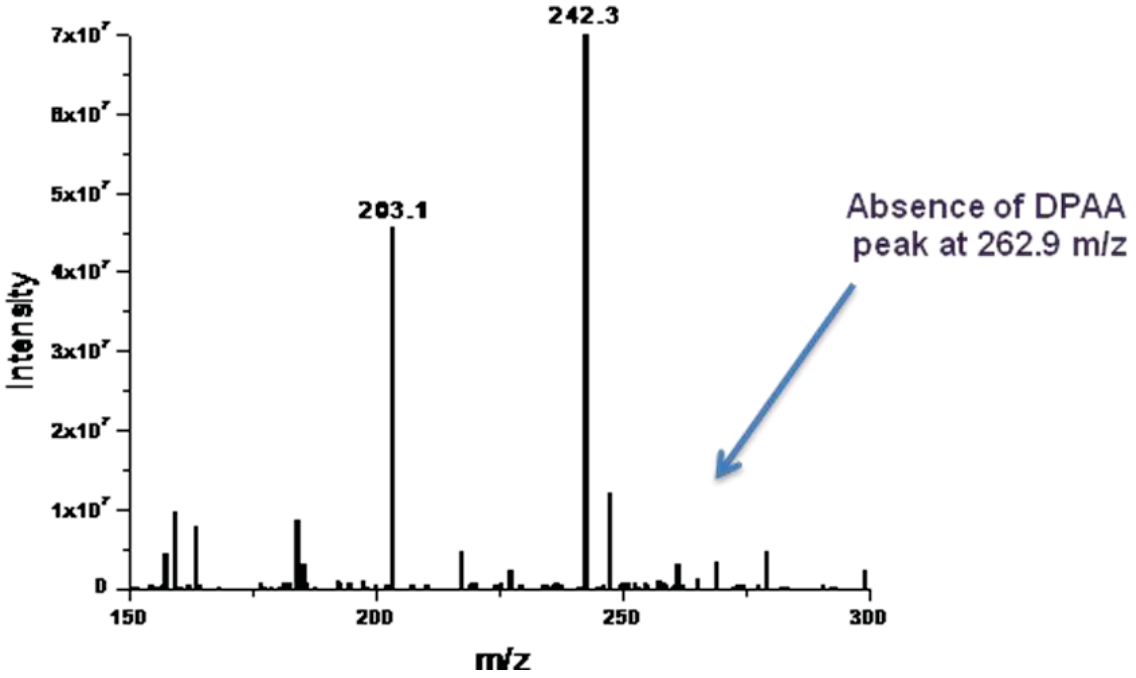

Figure 6.11.b. ESI mass spectrum obtained for the unknown peak in Figure 6.11.a.

Evidence is shown for the molecular ion, $[PAA+H]^+$ at m/z = 203.1. The mass spectrum represents the fraction collected for the unknown peak in Figure 6.11.b. There is no evidence of this conversion in the medium. It is interesting to note in Figure 6.11.a how the $[DPAA+H]^+$ peak, expected at m/z = 262.9, is absent. In the cell medium instead, the mass spectrum performed under the same conditions, stands out with a relative abundance of 5 x 10^7 and no PAA mass peak is shown. LC-ICPMS with standard spike confirmed this observation. The outstanding peak at m/z 242.3, which also is present in the cell blank, requires further investigation by exact mass identification, currently underway. ESI-MS^2 data of this unidentified

compound show characteristic peaks at m/z = 279.0 and 372.9. T. Nakayama et al. [11] have suggested possible conversions involving phenylarsonic acid-diglutathione complex, PAA - $(GSH)^2$ and fragments of this might offer possibilities. Also no sulfur or phosphorous was detectable in the fraction taken from ICPMS for ITMS experiments. Further mass spectrometry is required for the identification of the 242.3 m/z peak.

Figure 6.12.a demonstrates that PAO metabolizes also to PAA, with a higher intensity yield. The ESI experiment (**Figure 6.12.b**) and LC-ICPMS std. spike analysis confirms the presence of this As species. The peak at m/z = 203.1 shows the presence of PAA The main peak of m/z = 169.1 $[PAA+H],^+$ due to PAO is completely absent. Peaks at m/z = 185.3 are due to water loss $[PAA-H_2O]^+$. Also an outstanding peak of m/z = 242.3 is present and not yet identified.

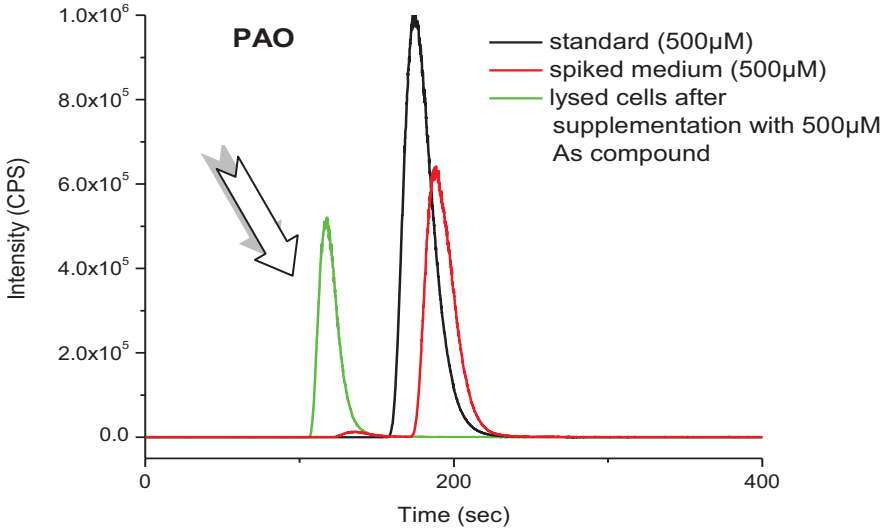

Figure 6.12.a. LC-ICPMS for speciation analysis with PAO standard, spiked medium and target cells.

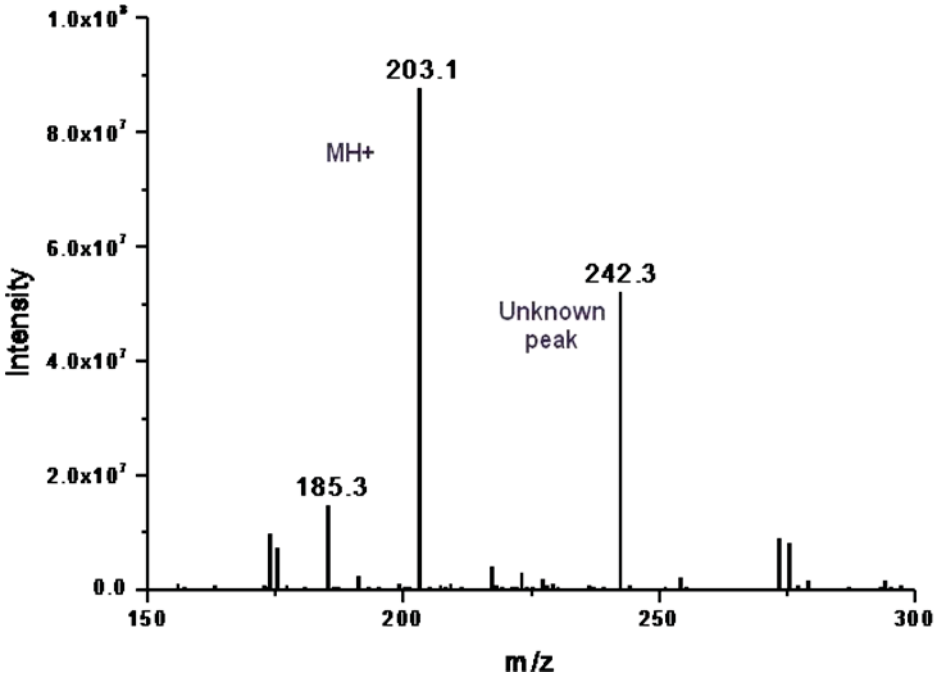

Figure 6.12.b.ESI-MS mass spectrum obtained for the unknown peak in Figure 6.12.a.

The fact that both arsenic containing CWDP compounds, DPAA and PAO, transform to PAA matches with their degradation pathways as reported by Oyama[5] (Figure 6.13).

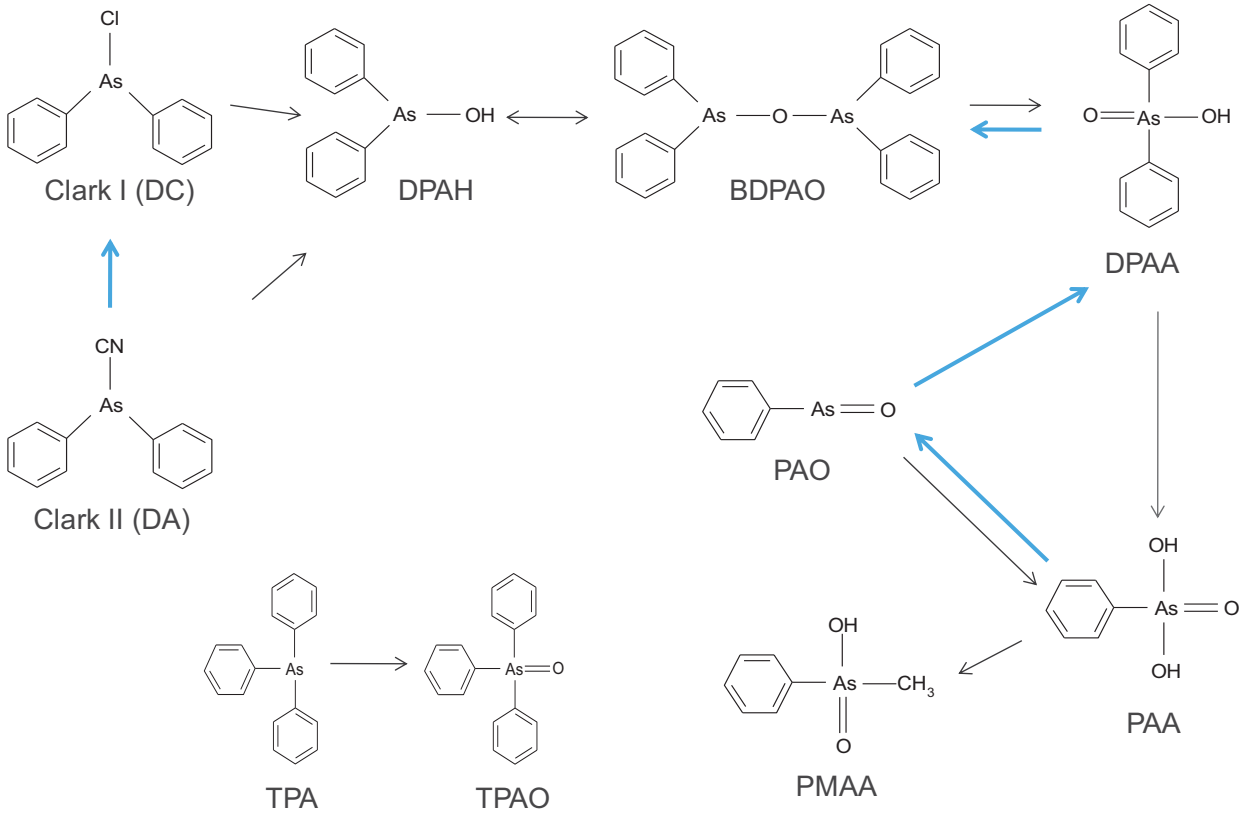

Figure 6.13. Degradation pathway of the sternutator agents Clark I and Clark II.[5]

TPA and TPAO, byproducts of the CWDPs degradation pathway, the two inorganic species As (III) and As (V), as well as the methylated species DMA and MMA gave poor intensity in the LC-ICPMS separation. The As uptake by the cells was sufficient for total analysis, but too low for speciation. Minimal sample is due to the logistics in preparing larger sample amounts. However, this is under study and larger sample quantities are being prepared.

6.7 Conclusions

The cytotoxicity experiments monitoring LDH activity show evidence for the chemical warfare degradation products, diphenylchloroarsine and diphenylcyanoarsine, PAO, PAA, DPAA, TPA and TPAO providing stronger cell death when compared to sodium arsenite, sodium arsenate, DMA and MMA. This enhanced interaction may be caused by greater membrane permeability through the phenyl groups. Generally, trivalent arsenic species demonstrate toxicity more quickly than the pentavalent species, as might be expected since MMA(III) is thought to be as toxic as As (III).

The study also indicates possible metabolic changes CWDPs might undergo after interaction with the African Green Monkey kidney CV-1 cells. Two degradation products, DPAA and PAO generate PAA in their degradation pathway and confirm that the metallomic approach of multiple mass spectrometries is highly viable.

6.8 References

(1) D. Hank Ellison, Handbook of chemical and biological warfare agents, CRC Press LLC, Boca Raton, 2000, Chap. 1, p. 40.

(2) Navy Warfare Library (located on the Reference Page) and the Navy Warfare Development Command SIPRNET Doctrine Discussion Group (DDG): http://www.nwdc.navy.mil/content/Library/Library.aspx

(3) Spring-8, Research Frontiers 2006, Chap. Environmental Science, p. 122.

(4) B. Daus, J. Mattusch, R. Wennrich, H. Weiss, *Talanta*, **75**: 376–379, (2008).

(5) S. Oyama, S. Hanaoka, *Cytotoxicityof Arsine Containing Chemicals related to OCWs in Japan,* CWD2007 (Brussels, 18 May, **2007**)

(6) Sang-Ho Nam, Jae-Jin Kim, Soung-Sim Han, *Bull. Korean Chem. Soc,* **24**(12): 1805-1808, (2003).

(7) LDH Cytotoxicity Detection Kit Manual, Takara Bio Inc., Cat.# MK401, v.03.10, p.4.

(8) C. Drahl, *Chemical & Engineering News*, **86**(34): 11, (2008).

(9) S. Hirano, Xing Cui, Song Li, S. Kanno, Y. Kobayashi, T. Hayakawa, A. Shiraim, *Archives of toxicology*, **77**(6), 305-312, (2003).

(10) T. Tsuchiya, T. Tanaka-Kagawa, H. Jinno**,** H. Tokunaga, K. Sakimoto, M. Ando, M. Umeda, *Toxicological Sciences*, **84**(2):344-351, (2005).

(11) T. Nakayama, T. Isobe, K. Nakamiya, J.S. Edmonds, Y. Shibata, M. Morita, *Magnetic Resonance in Chemistry,* **43:** 543-550, (2005).

Chapter 7

Protein phosphorylation studies of cerebral spinal fluid for potential biomarker development

Reproduced from Karolin K. Kroening, Julia Kuhlmann, Renee Easter, Joseph F. Clark, Gail Pyne-Gaithman, Joseph A. Caruso. Protein phosphorylation studies of cerebral spinal fluid for potential biomarker development. *Metallomics,* 2010; 2, 334–341.

7.1 Introduction

Mass spectrometry is a powerful tool for the identification of protein phosphorylation and phosphorylation sites that might be an indication of cell signaling associated with certain pathologies. Our point of departure is to investigate phosphorylation in the cerebral spinal fluid (CSF) of subarachnoid hemorrhagic stroke (SAH) patients for signaling changes prior to the deadly complications that may arise from the cerebral vasospasm condition (CV), with the ultimate goal of developing appropriate biomarkers.

The American Heart Association reported in 2009 that hemorrhagic stroke accounts for about 15% of all stroke cases. However, hemorrhagic stroke is significantly different from ischemic stroke where the vessel clogs, and prevents oxygen flow to parts of the brain. Hemorrhagic stroke results from a weakened artery that ruptures and bleeds into the surrounding brain tissue. The blood then accumulates and can lead to increases in intracranial pressure. There are two types of hemorrhagic strokes: intracerebral hemorrhage and subarachnoid hemorrhage.[1]

Our attention focuses on subarachnoid hemorrhage where the ruptured vessel is located in the subarachnoid space: the interval between the arachnoid membrane and *pia mater* in the central nervous system, which is fluid filled with cerebral spinal fluid. In 85% of the cases of spontaneous SAH, the cause is rupture of a cerebral aneurysm. An aneurysm is a weakness and/or ballooning in the wall of an artery in the brain. In 15 to 20% of cases of spontaneous SAH, no aneurysm is detected on the first angiogram. About half of these are attributed to non-

aneurysmal perimesencephalic hemorrhage, in which the blood is limited to the subarachnoid spaces around the midbrain (i.e. mesencephalon).[2,3]

After SAH, cerebral vasospasm post subarachnoid hemorrhage is the cause of death in 40 to 50% of patient.[4] "Vaso" refers to blood vessel and "spasm" refers to the vessel's "spastic", or "constricted" physical state.[5] The term "cerebral vasospasm" is commonly used to refer to both the clinical picture of delayed onset of ischemic neurological deficits associated with aneurysmal SAH ("symptomatic vasospasm") and the narrowing of cerebral vessels documented by angiography or other studies ("angiographic or arterial vasospasm"). Arterial vasospasm typically appears three to four days after rupture and reaches a peak in incidence and severity at seven to ten days. The incidence and time course of symptomatic vasospasm (CV in this study) parallels that of arterial vasospasm. However, while 40 to 70% of patients have evidence of arterial narrowing (detected by angiography or Doppler ultrasound), only 20 to 30% develop the clinical syndrome involving delayed ischemic neurologic deficit. The most important factors in determining the clinical effect of vasospasm are the severity and extent of vessel narrowing. Symptomatic vasospasm typically begins four to five days after the hemorrhage and is characterized by the insidious onset of confusion and a decreasing level of consciousness. When the arterial narrowing is marked, with concomitant ischemia, these symptoms may progress to focal neurological deficits, infarction, coma and death. In less severe cases, neurological recovery can be expected as the arterial narrowing resolves. The exact mechanism(s) by which SAH induces arterial vasospasm continues to be a subject of

considerable research and debate.[6-8] Therefore, the development of biomarkers that may predict CV after SAH is an interesting, but insufficiently studied research area.

Our focus in this study is to explore protein phosphorylation differences in cerebral spinal fluid between patients that have suffered from post-SAH CV (CSF V) and the ones that did not have CV post-SAH (CSF C); thereby expanding our preliminary study.[4] CSF samples from non-hemorrhage patients were also available and were used as a control (CSF Control). The phosphorylation of proteins on the amino acid residues of serine, threonine and tyrosine is estimated to affect 30% of the proteome and is a major regulatory mechanism that controls many basic cellular processes.[9] Phosphoprotein analysis in complex protein mixtures, such as CSF, involves identification and sequencing of phosphoproteins and phosphopeptides. Application of capillary liquid chromatography coupled to inductively coupled plasma mass spectrometry (capLC-ICPMS) combined with nano-liquid chromatography-electrospray ionization, ion trap mass spectrometry (nanoLC-CHIP/ITMS) represents a suitable technique for quantification of phosphoproteins and their phosphorylation degree by detecting the natural isotope ^{31}P. It also is a preferred method, since it avoids the use of the radioactive ^{32}P and ^{33}P labeling, often used in identifying protein phosphorylation.

Because of the complexity of CSF, the subdivision between two different regions (<5 kDa and 5-50 kDa) has been chosen to facilitate protein identification. The CSF samples were studied in the 5-50 kDa molecular weight range, which represents the common weight range for many proteins, but also the region <5 kDa has been taken in consideration. Important differences in

protein identifications are shown in this study and are promising for the development of biomarkers in order to predict the onset of CSF V.

7.2 Materials and Methods

The CSF samples were obtained through the Department of Neurology at the University of Cincinnati with appropriate institutional review board approvals. Double deionized (DDI) water was prepared by passing distilled water through a NanoPure (18 MΩ) treatment system (Barnstead, Boston, MA, USA). Acetonitrile (Tedia Company, Fairfield, OH, USA) has been used for mobile phase B in the capLC-ICPMS analysis. Formic Acid and Trifluoroacetic acid for the mobile phases A and B in the capLC-ICPMS separation have been purchased from Fisher Scientific (Fairlawn, NJ, USA). Solvents being used for the nanoLC-CHIP/ITMS, water and acetonitrile, were of high purity and have been purchased from Burdick and Jackson (Muskegon, MI, USA). Formic acid reagent grade (LOT: LB68266) for the ion trap and Spin Concentrators for Proteins (5kDa MWCO and 50kDa MWCO) are from Agilent (Agilent Technologies, Santa Clara, CA, USA). Top-Tip porous titanium dioxides tips were purchased from Glygen Corp. (Columbia, MD, USA).

Bovine ß-Casein, Iodoacetamide and dithiothreitol were acquired from Sigma-Aldrich (St. Louis, MO, USA). Ammonium bicarbonate was purchased from Fisher Scientific. Urea was from Mallinckrodt Baker (Canada). Sequence grade modified Trypsin and the suspension buffer acetic acid was obtained from Promega (Madison, WI, USA). Spin-X centrifuge tube filters (22

µm) were acquired Corning Inc. (Corning, NY, USA). Protein amounts in the cerebral spinal fluid samples determinations have been performed with the Pierce BCA assay (Pierce Chemical Company, Rockford, IL).

All information related to protein identifications are originated from Spectrum Mill rev. A. 03.03, Agilent Technologies and UniProtKB, the protein knowledge base, which consists of two sections: SwissProt and TrEMBL.

7.3 Sample preparation

The CSF samples were received at -80 °C and slowly thawed on ice before sample preparation in order to avoid protein degradation. Subsequently, they were loaded on a 5 kDa spin concentrator and subsequently spun and after that on a 50 kDa spin concentrator in order to obtain the desired MW regions of sample analysis. The samples were spun at 5000g for 20min at 4°C. Based on the protein amount present, previously determined by the *Pierce BCA assay* in the different samples received, a tryptic digestion was performed. The calculated amounts (1mg for Bovine ß-Casein, 12µL for CSF C, 20 µL for CSF V, 15 µL for CSF Control) were dissolved in water in a 1:1 ratio. 20 µL of a 0.4 M ammonium bicarbonate and 8M urea (pH 7.5) and 5 µL of 45mM dithiothreitol were added and incubated at 50°C for 15 min in order to reduce the protein. After cooling the sample to room temperature, 5 µL of 100mM iodoacetamide was added and left in the dark for 15 min, 5 µL of trypsin was added and the protein solution was incubated at 37°C for 22 hours. To halt the trypsin activity, formic acid was added. Samples were filtered through 0.22 µm, filters prior to the capLC separation.

After the fractions from the capLC-ICPMS were collected, they were passed through the TipTop titanium dioxide tips in order to enrich the phosphoproteins. Particular attention was focused on this part of the sample preparation. The sample and the elution buffer had to be pushed through the tip very slowly in order to give the phosphopeptides time to bind to the stationary phase.

7.4 Instrumentation

7.4.1 Capillary Liquid Chromatography (capLC)

An Agilent (Agilent Technologies, Santa Clara, CA, USA) 1200 series capillary liquid chromatography system equipped with a high pressure binary gradient pump, chilled autosampler, vacuum degasser, column compartment with Peltier heating/cooling, and UV detector was used to identify the phosphoprotein species being investigated in this study. An Agilent Zorbax SB-C18 column (0.5 x 150 mm, 5 µm) was used for the separation under gradient conditions with mobile phase A (1 % FA, 0.1 % TFA (v/v) in water) and B (80 % ACN, 1 % FA, 0.1 % TFA (v/v) in water). The gradient system was the following: 0-5 min, 3 % B; 5-10 min, 5 % B; 10-15 min, 10 % B; 15-20 min, 45 % B; 20-50 min, 75 % B; 50-60 min, 10 % B; 60-90 min, 0 % B. The column was re-equilibrated for 30 min after each run. 2 µL of digested CSF sample were injected into the capLC-ICPMS at a flow rate of 5.0 µL min^{-1}. The autosampler temperature was held at 4° C to prevent degradation of the protein samples.

7.4.2 Inductively Coupled Plasma Mass Spectrometer (ICPMS)

An Agilent 7500cx ICPMS (Agilent Technologies, Santa Clara, CA) equipped with a shield torch system and a collision/reaction cell was used for element specific detection of phosphorus. Coupling of the ICPMS with the LC was accomplished through the use of a PEEK coated silica tubing and a DS-5 capillary nebulizer (CETAC Technologies, Omaha, NE). ICPMS detection of the only phosphorus isotope (m/z = 31) was carried out using helium as a reaction gas at a flow rate of 3.7 mL min^{-1} and a quadrupole and octopole bias at -16 V and -18 V, respectively, for a net energy discrimination voltage of +2 V.

7.4.3 NanoLC-CHIP/ITMS

An Agilent 6300 Series HPLC-CHIP/Ion Trap XCTsystem (Agilent Technologies, Santa Clara, CA) coupled to a 1200 LC, equipped with both a capillary and nano pump was used for mass identification. The sample was loaded via the capillary pump on the on-chip enrichment column. The chip used, contained a Zorbax 300SB C18 enrichment column (4 mm × 75 μm, 5 μm) and a Zorbax 300SB C18 analytical column (43 mm × 75 μm, 5 μm). Samples were loaded on the enrichment column at a flow rate of 4 μL min^{-1} with a 97:3 ratio of solvent A (0.1 % FA (v/v) in water) and B (90 % ACN, 0.1 % FA (v/v) in water). After the enrichment column was loaded, the on-chip microfluidics switched to the analytical column at a flow rate of 0.4 μL/min. The following gradient conditions were used in the analysis: 0-5 min, 3 % B; 5-50 min, 40 % B; 50-60 min, 70 % B; 60-70 min, 50 % B; 70-90 min, 0 % B.

The MS conditions have been adopted from Ellis *et al* [4]. The analysis was achieved using nitrogen as a drying gas at a flow rate of 4 L min^{-1} and a temperature of 350° C. The capillary voltage was set to 1900 V, with a skimmer voltage of 30.0 V (capillary exit: 70.0 V; trap drive: 85.0 V). Two averages were taken for each precursor ion. The target number of ions was 500,000 with a maximum accumulation time of 150 ms. The MS scan range was 50-2200 *m/z* in standard-enhanced scan mode. MS^2 experiments were performed with five precursor ions per cycle and fragmentation amplitudes of 1.30 V. ESI-MS, MS/ESI-MS^2, and MS/ESI-MS^3 experiments were completed as well.

7.5 Results and Discussion

7.5.1 Analysis of standards for method confirmation

A study of detection limit (LOD) for ^{31}P has been performed to assess the efficiency of the chromatographic method coupled to ICPMS. A tryptic digest of bovine ß-casein was the standard of choice for the LOD determination**.** The concentration range of this protein was 0, 5, 10, 25, 50 ng mL^{-1} and R^2 for the calibration curve was 0.989. The linearity of the calibration curve has been verified with Mandel's fitting test. Detection limits (3σ) based on three times the standard deviation of seven replicates of the blank areas (IUPAC definition) for the analysis of ^{31}P of bovine ß-casein, based on 2 µL injection volume, was 10 ng mL^{-1}. The ^{31}P fraction in the chromatogram was collected offline and taken to the nanoLC-CHIP/ITMS for further identification. The base peak chromatogram (BPC) shows a peak at 30.4 min. Fragmentation analysis confirms the presence of bovine ß-casein showing MS fragments at m/z

278.4, m/z 147.2, m/z 284.3 and m/z 749. These are some examples of the characteristic fragments at the sequence positions 2, 44, 122 and 128 from bovine ß-casein after tryptic digestion.

The method of using capLC-ICPMS and nanoLC-CHIP/ITMS has been confirmed to be an excellent tool for phosphorylation site identification in previous studies, where phosphopeptide standards such as Pp60-src and P60 c-src showed validity for the techniques applied in this study [10].

7.5.2 Analysis of CSF samples (5-50 kDa) with capLC-ICPMS and nanoLC-CHIP/ITMS

The chromatograms of CSF Control, CSF V and CSF C samples show distinct differences. Although the separations are not exemplary, the aim of this study was the investigation of differences in phosphorylation and to determine which proteins those differences are related to. However, not only the differences are interesting to see, but also the similarities on certain samples, since they can indicate a disease state as well.

The CSF V sample presented a peak at 67.2 min as shown in **Figure 7.1**. This peak was not present in the CSF Control or in the CSF C sample and therefore, indicates a difference in phosphorus containing species. Furthermore, a peak at 74.6 min was present in the CSF Control, but not in the CSF samples from patients that had suffered from subarachnoid hemorrhage, CSF C, with subsequent vasospam, CSF V.

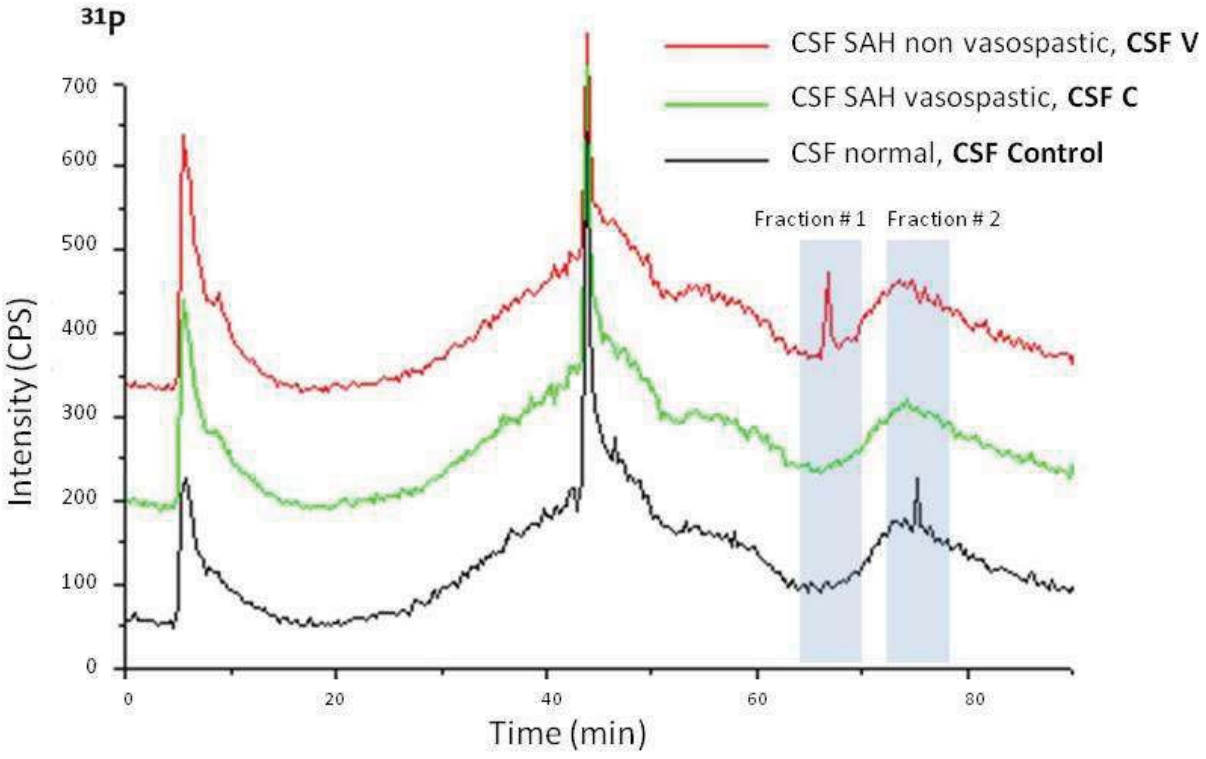

Figure 7.1. CSF Control, CSF C, CSF V (5-50 kDa molecular weight region) capLC-ICPMS chromatograms. A peak at 67.2 min in the CSF V is different from CSF Control and CSF C. Also, a peak at 74.6 min in the CSF Control sample is not present in the samples from patients that have suffered a SAH.

Both peaks were collected offline, Fraction #1 for the peak present in the CSF V sample and Fraction #2 for the peak present in the CSF Control, and analyzed with nanoLC-CHIP/ITMS for further mass identification. A relatively long time span of 30 min with a gradient from 45 % to 75 % ACN was chosen in order maintain spray stability. The base peak chromatogram (BPC) and average mass spectrum for the collected fraction (Fraction #1) of the peak at 67.2 min are

shown in **Figure 7.2**. The BPC of this peak shows high intensity peaks (x 10^9) between 12.1 and 18.6 min.

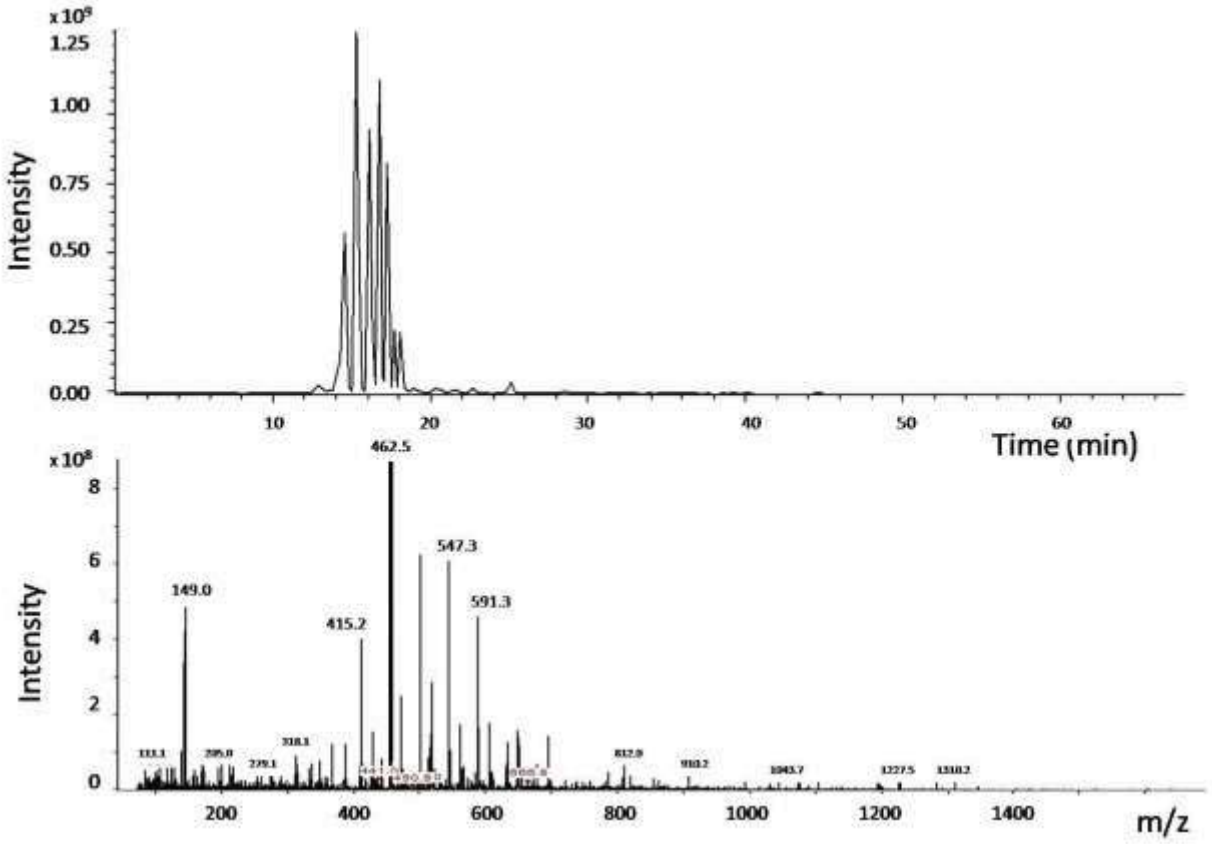

Figure 7.2. Base peak chromatogram and mass spectrum of Fraction #1 from CSF V sample of chromatogram of Figure 7.1.

The results of the protein database research of the region of high intensity with Spectrum Mill, with the SwissProt database, are presented in **Table 7.1**, based on statistical matches as score (which reflects information content, such as the amount of useful fragmentation), spectrum intensity, and Fwd-Rev score (which is the difference between scores for top hits from a database search of the matched peptide sequence, both for the forward sequence reading

direction and the reverse direction). The phosphorylation sites are listed in column 4. Not all the proteins shown are necessarily related to stroke complications; on the other hand they may be an indication that a protein, whose function is not currently known to be related to SAH, may actually play a role.

Score	FrwRev Score	Spectrum Intensity	Variable Sites	Sequence	Ret. Time (min)	Accession #	Name
7.86	1.76	4.88E+05	S879s	(R)sLNEELGDE DSEKKR(K)	43.66	O14924	Regulator of G-protein signaling 12 (RGS 12) Homo Sapiens (Human)
6.57	-0.83	2.56E+05	T1123t	(K)VKTDEVVTL tPRIGPK(V)	41.53	P13611	Versican core protein precursor (Large fibroblast proteoglycan) (Chondroitin sulfate proteoglycan core protein 2) (PG-M) (Glial hyaluronate-binding protein) (GHAP) - Homo sapiens (Human)
5.95	0	4.14E+05	S2032s	(K)KTGSKNLCA VELPSsVK(L)	37.9	Q9NZJ4	Sacsin - Homo sapiens (Human)
5.1	0.39	6.90E+05	S4077s	(R)sSRRTGPQS PCER(T)	40.88	Q12955	Ankyrin-3 (ANK-3) (Ankyrin-G) - Homo sapiens (Human)
5.01	0.12	1.23E+06	T129t	(K)AERIGEtPEL CALTGPFER(G)	54.63	O60294	Leucine carboxyl methyltransferase 2 (EC 2.1.1.-) (p21WAF1/CIP1 promoter-interacting protein) (tRNA wybutosine-synthesizing protein 4 homolog) - Homo sapiens (Human)
5	0.47	8.46E+05	S129s	(K)GAAVNGPV SHSSLTKTsNM NK(G)	44.14	Q9H582	Zinc finger protein 644 (Zinc finger motif enhancer-binding protein 2) (Zep-2) - Homo sapiens (Human)
4.8	-0.09	3.38E+05	S358s S360s	(K)QRNAEALA ELsEsLRNR(A)	42.69	Q9H1B7	RING finger protein C14orf4 - Homo sapiens (Human)
4.44	4.44	5.88E+05	S59s	(K)GPNANs(-)	50.96	P62861	40S ribosomal protein S30 - Homo sapiens (Human)

Table 7.1. Results from Spectrum Mill of collected Fraction #1 from CSF V sample in chromatogram from Figure 7.1.

The results with highest statistical validity for the CSF V sample (**Table 7.1**) show the regulator of G-protein signaling 12, homo sapiens. It inhibits signal transduction by increasing the GTPase

activity of G-protein α-subunits, thereby, driving them into their inactive GDP-bound form. Isoform-3 of this protein is brain specific. It is phosphorylated upon DNA damage, probably by ATM, ataxia telangiectasia mutated, or ATR, ATM and Rad3-related, and the database SwissProt reports phosphorylation on serine 879 in the sequence. G-protein-coupled receptors (GPCRs) are major targets for drug discovery. The regulator of G-protein signaling (the RGS)-protein family has important roles in GPCR signal transduction. RGS proteins represent a large set of tantalizing new central nervous system (CNS) drug targets with potential therapeutic actions in a wide range of clinical situations, such as Alzheimer‘s and Parkinson’s Diseases, Spasticity and Epilepsy.[11]

The following significant protein is Sacsin, which is highly expressed in the central nervous system. It may function in chaperone-mediated protein folding and it is known that chaperones, especially the stress inducible Hsp70, have been studied for their potential to protect the brain from ischemic injury. Giffard *et al.* showed that over expression of Hsp70 *in vivo* by, either viral or transgenic induction, before ischemia protects neurons from injury. The protection may be mediated by one or more of the many activities ascribed to Hsp70, including refolding denatured proteins and preventing unfolded and damaged proteins from aggregating, or by a direct anti-apoptotic mechanism.[12]

Of interest is also the 40S ribosomal protein S30 protein (Fau). Fau is a ribosomal protein synthesized as a *C*-terminal extension protein (CEP) of an ubiquitin-like protein. This may be of importance, since transient cerebral ischemia activates various post-translational protein modifications, such as phosphorylation and ubiquitin conjugation. These are believed to play a

major role in the pathological process triggered by an interruption of blood supply and culminating in cell death.[13]

These aforementioned are few examples of the proteins that have been identified in the BPC of the peak at 67.2 min of the CSF V sample. None of the above mentioned proteins were found in the CSF Control or CSF C; thus indicating a different phosphorylation profile in the CSF V patients' CSF compared to CSF C or CSF Control which may be diagnostic, prognostic or mechanistically relevant to the clinical condition. The authors are aware that for these examples and those below, only proof of concept is suggested. A statistically valid study to trigger clinical interventions or enhance treatments will require 30 patients in the SAH CSF C group and 30 additional in the SAH CSF V group. A research proposal has been submitted requesting funding for such a study.

The CSF Control collected peak, Fraction #2, gave the following results: The protein FAM38A (score: 8.25, peak intensity: 4.55×10^6 cps indicating relatively high statistical validity), which is a membrane protein induced by β-amyloid treatment, has been identified. It is expressed in numerous tissues. In normal brain tissue, it is expressed exclusively in neurons, but not in astrocytes. It was found to be expressed in about half of the activated astrocytes located around classical senile plaques in Alzheimer's disease.[14] This protein gave an eminent value of 3.32 for the Fwd-Rev score, which indicates the difference between scores for top hits from a database search of the matched peptide sequence both in for forward sequence reading direction and the reverse direction. The larger the score the greater the confidence in the sequence reported, accordingly to the score and spectrum intensity.

The Cystatin-SA precursor (Cystatin-S5) has also been identified. Cystatin-SA (CST2) is a human gene and a member of the family of cysteine protease inhibitors. Although cystatin-SA has not been associated with stroke, elevated cystatin-C levels were independently associated with both ischemic and hemorrhagic stroke, while cystatin-C is used as predictor for the risk of cardiovascular events and death.[15]

Although it has a slightly lower score and peak intensity and a negative value of the Fwd-Rev score (-0.02), an uncharacterized protein KIAA1383 has been identified. KIAA genes are protein-coding sequences of uncharacterized human genes. Since the protein is uncharacterized and its function and location is not known, it may trigger high interest.

7.5.3 Analysis of CSF samples (< 5 kDA) with capLC-ICPMS and nanoLC-CHIP/ITMS

A significant difference between the CSF SAH non vasospasm sample, CSF C, and the SAH vasospasm, CSF V, and normal sample, CSF Control, in the molecular weight region below 5 kDa can be seen as shown in **Figure 7.3**.

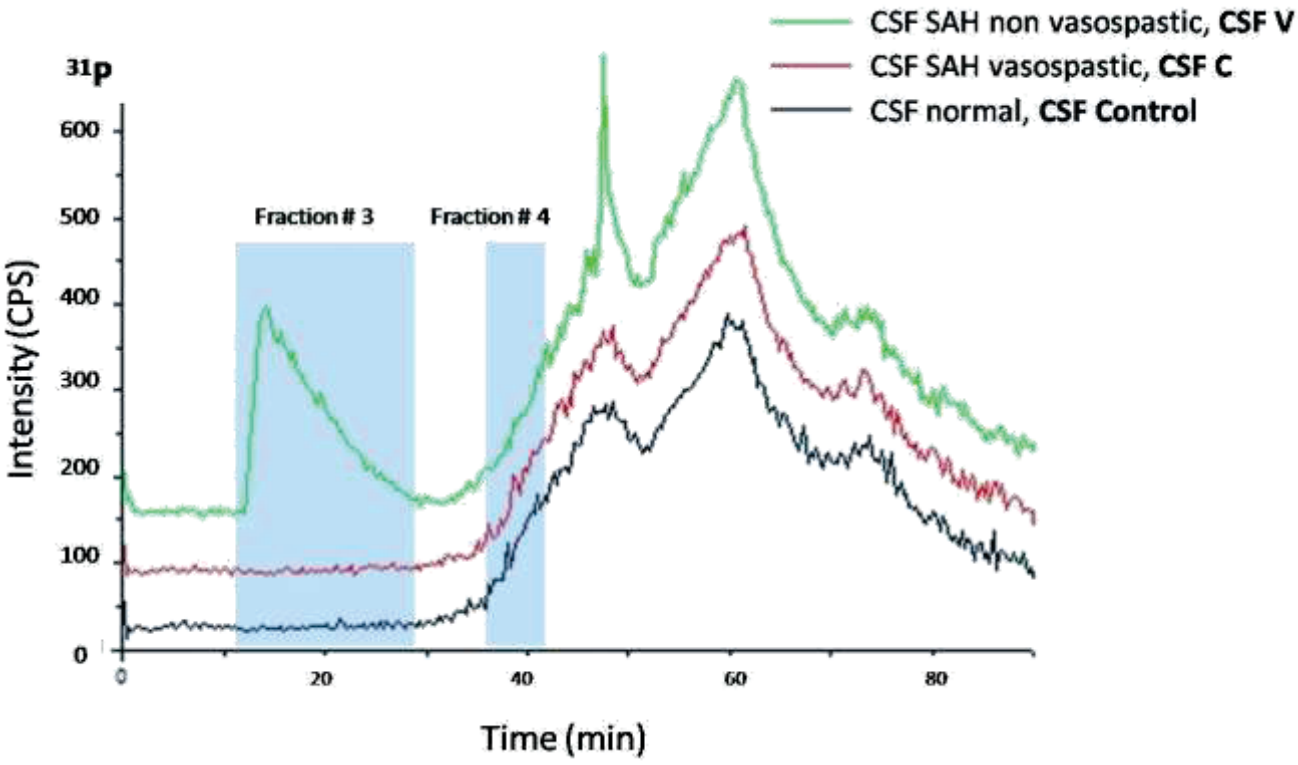

Figure 7.3. CSF Control, CSF C, CSF V (< 5 kDa) LC-ICPMS chromatograms. A peak at 12.1 min in the CSF C is being distinguished from CSF Control and CSF V. Also, a peak at around 38 min in the CSF Control and CSF V samples is not present in the samples from patients that have suffered a SAH without vasospasm.

The peak from 12.1-31.0 min is only present in the CSF C sample, which is the CSF SAH non vasospasm sample, and might be indication of important phosphoproteins. This peak was collected for further capLC-CHIP-ITMS analysis (Fraction # 3).

The database search resulted in a large number of brain protein phosphorylation hits for Fraction # 3: A very good hit (Score: 12, Spectrum Intensity: 1786325) at retention time 35.54

min was uncharacterized protein C11orf63. The cytolocation of this protein is unknown. C11orf63 is *homo sapiens* chromosome 11 open reading frame 63, type: mRNA, gene: C11orf63. As of this writing, the protein is uncharacterized and its function and location is not known.

Another protein match with the highest phosphorylation hits is protein73 which is a p53-like transcription factor (p53-related protein) and signifies enhanced signaling or protein activation. It participates in the apoptotic response to DNA damage. Isoforms containing the transactivation domain are pro-apoptotic, isoforms lacking the domain are anti-apoptotic and block the function of p53 and transactivating p73 isoforms. It is present in brain tissue as well as in other organs like kidney, placenta, colon, heart, liver; mainly in almost every organ and, therefore, very important in regulating apoptosis.

Further interesting proteins found include the Microtubule-associated serine/threonine-protein kinase 1. These suggest at this point that CSF C may exhibit similar phosphorylation responses to other neurodegenerative diseases. Accumulating evidence indicates that serine/threonine protein phosphatases (PPs), such as PP1, PP2A and PP2B, participate in the neurodegenerative progress in Alzheimer's disease. The general characteristics and pathologic changes of PP1, PP2A and PP2B in Alzheimer's, and their relations with microtubule-associated proteins, focusing mainly on τ-protein, neurofilament (NF), amyloid precursor protein (APP) processing and synaptic plasticity is a topic of active investigation and effective therapeutic intervention in the future.[16]

The Ubiquitin protein has been found in this fraction and was also reported in a previous study (J. Ellis *et al*)[10]. It is an important protein since it has been linked to neurodegenerative diseases like Parkinson's and Alzheimer's. Alzheimer's disease is the most common form of dementia and is characterized by degeneration of neurons and their synapses. The dementia can be sometimes attributed to a vascular dementia associated with perfusion deficits. Thus, there is a pre-existing cerebral vascular pathology in a subset of Alzheimer's patients. A higher number of senile plaques (SP) and neurofibrillary tangles (NFT) compared to non-demented individuals of the same age are often found *post mortem*. NFT are composed of a hyperphosphorylated and ubiquitinated forms of tau protein (τ-protein). Previous studies have shown that both tau and ubiquitin concentrations are increased in the cerebrospinal fluid (CSF) in Alzheimer's disease.[17]

An additional difference can be seen at 34.0-41.0 min as highlighted in the capLC-ICPMS chromatogram in Figure 3. CSF V and CSF Control seem to present low counts peaks that are not shown in the CSF C chromatogram. Fractions of these low intensity peaks were collected offline (Fraction # 4) for further analysis with capLC-CHIP-ITMS.

Results for Fraction # 4 are the following: This fraction from CSF C sample (SAH non vasospasm) has reported only 4 proteins with phosphorylation sites. The first one is the Gamma-aminobutyric acid (GABA) receptor subunit beta-2. GABA is a major inhibitory neurotransmitter in the vertebrate brain and mediates neuronal inhibition by binding to the GABA/benzodiazepine receptor which leads to the opening of an integral chloride channel. Generally serine/threonine phosphorylation of GABA receptors has been found to reduce GABA receptor activity, and conversely, dephosphorylation of the receptor is often associated with

the enhanced receptor function.[18,19] The concentration of GABA in CSF has been studied extensively and has been shown to be related to Parkinson's disease as well as epileptic seizures.[20,21] The GABA level in CSF was found to be reduced in patients with idiopathic Parkinson's disease when compared with age matched controls, but the difference was not significant. However, GABA levels in CSF were lower in patients treated with levodopa than in untreated patients and controls. There was no difference in plasma GABA levels between Parkinsonian patients and controls.[19]

Another protein that was found is ubiquilin-4, which has been also identified in Fraction # 3, and was also reported in a previous study *Ellis et al*.[10] As mentioned earlier, this protein is important in the stabilization of other brain proteins. It has also emerged as a therapeutic target for Huntington's disease, as it binds to protein aggregates found in Huntington's, Alzheimer's, and Parkinson's Diseases.[22]

7.5.4 Protein and Protein Phosphorylation Identification with analytical tools

In confirming one example from the above described proteins, Regulator of G-protein signaling 12 (RGS12) was selected. The mass spectrum shows evidence of the characteristic peaks that may follow tryptic digestion. For example in **Figure 7.4** the masses m/z 391.2 corresponding to the peptides fragments ATK, m/z 575.3: AQSNR, m/z 728.4: m/z GWLKPK, m/z 1193.6: LAFSAVCPDDR, m/z 1796.9: INLDEAEEFFELISK etc.

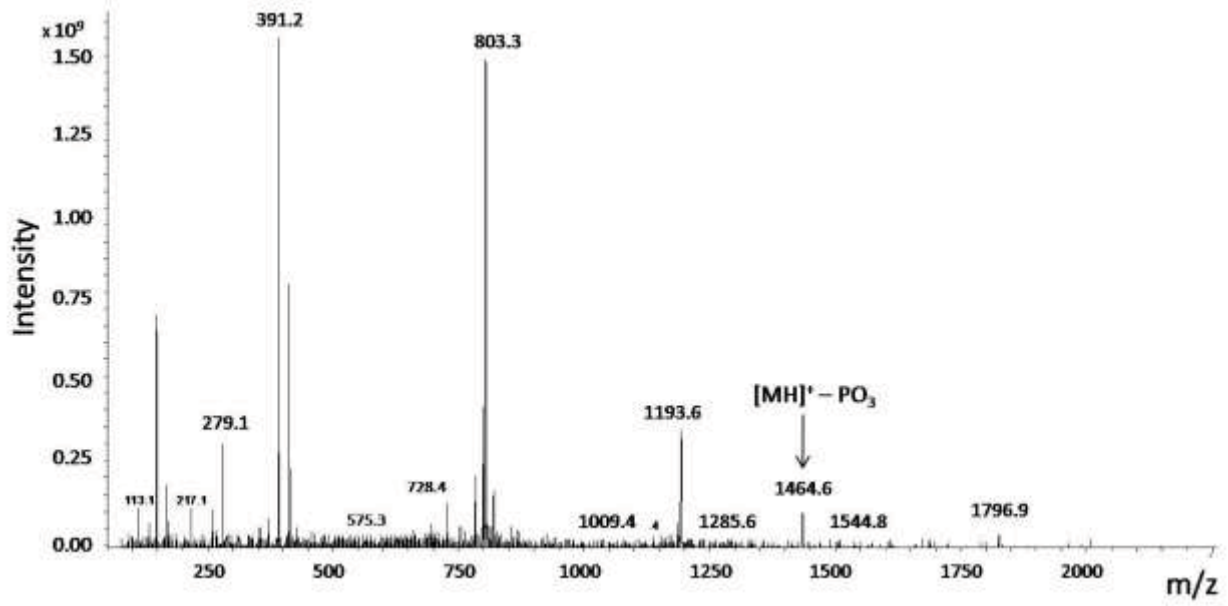

Figure 7.4. Regulator of G-protein signaling 12 (RGS12) average mass spectrum showing characteristic masses as ATK, m/z 575.3: AQSNR, m/z 728.4: m/z GWLKPK, m/z 1193.6: LAFSAVCPDDR, m/z 1796.9: INLDEAEEFFELISK etc., being indication of peptide fragmentation.

Serine at the sequence position 879 was identified as a phosphorylation site. The loss of -PO_3 is indicated in the mass spectrum at m/z 1544.8 with a low intensity of 6130 counts (figure 4). The peak m/z 1464.6 at higher intensity indicating the loss of -78 Da. Therefore, even if Spectrum Mill gives a statistical indication at what position the loss of the phosphate group can occur, the ESI mass spectrum analysis permits a precise and simplified identification of the suggested results from Spectrum Mill, thereby providing further verification. It is clear that mass spectrometry for peptide identification and the identification of phosphorylation sites can be very powerful when combining direct mass spectral information with an appropriate data base search. In almost all the other identified proteins the phosphorylation sites from the mass

spectra matched with the ones suggested from the database. In most of the mass spectra the neutral loss of a phosphate group or a phosphate group plus water (H_3PO_4) occurred at phosphoserine and phosphotyrosine containing phosphopeptides.

7.6 Conclusion

Phosphoproteins in CSF and particularly the lower copy numbers of many signaling proteins are difficult to detect, but mass spectrometry is an excellent tool for the identification of phosphoproteins and the indication of phosphorylation sites. The capLC-ICPMS method permits a simplified screening of differences in ^{31}P in CSF Control or diseased SAH/CV post SAH patients at low level for phosphorus containing species. NanoLC-CHIP/ITMS provides a relatively modestly expensive option to generate MS^n spectra for the data base search engines and, thereby, a route to confirm statistically based results via the losses or gains to the mass spectra. In this study differences have been shown in the variety of the two molecular weight regions, < 5KDa or 5-50 kDa, of three different sample types,CSF V, CSF C and CSF Control, and the approach is promising for future studies to inform the identification of biomarkers with putative implications for therapeutic targets.

7.7 References

(1) Association, A.H. *American Heart Association, Inc.* 2009 [cited; Available from: \http://www.americanheart.org/.

(2) GJ Rinkel, J.v.G.a.E.W., *Subarachnoid hemorrhage without detectable aneurysm. A review of the causes.* Stroke, 1993. **24**: p. 1403-1409.

(3) van Gijn, J., R.S. Kerr, and G.J.E. Rinkel, *Subarachnoid haemorrhage.* The Lancet, 2007. **369**(9558): p. 306-318.

(4) Ellis, J., et al., *A Preliminary Study of Metalloproteins in CSF by CapLC-ICPMS and NanoLC-CHIP/ITMS.* Journal of Proteome Research, 2008. **7**(9): p. 3747-3754.

(5) Khurana, G. *Brain aneurysm*. 2006 [cited; Available from: http://www.brain-aneurysm.com/.

(6) D, H.E.D.M.J.M.M.E., *Therapeutic potential of the lazaroids (21-aminosteroids) in acute central nervous system trauma, ischemia and subarachnoid hemorrhage.* Advances in pharmacology, 1994. **28**: p. 221-68.

(7) Hall, E.D., *Efficacy and mechanisms of action of the cytoprotective lipid peroxidation inhibitor tirilazad mesylate in subarachnoid haemorrhage.* European Journal of Anaesthesiology, 1996. **13**(3): p. 279-289.

(8) Sarah L. Smith, M.A., Heidi M. Scherch, B.S., and Edward D. Hall, Ph.D., *Protective effects of tirilazad mesylate and metabolite U-89678 against blood-brain barrier damage after subarachnoid hemorrhage and lipid peroxidative neuronal injury.* Journal of Neurosurgery, 1996. **84**(229-33).

(9) Ptacek, J., et al., *Global analysis of protein phosphorylation in yeast.* Nature, 2005. **438**(7068): p. 679-684.

(10) Ellis, J., et al., *Studying Protein Phosphorylation in Low MW CSF Fractions with capLCâˆ'ICPMS and nanoLCâˆ'CHIP-ITMS for Identification of Phosphoproteins.* Journal of Proteome Research, 2008. **7**(11): p. 4736-4742.

(11) Neubig, R.R. and D.P. Siderovski, *Regulators of G-protein signalling as new central nervous system drug targets.* Nature Reviews. Drug Discovery, 2002. **1**(3): p. 187-197.

(12) Giffard, R.G., et al., *Chaperones, protein aggregation, and brain protection from hypoxic/ischemic injury.* J Exp Biol, 2004. **207**(18): p. 3213-3220.

(13) Yang, W., et al., *Cerebral ischemia/stroke and small ubiquitin-like modifier (SUMO) conjugation--a new target for therapeutic intervention?* Journal Of Neurochemistry, 2008. **106**(3): p. 989-999.

(14) Satoh, K., et al., *A novel membrane protein, encoded by the gene covering KIAA0233, is transcriptionally induced in senile plaque-associated astrocytes.* Brain Research, 2006. **1108**(1): p. 19-27.

(15) Ni, L., et al., *Cystatin C, Associated With Hemorrhagic and Ischemic Stroke, Is a Strong Predictor of the Risk of Cardiovascular Events and Death in Chinese.* Stroke, 2007. **38**(12): p. 3287-3288.

(16) Tian, Q. and J. Wang, *Role of Serine/Threonine Protein Phosphatase in Alzheimer's Disease.* Neurosignals, 2002. **11**(5): p. 262-269.
(17) Skoog, I., et al., *A Population-based Study of tau Protein and Ubiquitin in Cerebrospinal Fluid in 85-year-olds: Relation to Severity of Dementia and Cerebral Atrophy, but not to the Apolipoprotein E4 Allele.* Neurodegeneration, 1995. **4**(4): p. 433-442.
(18) Levitan, I.B., *Modulation of ion channels by protein phosphorylation and dephosphorylation.* Annual Review of Physiology, 1994. **56**: p. 193-212.
(19) Raymond, L.A., C.D. Blackstone, and R.L. Huganir, *Phosphorylation of amino acid neurotransmitter receptors in synaptic plasticity.* Trends in Neurosciences, 1993. **16**(4): p. 147-153.
(20) Abbott, R.J., I.F. Pye, and S.R. Nahorski, *CSF and plasma GABA levels in Parkinson's disease.* Journal of Neurology, Neurosurgery & Psychiatry, 1982. **45**(3): p. 253-256.
(21) Wolfgang, L., *Relationship Between GABA Concentrations in Cerebrospinal Fluid and Seizure Excitability.* Journal Of Neurochemistry, 1982. **38**(1): p. 293-295.
(22) Mah, A.L., et al., *Identification of Ubiquilin, a Novel Presenilin Interactor That Increases Presenilin Protein Accumulation.* J. Cell Biol., 2000. **151**(4): p. 847-862.